International Journal of Disaster Risk Reduction 143 (2026) 106252

Contents lists available at ScienceDirect

International Journal of Disaster Risk Reduction

journal homepage: www.elsevier.com/locate/ijdrr

review article

Spatio-temporal variability of landslides as indicator of climate change impact: Towards an Italian national scale integrated procedure for the rainfall role analysis in landslide dynamics

M. Delchiaro [a], V. Ruscitto [a,*], G. Iacobucci [a], D. Piacentini [a], F. Troiani [a], E. Dallan [b], M. Borga [b], M.V. Struglia [c], A. Montanari [d], M. Marani [e], S. Silvestri [f], C. Puglisi [c], L.M. Falconi [c], G. Righini [g], S. Segoni [h], M. Pirone [i], R. Tufano [j], R. Narcisi [k], F. Vagnon [k], G. Taddia [k], P. Mazzoglio [k], P. Claps [k], C. Martinello [l], E. Rotigliano [l], G. La Porta [m], M. Ferrarotti [a,n], M. Pirulli [m], G. Pepe [o], B. Antonielli [p], L.M. Giannini [a], C. Esposito [a], S. Martino [a], F. Bozzano [a], D. Calcaterra [j], D. Di Martire [j], M. Della Seta [a]

[a] Department of Earth Sciences, Sapienza University of Rome, Rome, Italy
[b] Department of Land Environment Agriculture and Forestry, University of Padova, Padova, Italy
[c] ENEA Italian National Agency for New Technologies, Energy and Sustainable Economic Development, Rome, Italy
[d] Department of Civil, Chemical, Environmental, and Materials Engineering, University of Bologna, Bologna, Italy
[e] Department of Geosciences, University of Padova, Padova, Italy
[f] Department of Biological, Geological, and Environmental Sciences, University of Bologna, Ravenna, Italy
[g] ENEA Italian National Agency for New Technologies, Energy and Sustainable Economic Development, Bologna, Italy
[h] Department of Earth Sciences, University of Florence, Florence, Italy
[i] Department of Civil, Architectural and Environmental Engineering, University of Naples Federico II, Naples, Italy
[j] Department of Earth Sciences, Environment and Resources, University of Naples Federico II, Naples, Italy
[k] Department of Environment, Land and Infrastructure Engineering (DIATI), Politecnico di Torino, Turin, Italy
[l] Department of Earth and Marine Sciences, University of Palermo, Palermo, Italy
[m] Department of Structural, Geotechnical and Building Engineering (DISEG), Politecnico di Torino, Turin, Italy
[n] SPERI S.p.A., Rome, Italy
[o] Department of Earth, Environment and Life Sciences, University of Genova, Genoa, Italy
[p] Serco Italia S.p.A., Rome, Italy

ARTICLE INFO

Keywords:
Climate change
Landslides
Rainfall
Multi-hazard
National Recovery and Resilience Plan (PNRR)

ABSTRACT

Ground instabilities such as landslides, subsidence, sinkholes, and soil liquefaction are highly sensitive to climate change. In Italy, these phenomena represent a major component of hydrogeological risk, particularly in mountainous and hilly regions where recent extreme events have highlighted the growing influence of climatic stressors on slope instability. Intense and prolonged rainfall acts both as a preparatory factor, gradually weakening slopes, and as a triggering factor, directly inducing failures. Despite the increasing frequency and severity of rainfall extremes, a comprehensive conceptual framework integrating extreme precipitation behaviour into landslide dynamics is still lacking.

* Corresponding author.
E-mail address: valeria.ruscitto@uniroma1.it (V. Ruscitto).

https://doi.org/10.1016/j.ijdrr.2026.106252
Received 8 February 2026; Received in revised form 11 May 2026; Accepted 5 June 2026
Available online 6 June 2026

This work reviews current knowledge on rainfall induced landslide processes, with specific attention to the distinction between preparatory and triggering mechanisms and to their sensitivity to evolving climatic conditions. Focusing on shallow landslides, where rainfall exerts a more direct and immediate influence than in deep-seated processes, we analyse the spatio-temporal variability of landslide occurrence as an indicator of climate change impacts.

Building on this review, we develop a national scale conceptual framework composed of standardized toolchains designed to assess and systematically integrate the role of rainfall in landslide dynamics. The toolchains are evaluated through virtual test beds, which provide a controlled yet geomorphologically realistic environment for exploring multi hazard interactions and assessing the internal coherence of modelling workflows. This conceptual validation highlights both the potential and the limitations of existing approaches, particularly the difficulty of translating rainfall information into soil moisture and pore pressure conditions -an essential but still critical step for reliably modelling preparatory processes.

1. Introduction

Climate change refers to long-term shifts in climate variables. While natural processes such as volcanic activity, solar fluctuations, and internal variability contribute to climatic oscillations [1], recent changes are predominantly driven by human activities [2,3]. Anthropogenic emissions have raised atmospheric CO_2 from ~278 ppm in pre-industrial times to over 417 ppm in 2022 [3,4] , altering the Earth's energy balance and intensifying extreme events such as heavy rainfall, heatwaves, droughts, and windstorms [5–9]. Climate-change parameters describe how the climate system evolves, whereas impact indicators measure the consequences on natural and human systems [3], including changes in landslide frequency, floods, glacier retreat, and drought severity (Fig. 1).

Landslides are particularly sensitive to climatic variations, as shown by several studies [11–14], with annual damages exceeding €6 billion in industrialized countries. Indirect impacts are also substantial: in Italy, hydrogeological events increase firm exit probability by 7.3% and reduce revenues and employment by 4.9% and 2.2% [15]. Large-scale climate drivers further modulate landslide occurrence: intense El Niño phases amplify rainfall-induced landslides [12]; atmospheric rivers dominate triggering storms in the subtropical Andes [16,17]; and random rainfall patterns influence landslide timing and cumulative area [18]. Additionally, warming and extreme rainfall affect vegetation dynamics, sometimes degrading stabilizing cover [19] and other times enhancing slope resistance [20].

In Italy, the effects of ongoing climate change have become increasingly evident in recent years. The years 2022 and 2023 were the warmest years since 1961, considering the mean and the maximum temperatures with an average anomaly of +1.14°C (SNPA Report 2023 [21]). These anomalies have strongly influenced the national water balance, especially in northern and central Italy, causing several extreme floods and prolonged droughts. For example, extreme rainfall events occurred in Emilia Romagna (326 mm/day; [22]) and Tuscany regions (200 mm in 3 h; [23]) in May and October 2023, and November 2023, respectively, although the cumulative rainfall in Italy during 2023 was overall lower than climatological average of about 4% [21]. In particular, during the May 2023

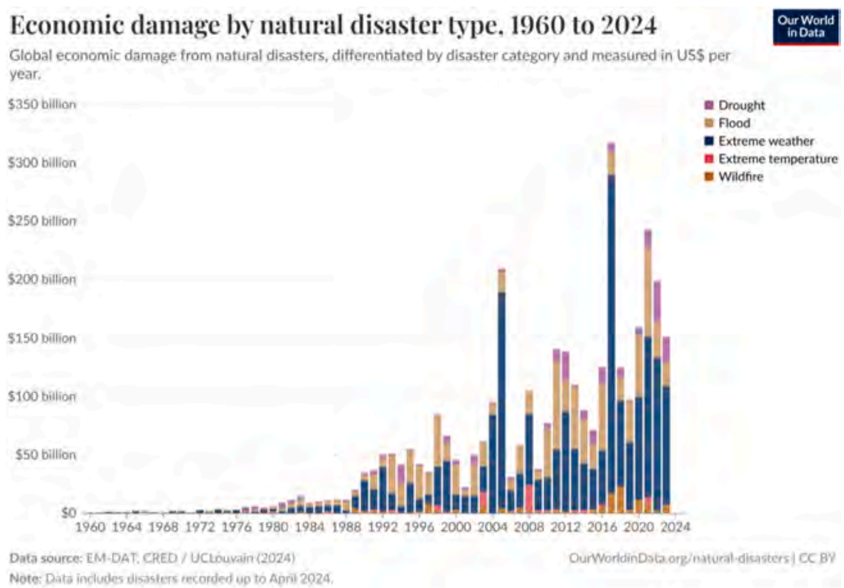

Fig. 1. Global economic damage by natural disaster from 1960 to 2024. The amount of damage to property, crops, and livestock is given in US$ (EM-DAT, CRED/UCLouvain, 2024 10). Data includes disasters recorded up to April 2024.

Emilia-Romagna event more than 80,000 rainfall-induced landslides (mostly first-failure) occurred over an area of more 6000 km^2, with density reaching as high as 200 landslides per square kilometer [24]. Moreover, prolonged dry periods occurred in the regions of Piedmont, Liguria, Emilia Romagna, Apulia, Sicily and Sardinia regions with more than 330 dry days. Even so, in the autumn of 2024 some exceptional events occurred: on 19th and 20th October the municipal area of Bologna recorded the absolute record of daily rainfall since 1900 [25].

In the Mediterranean region, waterspouts, cyclones, floods, and storm surges have increased in frequency and intensity [26–28], like Ciarán and Domingos Storms in November 2023. During these events, along the Ligurian coast the wind speed reached 100 km/h (classified as a violent storm in the Beaufort Wind Force Scale), locally exceeding 200 km/h (hurricane), and causing severe storm surges comparable to the Vaia Storm, which occurred in northeastern Italy in October 2018 [29]. Exceptional high tides were recorded in the Northern Adriatic Sea, reaching the third highest value since 1869 (110 cm Punta della Salute zero tide gauge in Venice) at the end of October - beginning of November 2023 [30].

Landslides, whose spatio-temporal variability has been recognized as an indicator of climate change impact, are influenced by a complex interaction of static (predisposing) and dynamic (preparatory and triggering) factors. While static factors define the inherent susceptibility of a slope to failure [31–33], only dynamic factors allow for the assessment of climate change impacts on slope instability. On one hand, the study of the predisposing static factors includes the analysis of landslide susceptibility, which can be carried out using qualitative (heuristic, descriptive) or quantitative (numerical, probabilistic) methods (e.g., Ref. [13,34–38]). On the other, the study of dynamic factors, encompassing both preparatory and triggering phases, focuses on the time-dependent processes that control slope instability. These factors respond directly to variations of meteorological and environmental conditions. Among these, rainfall, taken here as a representative variable, plays a dual role, acting as both a preparatory and a triggering factor. In general, intense and prolonged precipitation progressively reduces slope stability by altering soil moisture, increasing pore pressure, and decreasing shear strength [39–41]. The preparatory phase is further modulated by antecedent and cumulative rainfall, as well as seasonal trends [42 43,44], which promote soil saturation, internal erosion, and progressive weakening [45–48]. However, the impacts of climatic forcing vary spatially due to differences in soil properties, vegetation cover, topography, and land use, and are further influenced by microclimatic variability and climate change, which is intensifying heavy rainfall events. Anthropogenic topographic changes can further modify local slope stability conditions [49], altering drainage patterns, erosion susceptibility, and sediment connectivity. Consequently, the response of shallow landslides to evolving climatic patterns remains highly region-dependent [50–52].

Despite the intensification of extreme rainfall events observed in recent decades due to climate change [3], a comprehensive understanding of how climate influences the preparatory and triggering factors of landslides is still lacking. Moreover, although

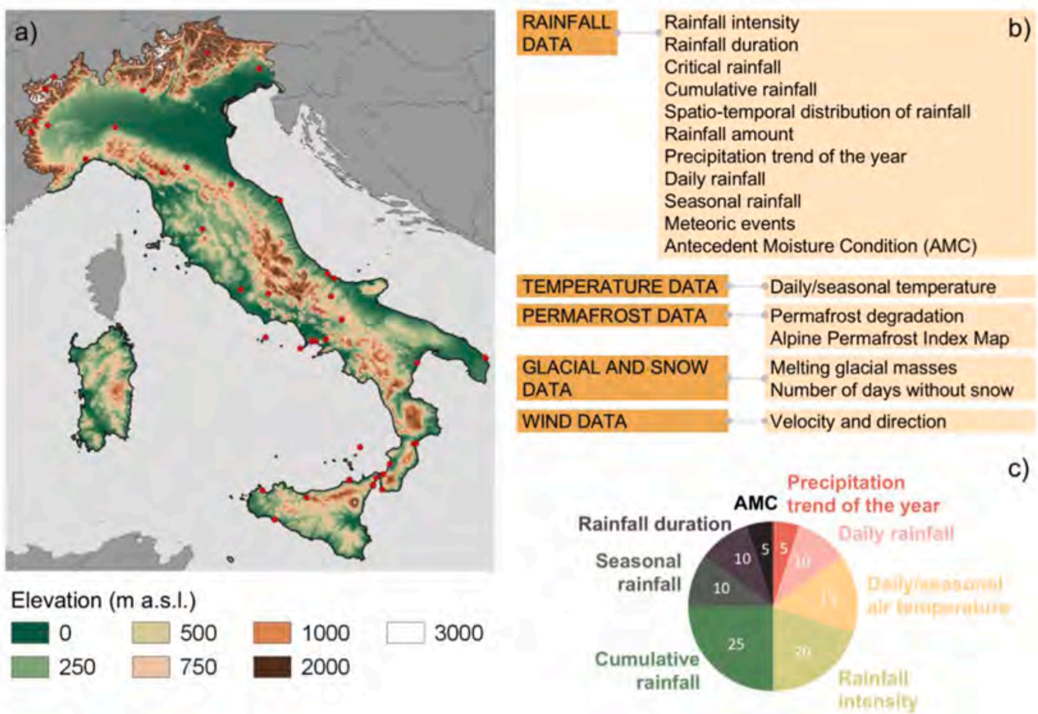

Fig. 2. Location of the Learning Examples (LEs) selected within the RETURN project across the Italian territory (a), and classification of the associated climate indicators, as reported in the literature of each LE (b, c). The pie chart in panel c displays the relative frequency of indicators used to assess landslide preparatory and triggering conditions, highlighting the predominance of rainfall-related variables, particularly cumulative rainfall (∼25%) and rainfall intensity (∼20%). Panel b summarizes the types of climatic and environmental indicators categorized by data domain (e.g., rainfall, temperature, permafrost, snow/glaciers, wind).

numerous site-specific studies in Italy have explored the preparatory and triggering role of rainfall in gravitational processes; however, these investigations remain fragmented and localized. Currently, there is no shared procedural framework or standardized toolchain at the national level to systematically assess and integrate the impacts of climate on landslide dynamics.

An opportunity to address this shortcoming is provided by frameworks, such as the RETURN partnership, that facilitate the transdisciplinary approaches necessary for studying phenomena involving multiple aspects. The methodological approach described in this paper was first focused on the study of the state of the art grounded on the identification of a series of case studies (defined as Learning Examples) which represent best practice experiences and forefront analyses. Furthermore, a total of 38 impact-oriented hazard indicators were selected, considering the most common weather-climatic parameters, including precipitation, temperature, snow and glacial data, wind, and marine data (Fig. 2). In this perspective, the identification of climatic stressors responsible for ground instabilities has been carried out by specific tasks, also benefiting from recent advances in geomorphological approaches on climate services [53–57]. Within this framework, landslides and other ground instabilities were categorized as reported in Table 1. The landslides are classified according to their kinematics (i.e., slow and fast movements) and types (i.e., flows, slides, spreads and slope deformations, falls, and topples).

Concluding, the aim of this study is to investigate the spatio-temporal variability of landslide occurrence as an indicator of climate change impact, with a specific focus on the preparatory and triggering factors to better understand the role of rainfall in landslide dynamics. The analysis primarily focuses on shallow landslides, where the rainfall-induced dynamics of preparation and triggering are more direct and clearly linked to short-term hydro-meteorological conditions, rather than on deep-seated landslides, whose response to rainfall is more complex and delayed (e.g., Ref. [58]). Building on this review, we develop a national-scale conceptual framework supported by standardized toolchains designed to systematically assess the role of rainfall in landslide dynamics. These toolchains are evaluated through a virtual test bed (VTB), which offers controlled yet geomorphologically realistic environments for exploring multi-hazard interactions and verifying the internal coherence of modelling workflows. This conceptual validation helps to identify key gaps in current methodologies, providing a structured basis for future operational developments, adaptable to diverse geographical and climatic contexts.

2. Literature review on present climate and expected future changes of precipitation in Italy

2.1. Precipitation climatology

Italy's annual and extreme precipitation climatology is shaped by complex atmospheric and topographic influences [59–61]. In northern Italy, precipitation is mainly generated by cyclonic systems originating from the North Atlantic or near the Iberian Peninsula [62,63], which often intensify over the Gulf of Genoa which is also known as the “Genoa cyclogenesis” region [64]. Coupled with orographic uplift, this leads to high annual precipitation (in the range 1500–2500 mm) across northern windward regions such as Liguria, northern Tuscany, southern Alpine foothills, reaching 3000 mm in Friuli, the north-easternmost area [65,66]. Conversely, the whole Po River valley, leeward regions like the Adriatic coast, and the inner part of the Alps like South-Tyrol receives significantly less precipitation amounts (<1000 mm; [67]). In southern Italy, precipitation is mainly driven by convective systems and cyclones over the Tyrrhenian and Ionian Seas [64], especially in winter. The higher precipitation totals range from 1000 to 1300 mm on Sicily's northern and eastern coasts to 1200–1800 mm in the Calabrian Apennines [68], while much drier conditions are present in the rest of the central-southern Italy (<600 mm). More detailed information on the annual precipitation distribution over Italy is available in Crespi et al. [66].

Strong spatial variability is also evident for extreme precipitation in Italy, particularly for short durations, as shown in Avanzi et al. [59]. They estimated the highest values of 1-h extreme precipitation events (e.g. 50-year return period quantiles, ranging from ~17 to 220 mm) along much of Italy's coastline, especially the southern coast of Friuli–Venezia Giulia, the western coast of central Italy, and the eastern coasts of Sicily, Calabria, and Sardinia, with values exceeding 200 mm. High values are also found inland, notably across the Po Valley, Venice lagoon, and mountainous Apennine regions, highlighting the widespread nature of convective storms in lowland

Table 1
Categories of ground instabilities as conceptualized in the Extended Partnership RETURN. In bold the kinematics and typologies considered in the present work.

Ground Instabilities	**Subaerial Landslides**	**Subaerial Slow Landslides Typologies**	**Slow Flows (Earthflows)**
			Slow Slides (Rotational and Planar Slides, Soil slips)
			Slow Spread & Slow Slope Deformations (Spread (except Liquefaction), Rock/Soil Slope Deformations, Creep, Deep-Seated Gravitational Slope Deformation)
		Subaerial Rapid Landslides Typologies	**Rapid Flows (Debris flows, Mudflows)**
			Rapid Slides (Rock Slides, Rock Avalanches)
			Falls & Topples (Rock Falls, Rock Topples)
	Submarine Landslides	Submarine Landslides Typologies	Slow Submarine Landslides (Creep, Deep-seated Gravitational Slope Deformation)
			Rapid Submarine Landslides (Flows, Avalanches, Slides)
	Sinkholes	Slow Sinkholes Typologies	Slow Sinkholes (Suffosion Sinkholes, Solution Sinkholes)
		Rapid Sinkholes Typologies	Rapid Sinkholes (Collapse Sinkholes, Cover-collapse Sinkholes)
	Subsidence	Subsidence Typologies	Subsidence (all types)
	Liquefaction	Liquefaction Typologies	Liquefaction (all types)

and coastal areas. As the duration increases to 24 h (50-yr quantiles in the range ∼40–1010 mm), the highest values are concentrated in narrower regions like the northwestern Alps, the Italian western coast, eastern Sardinia, southern Calabria, and eastern Sicily. As discussed in Avanzi et al. [59], this variability reflects the transition from convective systems (dominant at short durations) to stratiform precipitation (more common over longer durations) in combination to the Italian topography. Indeed, although convective storms (e.g., 1-h events) are smaller in extent than stratiform systems, their presence is more widespread, especially over large plains like the Po Valley owing to strong vertical instability. In contrast, extreme daily precipitation events are spatially confined where moist airflows are uplifted by the presence of relief.

2.2. Observed trends

In recent years, growing attention has been given to quantifying and understanding trends in precipitation amounts, particularly on extreme precipitation to establish empirical baselines for climate impact studies. On an annual scale, a review by Caporali et al. [69] found general consensus on the decreasing trend in the number of wet days across Italy, with only minor regional variations, and a less-pronounced decline in total precipitation, particularly during the winter months. A recent study by Vicente-Serrano et al. [70] over the Mediterranean Region, spanning a period from 1871 to 2020, highlights the variability of detected trends on the considered period and region, while a long-term trend over the whole region is not emerging. They attribute the detected trend mostly to the variability of atmospheric circulation patterns, that is internal variability of climate. However, over most of Italy a tendency of decreasing annual precipitation is found from long-term analysis, while in the last decades they found increasing trends.

In the past 20 years many studies have been developed on trend in extreme precipitation over Italy at regional extent (e.g. Refs. [71–77]). Most of them show a lack of statistical significance in the trends over large parts of the investigated areas, while significant trends could emerge over smaller regions. This clearly emerges from a couple of studies recently carried over the whole Italy by using long-term records of annual maxima at sub-daily durations [9,78]. By using a quantile regression approach and analyzing data from 1960 to 2022, Mazzoglio et al. [9] provide a broader picture of trends in extreme precipitation. Their results suggest that rarer extremes (high quantiles) exhibit greater spatial and temporal variability than ordinary ones, and higher magnitude of the trend. Notably, 1-h extremes show mostly increasing trends, especially in parts of northern Italy and Sardinia, and part of central Italy, while 24-h extremes reveal both positive and negative trends depending on the region. For sub-hourly durations, the study of observed trends is much more limited due to the reduced availability of long records or good-quality weather radar data, even if it would be of great interest for impact study of precipitation-driven hazards such as debris flows and flash floods. Indeed, a few recent studies highlight a tendency for a much faster increasing trend at those short durations compared to hourly or higher durations (e.g. Ref. [79] nearby Sydney, Australia; [80] from climate projection in UK). Over Italy, just a few studies analyzed trends in sub-hourly rare extremes in the last 20-30 years, in the Eastern Alps [81] and in Sicily Island [76], both confirming a more significant increasing trend at sub-hourly durations with respect to hourly duration. All these findings highlight Italy's high climatic variability and the need for spatially resolved, duration-specific analyses when evaluating the impacts of (climate) change on precipitation extremes.

2.3. Climate change modelling

Recent advances in climate modeling have significantly enhanced projections of future precipitation, particularly in climate-sensitive regions like the Mediterranean, which has been recognized as a primary hotspot of climate change [82]. Global climate models (GCMs) have proven insufficient for the representation of intense precipitation at the regional and local scales, and downscaling methods have been developed to better resolve sub-grid processes [83,84]. Among these, dynamic downscaling with regional climate models (RCMs) has played a key role, and the possibility of accounting for interactions between the atmosphere and the ocean first led to the development of coupled regional systems for the Mediterranean basin [85] that are rapidly evolving into the development of Earth System Models. However, in the last decade the increasing availability of computational power has allowed the development of atmospheric convection-permitting models (CPMs), which operate at grid spacings below 4 km. These models explicitly resolve convective processes, eliminating the need for parameterization schemes, and offer improved simulation of hourly precipitation characteristics, including diurnal cycles, spatial patterns, intensity distributions, and extremes [86–88]. CPMs also allow for more accurate representation of land-surface heterogeneities, such as mountains, coastlines, and urban zones, and of land-atmosphere feedback that influence other climatic extremes like droughts and heatwaves. In the European context, within the CORDEX-FPS Convection project, Ban et al. [89] and Pichelli et al. [90] introduced the first 10-year CPM ensemble simulations at ∼3 km resolution over the greater Alpine region. Ban et al. [89] showed that CPMs driven by ERA-Interim reanalysis better reproduce observed daily and hourly precipitation extremes than coarser RCMs. Pichelli et al. [90] extended this by evaluating CPMs driven by CMIP5 GCMs under the RCP8.5 scenario, finding that these high-resolution models not only refine the spatial detail of projected changes but can even alter the sign of projected intensity and extreme trends compared to RCMs. Over Italy, in summer, Pichelli et al. [90] report a future intensification of heavy precipitation (here evaluated as high percentiles) across both hourly and daily timescales. Autumn projections reveal a north-south increase-decrease pattern in precipitation changes, although substantial inter-model variability limits certainty. Further analysis by Dallan et al. [91,92] assessed changes in extreme precipitation from sub-daily to daily durations, with return periods up to 100 years. Their results show a general intensification of precipitation extremes across all durations, with the strongest increases found at the shorter durations and for rarer events (that is, higher future intensification at 100 year than at 20 year return period) and in the mountainous regions, particularly the Eastern Alps and Northern Apennines. These results point to a shift in the statistical distribution of precipitation toward heavier tails. The relation of the changes with elevation is summarized in Fig. 3, showing the projected changes for the 20yr return level at sub-daily durations. At 1, 3, 6 h, it clearly emerges how the future increase is generally higher in both the more elevated areas and in lowlands, and how, in orographically complex terrains, it enhances with elevation.

This study suggests that the most intense events are becoming more dominant, especially in elevated areas potentially prone to ground instabilities, which may be critical information for hydro- and geomorphological risk management and climate adaptation.

A national-scale perspective over Italy is provided by the VHR-PRO_IT model [93], which is, since recently, the only convection-permitting projection that covers the entire country and spans a 90-year simulation window (1981–2070) under both RCP4.5 and RCP8.5 scenarios. Results indicate a consistent increase in average precipitation intensity under both scenarios, with stronger increases under RCP8.5. In contrast, the frequency of precipitation events decreases, especially in complex terrain such as the Alpine region. These changes, higher average intensities but less frequent events, align with the multi-model findings of Pichelli et al. [90]. Notably, increases in heavy precipitation intensity (characterized here as high percentile of hourly values) are expected in the Alps, Po Valley, and Eastern Mediterranean, while decreases are projected for southern and insular regions like Sicily and Sardinia. The spatial distribution of these changes remains similar between scenarios, but with lower magnitudes under RCP4.5. Lompi et al. [94] applied a non-stationary statistical frequency analysis to exploit the multi-decadal simulation and assessed the changes in extreme sub-daily precipitation characterized by high return periods. Their study confirms a general increase in extremes in a warmer climate, with larger areas of statistically significant change for shorter durations and higher return periods, but the heaviest increases for longer-duration extremes.

By the best of our knowledge, the aforementioned studies are the only studies based on CPM projections covering completely the Italian territory and refer to global scenarios produced in the CMIP5 context. Most recently, in the framework of the RETURN project, a regional downscaling of CMIP6 global climate projections has been performed, aiming to produce high-resolution (5 km) climate information for the assessment of climate change signals over the Italian regions. The experiments cover hindcast (i.e. ERA5-driven) and historical simulations (driven by the MPI-ESM1-2-HR model) to simulate the present (1980-2014) and future (2015-2100) climate under three different emission scenarios (SSP1-2.6, SSP2-4.5, SSP5-8.5) [95]. Although the resolution adopted does not allow to switch off the convective parameterization, the authors show that, with the model configuration adopted, most of the precipitation, either large scale or convective, is explicitly resolved. This suggests that the model mimics a convection permitting model. Doing so [95], were able to cover a domain that includes all the italian territory and to perform scenario simulations long enough to speculate on the impacts of extreme events under climate change conditions. The authors analyzed the seasonal projections of precipitation change at the end of the century across the three scenario experiments finding only in the scenario SSP1-2.6 a significant increase of the mean precipitation over most of the Italian peninsula in winter and spring. The other two scenarios project a decrease in mean precipitation for all seasons that intensifies with the scenario severity. The only exception to this signal in SSP2-4.5 and SSP5-8.5 is the projected increase of precipitation in the alpine regions during winter and fall. On the other hand, the analysis of change in extreme events highlights that at the end of the century, the SSP2-4.5 and SSP5-8.5 scenarios project higher probabilities for extreme events as well as events of unprecedented intensity with respect to the present climate simulations. Seasonal analysis of the difference between the values of the 99th percentile (P99) of daily rainfall during the period 2071–2100 and the corresponding values computed for the period 1985–2014 clearly shows that this intensification of extreme events is mostly concentrated in fall (SON) almost over all italian regions. It is worth noting that in Ref. [95] is also presented an intercomparison through different datasets (observations, reanalysis and the newly produced hindcast simulations) of the current spatial distribution of extreme precipitation events in Italy (P95, P97 and P99 values) which show that the most affected regions are Liguria and north of Tuscany, as well alpine regions and the Appennines in central and southern Italy and northern part of Sicily. For all these regions, an increase in the intensity and frequency of extreme events is expected, especially in the autumn season. With a view to analysing the spatial and temporal variability of landslide phenomena as

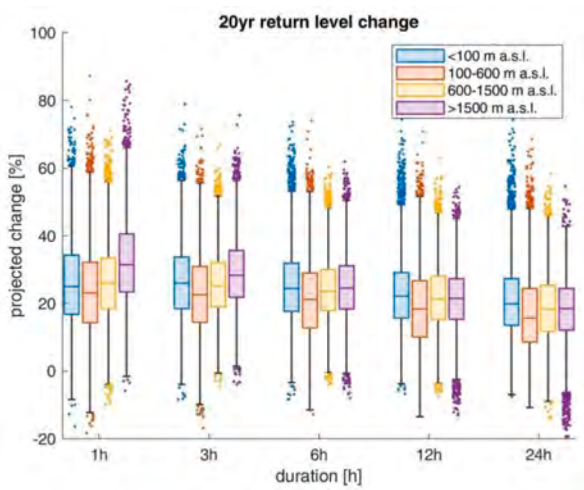

Fig. 3. Future relative changes for 20yr return level based on results by Dallan et al. [92] on Great Alpine Area and North Italy, using an ensemble of CPMs (scenario RCP8.5, end of century changes). Grid-points in the area are grouped in equally populated elevation ranges.

indicators of climate change impact, considering that precipitation is one of the main drivers of these phenomena, we can therefore conclude that, under the most severe scenario, the spatial variability of these phenomena is expected to be altered in a non-obvious way by the combination of a trend towards a reduction in average precipitation with a consequent increase in drought periods and an increase in extreme events.

Based on this review about extreme precipitation projections over Italy, it emerges that only a limited number of studies have used CPM ensembles to investigate rare-event statistics such as annual exceedance probabilities or long return periods [91,92,96], which are critical for engineering and hydrological planning and impact studies. Further developments are thus needed in the context of climate models, for increasing availability of multi-model long simulations at CPM resolution. Equally important is the validation of such high-resolution simulations against dense observational datasets, which remains a key challenge for ensuring their reliability in reproducing extremes at different sub-daily durations and supporting their operational use [97]. Many of these studies focus on fixed-time-window rainfall durations, and caution should be taken in transferring their findings in the context of landslide triggering. Recent studies emphasize that intensity–duration (ID) thresholds for landslide initiation and intensity–duration–frequency (IDF) curves for rainfall probability represent fundamentally different concepts and conflating them can lead to significant misinterpretations of landslide-triggering probabilities [98].

3. Rainfall: preparatory vs. triggering factors

3.1. *Rainfall as preparatory factor in rapid landslides*

Numerous studies analyzed how climate change in terms of variations in precipitation and temperature affect hydrological regimes and, consequently, the intensity of shallow landslide phenomena [51,99–107]. In this regard, rainfall is widely recognized as a primary triggering factor for shallow and rapid landslides. However, the rainfall preparatory role has historically received less attention, and the effects of climate change remain controversial and are not easily generalizable.

3.1.1. *Empirical thresholds and antecedent rainfall indicators*

Traditionally, shallow and rapid landslides have been considered influenced mainly by intense rainfall which is considered to play a crucial role as a triggering factor [108,109]. The preparatory role of rainfall was considered of secondary importance or even negligible, depending on the hydrological characteristics of the material involved (the coarser and permeable the material, the less relevant the role of antecedent rainfall in preparing the ground instability). This was clearly reflected in empirical approaches, in which the triggering process is modeled through statistical correlations between a few key parameters, completely neglecting any preparatory role [110,111].

However, a relevant number of works have been published where triggering thresholds were defined using rainfall indicators based on antecedent rainfall [109,111]. Besides the technical advantage that antecedent rainfall indexes do not require rainfall measurements acquired at high temporal resolution [112,113], many studies observed that antecedent rainfall better captures the preparatory role of precipitation, in addition (or in alternative, depending on the models) to the triggering role. Indeed, antecedent rainfall has been taken into account in a wide variety of ways: Tien Bui et al. [114] combined daily rainfall (considered as triggering process) and 15-day antecedent rainfall (as a preparatory role), Saadatkhah et al. (2015) [115] considered 3- and 30-day antecedent rainfall, Lee et al. [116] used daily and 3-day cumulated rainfall. Moreover, some authors do not use directly the rainfall measures, but process them to calculate weighted antecedent rainfall indexes, trying to better account for the preparatory role of antecedent rainfall in influencing the degree of saturation of the terrain [117–122]. Martelloni et al. [123] introduced the use of the standard deviation from the mean rainfall amount accumulated during progressively increasing time steps (up to the whole duration of the wet season). Greco et al. [124] used a mobility function defined as the convolution integral of rainfall intensity with an empirical transfer function.

However, in the same research topic (empirical rainfall thresholds) recent advances proposed a more complete integration of preparatory and triggering rainfall indicators. Rosi et al.[125] and Nocentini et al. [126] merged the classical I-D (intensity-duration) approach with a third rainfall parameter based on the average antecedent rainfall. While the first couple of parameters accounts for the triggering effect of the peak rainfall intensity, the third parameter accounts for the preparatory role played by antecedent rainfall, identifying a third dimension of the threshold (which is thus constituted by a plane in 3D rather than a line in 2D). Accounting for the preparatory role of antecedent rainfall by means of the third parameter allows identifying uninfluential rainstorms and filters off many false alarms usually committed by traditional I-D approaches.

Moving forward on the same conceptual line, another series of approaches tried to directly include soil moisture ([127–129]), soil saturation [130] or soil volumetric water content [131,132] in the models, thus defining hydro-meteorological thresholds, where the preparatory role of rainfall is directly accounted by indicators quantifying its hydrological effects in the soil.

3.1.2. *Data-driven and machine learning approaches*

Building on the increasing effectiveness of available technology and on the hybridization of different approaches, a recent trend in empirical landslide forecasting is the use of machine learning to handle a more complete set of input parameters, including a wide range of rainfall indexes to be used simultaneously (overcoming the traditional limitation of selecting only two or three of them). This approach allows testing and including in the modelling several indicators to account for the preparatory role of rainfall. For instance, Ng et al. [133] apply several machine learning models only for a rainstorm-based landslide inventory with related short and antecedent rainfall. Similarly, Liu et al. [134] uses a landslide inventory related to the same rainstorm triggering event for the application of various machine learning models. Stanley et al. [135] added snow water equivalent and soil moisture content data as dynamic input parameters for an eXtreme Gradient Boosting model, representing the non-occurrence of landslide cells by selecting them across space and time. Distefano et al. [136] used Artificial Neural Networks to automatically identify the intensity-duration rainfall thresholds with higher predictive power. Nocentini et al. [126,137,138], working in two very different test sites (in Italy and in Norway) included rainfall amounts recorded over durations from 1 day to 30 days, discovering that this approach allows accounting for the preparatory effect of antecedent rainfall. In addition, and surprisingly, they discovered that a simple categorical variable consisting in the month of the year had a good predictive capability if used together with the others. Although the spatio-temporal prediction of landslides combining static and dynamic parameters in machine learning algorithms is still in a preliminary phase [136,139,140], the cited series of studies clearly shows that even for shallow rapid landslides the preparatory role of rainfall can be relevant, and can be better considered with complex data-driven models.

Also in landslide susceptibility studies, which traditionally are based on the study of predisposing factors, indicators based on rainfall have been recently included in a growing number of works [141,142]. This recent advance aims at implicitly or explicitly accounting for the preparatory role of rainfall, which has been considered to characterize the general climate or peculiar micro-climates of the studied area. Traditionally, the preparatory role of rainfall has never been explicitly accounted for in susceptibility studies. At best, it can be considered somehow implicitly included in some hydrological indexes which quantify the propensity of each spatial unit to retain water into soil. Among these indexes, the most used are the Topographic Wetness Index, the upslope drained area, and planform curvature (indicating convergence or divergence of surface and subsurface flow) [34,143]. It is worth noting that in most of the works where the shallow landslide susceptibility assessment is completed by a quantitative evaluation of the importance of each input parameter, the aforementioned hydrological factors are ranked among the most important ones. This outcome clearly indicates that terrain features, combined with rainfall, play a key role in preparing shallow landslides. Some studies, instead, use the mean annual precipitation to characterize the climate of the study area [144]. Spatial variations in this index highlight micro-climatic differences that may be correlated with the preparatory effect of new rainfall. However, in the framework of the ongoing global warming and changing precipitation trends, several authors identified a shift in landslide activities, thus highlighting the necessity of considering rainfall anomalies rather than rainfall regimes characterized with data pertaining to decades ago.

For this reason, more recently, an increasing number of researchers are using compound rainfall indicators to characterize rainfall anomalies rather than rainfall amounts *sensu strictu*. For instance, Catani et al. [145] used the return period of rainfall at varying duration and intensity, using in particular combinations of short durations and high intensities to account for the effect on shallow rapid movements and combinations of long durations and low intensities for deep seated landslides; they also found that these factors held a high predictive power. Marc et al. [146] used the 10-years return time rainfall anomaly to characterize the spatial pattern of storm-induced landslides. More recently, Caleca et al. [147] used a rainfall anomaly index (defined as the ratio between the event rainfall and the mean annual precipitation) demonstrating that spatial variations of this index have a strong influence on landslide susceptibility.

3.1.3. *Physically-based methods: soil moisture monitoring*

There is a close relationship between soil moisture and intense rainfall [108,109,148]. For instance, while an increase in average temperatures and a decrease in precipitation could lead to a reduction in the average volumetric water content (VWC), an increase in rainfall intensity could result in a higher frequency of sudden VWC increases. Notably, the effects of extreme temperatures and reduced precipitation on the ground can also lead to opposing outcomes. Prolonged drought periods may result in the formation of a

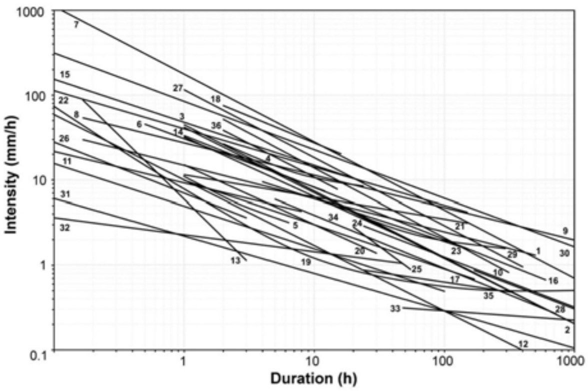

Fig. 4. Empirical Rainfall intensity-duration (I-D) thresholds for the initiation of landslides at global, regional and local scale. threshold. 1, Caine [108]; 2, Moser and Hohensinn [166]; 3, Cancelli and Nova [167]; 4, Cannon and Ellen [168]; 5, Wieczorek [169]; 6, Jibson [170]; 7, Guadagno [171]; 8, Rodolfo and Arguden [172]; 9, Ceriani et al. [173]; 10, Larsen and Simon [174]; 11, Arboleda and Martinez [175]; 12, Clarizia et al. [176]; 13, Tungol and Regalado (1996) [177]; 14, Zimmermann et al. [178]; 15, Paronuzzi et al. [179]; 16, Calcaterra et al. [159]; 17, Montgomery et al. [180]; 18, Wieczorek et al. [181]; 19, Crosta and Frattini [182]; 20, Marchi et al. [183]; 21, Ahmad [184]; 22, Jakob and Weatherly [185]; 23, Aleotti [186]; 24, Floris et al. [187]; 25, Baum et al. [188]; 26, Cannon and Gartner [189]; 27, Chien-Yuan et al. [190]; 28, Corominas et al. [191,192]; 29, Hong et al. [193]; 30, Zezere et al. (2005); 31-33, Guzzetti et al. [109]; 34, Dahal and Hasegawa [194]; 35, Kanungo and Sharma [195]; 36, Zhou and Tang [196]. Modified after Guzzetti et al. [109].

low-permeability surface crust, which increases runoff and reduces effective infiltration, making it harder to reach critical soil moisture levels. Conversely, drought events may also cause soil fractures, which can enhance effective infiltration.

A rapid, shallow landslide typically occurs when a thin, granular, partially saturated layer resting on steep bedrock increases its degree of saturation due to changes in moisture content caused by the vertical infiltration of water following rainfall events or snowmelt. As soil moisture increases, the suction decreases, leading to a reduction in cohesion and shear strength. When the soil becomes saturated, a temporary water table within the debris cover is generated, supported by the less permeable underlying layer, increasing pore pressures, weakening the soil structure and destabilizing the slope. Critical soil moisture can be reached through either intense or prolonged rainfall, depending on the antecedent rainfall, infiltration rate and soil's pre-existing moisture condition [105]. If the shear forces exceed the shear strength, [149], a failure plane forms within the soil layer or on the bedrock-soil interface, causing it to slide downslope.

The importance of hillslope hydrology in rainfall-induced landslides has gained attention, leading to the replacement of antecedent rainfall with average soil saturation measured over the same period. Ponziani et al. [150] identified a linear relationship between rainfall thresholds and initial soil moisture conditions, with correlation coefficients reaching up to 0.60. Their study proposed a procedure for landslide warning by integrating rainfall thresholds with soil moisture estimates derived from a calibrated and locally tested soil water balance model. Mirus et al. [130] demonstrated the advantages of incorporating soil saturation data into landslide prediction models. For the Seattle area in Washington, USA, they found that replacing 15-day antecedent rainfall data with average soil saturation significantly improved the accuracy of established rainfall-only thresholds, which also used 3-day recent rainfall data. Similarly, Marino et al. [127] emphasized the potential of incorporating soil moisture information into hydro-meteorological thresholds, noting that such data is increasingly accessible through remote sensing and sensor networks. In fact, soil moisture can be measured locally using various on-site techniques or remotely through satellites and airborne systems. Alternatively, hydrological models, such as those discussed by Abraham et al. [113], are being employed to predict moisture content over larger areas. These measurements, whether direct or modeled, can complement empirical and statistical landslide-triggering thresholds, which are often formulated in terms of rainfall intensity and duration [151,152].

Soil moisture data is increasingly available through a variety of monitoring systems, ranging from ground-based monitoring to remote sensing technologies [153–156]. In-situ monitoring involves installing sensors directly in the ground to measure Volumetric Water Content (VWC) or matric suction at various depths. Although such systems are expensive and have limited spatial coverage, they provide continuous, real-time data that is invaluable for understanding localized moisture dynamics. Remote sensing technologies, such as satellite-based systems (e.g., SMAP, Sentinel-1), offer broader spatial coverage and can estimate surface soil moisture over large areas. These systems use microwave radiometry and radar to detect soil moisture at shallow depths, typically up to 5 cm.

Remote sensing provides valuable regional data, but challenges with data resolution and accuracy at deeper soil layers persist. Ground-based monitoring offers greater precision and is often used to calibrate remote sensing data. Integrated monitoring networks that combine both approaches, along with hydrological models, can offer more comprehensive soil moisture spatial data [157,158] useful to improve landslide early warning systems as well as long-term hazard scenarios.

3.2. *Rainfall as triggering factor in rapid landslides*

Rainfall is widely recognized as the most common cause of landslides. High-intensity short duration rainfall mainly triggers shallow soil slips and flow-like landslides. Shallow landslides are often initiated during intense rainfall events due to a rapid increase in pore pressure or the loss of apparent cohesion caused by partial saturation. Factors influencing the occurrence and distribution of shallow landslides can be broadly divided into two categories: almost-static variables and dynamic variables. Almost-static variables include soil properties, seepage in the bedrock, and topographic features, which define the inherent predisposition of slopes to failure and

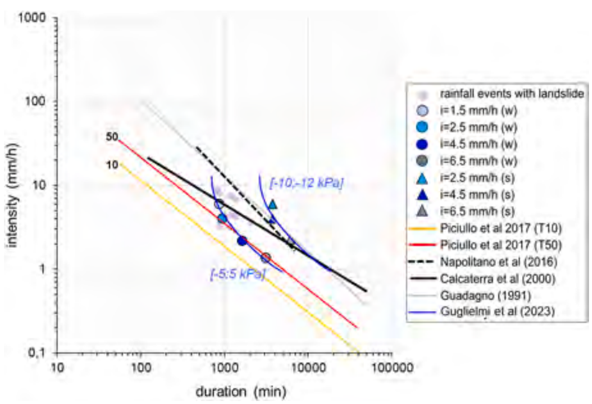

Fig. 5. Symbols colored according to rainfall intensity, represent points obtained from numerical analyses, where circles and triangles correspond to winter-like (w) and spring-like (s) initial hydrological conditions, respectively. Purple symbols indicate past flow-like landslide events that occurred in the Lattari Mountains. These results are compared with regional rainfall thresholds reported in the literature, developed using both empirical and physically-based approaches [159,171,198,228] (Adapted from Ref. [231]).

determine the spatial distribution of landslide susceptibility. In contrast, dynamic or transitory variables, such as the degree of soil saturation and cohesion influenced by root systems or partial saturation, primarily control the initiation of landslides on predisposed slopes. Both predisposing and preparatory factors have already been discussed in the previous sections; here, the role of the triggering factor is addressed. Approaches to comprehend rainfall-triggered landslides can be categorized as empirical (historical, statistical) and physically-based (simplified or advanced) [111].

3.2.1. Empirical methods

The empirical relationship between rainfall intensity, rainfall duration and slope instability has been extensively documented. Empirical rainfall thresholds are defined by studying rainfall events that have triggered landslides [159]. Rainfall intensity refers to the amount or rate of precipitation over a specific period, typically measured in millimeters (or inches) per hour. These thresholds are often established by plotting the rainfall conditions leading to landslides on Cartesian, semilogarithmic, or logarithmic scales and drawing lower-bound lines. Depending on the area investigated, empirical thresholds for the initiation of landslides can be loosely defined as global [108], national [42,160–162] or regional [163–165]. A global threshold attempts to establish a general ("universal'') minimum level below which landslides do not occur, independently of local morphological, lithological and land-use conditions and of local or regional rainfall pattern and history. For example, based on 73 events across diverse geological and climatic settings, Caine [108] first proposed a global threshold applicable for time periods ranging from 10 min to 10 days. Subsequently, many Authors developed empirical thresholds working at different scales and based on combinations of precipitation measurements obtained from individual or multiple rainfall events that resulted (or did not result) in landslides (i) intensity-duration (I-D) thresholds, (ii) thresholds based on the total event rainfall, (iii) rainfall event-duration (E-D) thresholds, and (iv) rainfall event-intensity (E-I) thresholds. Among these, the most common type are the intensity-duration thresholds (Fig. 4).

Statistical methods have also been used to define empirical rainfall thresholds at national [197] and regional levels [123,198]. For example, Brunetti et al. [199] proposed new national thresholds for Italy and regional thresholds for the Abruzzo Region by employing two independent statistical approaches: a Bayesian inference method and a Frequentist approach. Martelloni et al. [123] defined statistical rainfall thresholds using a single parameter (cumulative rainfall anomalies expressed in terms of standard deviation from historical average values) for the Emilia Romagna region of Italy. Gariano et al. [200] analyzed a catalog of 200 rainfall events linked to 223 shallow landslides in Sicily, southern Italy, over an 11-year period (2002–2011). They determined regional event duration–cumulative rainfall (E-D) thresholds for shallow landslide occurrence, calculated thresholds for different exceedance probability levels, and assessed uncertainty using a bootstrap nonparametric technique. Their study also examined the influence of lithology and seasonal patterns on shallow landslide initiation in Sicily.

3.2.2. Physically-based methods

Physically-based methods for analyzing shallow landslides often combine hydrological models with infinite slope stability analysis. These approaches typically use two modules: one to predict pore water pressure changes due to rainfall (e.g., TOPMODEL - [201]; TOPOG - [202,203]) and another to evaluate slope stability (e.g., Level I Stability Analysis LISA – [204]), either coupled or uncoupled. The first simplified models combined the slope stability analysis, generally considering an infinite slope model approach, with a steady-state shallow subsurface flow model (SINMAP – [205]; SHALSTAB - [206]), a shallow groundwater flow model (dSLAM – [207]), or a transient infiltration model (Transient Rainfall Infiltration and Grid-Based Regional Slope-Stability TRIGRS - [39,208]; HIgh REsolution Slope Stability Simulator HIRESS – [209]). These last models are commonly based on the analytical solution of Richards' equation [210], first implemented by Iverson [211]. Subsequently, models that solve the 3D Richards' equation in both saturated and unsaturated conditions, combined with the slope stability analysis (GEOtop-FS - [212]; InHM - [213]) were developed in order to model the transient infiltration processes catchments characterized by complex topographic conditions (e.g. Ref. [214]), when stratigraphy of soils is known (e.g. Ref. [215]) or/and for well-defined bedrock positions (e.g. Ref. [216,217]).

Also, Capparelli and Versace [218] introduced a physics-based approach for predicting critical rainfall by developing the Saturated Unsaturated Simulation for Hillslope Instability (SUSHI) code. Following these foundational studies, global efforts have refined physics-based rainfall thresholds at regional [219–221] and basin scales [222–225]. Most of these applications employ the infinite slope model and the Limit Equilibrium Method (LEM) to calculate the safety factor [226]. Site-specific analyses have also provided valuable insights. For instance, De Vita et al. [227] evaluated the influence of seasonal variations on hydrological thresholds by studying ash-fall pyroclastic deposits covering the slopes surrounding the Somma-Vesuvius volcano. This study underscored the critical role of antecedent hydrological conditions in defining rainfall thresholds for slope instability. Additional site-specific applications, such as those by Napolitano et al. [228] and Fusco et al. [229], focused on areas prone to flow-like landslides in Southern Italy.

Recently, a new open-source and physics-based model for Spatial Prediction of Rainfall-Induced Shallow Landslides (SPRIn-SL; [230]) which implements the infinite slope method by incorporating the TOPOG and the Green-Ampt models to consider groundwater flow and transient rainfall infiltration, respectively, was developed and tested in a small coastal catchment of Cinque Terre (Liguria, Italy). At the slope scale, more complex physics-based models have emerged integrating vegetation dynamics into hydrological models by accounting for transpiration (e.g., Ref. [231,232]). These coupled hydro-thermal models have been validated using extensive geotechnical data and comprehensive on-site monitoring.

As an example of physically-based rainfall thresholds, Fig. 5 shows the critical Intensity–Duration (I–D) curves obtained through coupled thermo-hydraulic numerical modeling of an unsaturated pyroclastic slope monitored at Mount Faito, within the Lattari Mountains, Italy [231]. Specifically, different threshold curves were derived as a function of the initial matric suction within the slope prior to the triggering rainfall event. Most rainfall events recorded in this geological context are located above the threshold curve corresponding to an initial suction of approximately 5 kPa, suggesting that this value may depict a representative preparatory condition for triggering. These physically-based thresholds are also compared with regional rainfall thresholds available in literature.

A recent offline early warning procedure that combines multi-factor rainfall thresholds with on-site suction monitoring before rainfall events was proposed by Pirone et al. [233]. The authors developed site-specific multi-factor rainfall thresholds, integrating mean rainfall intensity, rainfall duration, and antecedent suction. This approach employs a physics-based model calibrated with hourly on-site measurements of suction and water content, subsequently validated against historical landslide occurrences. However, the practical application of such deterministic models, especially in terms of early-warning systems, is still limited to specific studies, due to the time effort and data demand [47]. In fact, the main limitations of physics-based thresholds are related to the most important disadvantages of the deterministic methods: (i) requiring a significant amount of geotechnical, mechanical, and hydrological parameters for model simulation; and (ii) reconstructing the boundary conditions which represent, in the best way, the real soil and slope behaviors [234].

3.3. *The role of rainfall in slow landslides: preparatory or triggering?*

Slow-moving landslide movements are generally linked to intense and prolonged precipitation [235–237]. Water content is undoubtedly the most influential factor in slope movements [238]. These slow-moving failures can accelerate within days to months following the beginning of the rainfall event and decelerate during dry periods eventually halting. The imbalance between driving forces and shear strength of slope materials, caused by extreme rainfall, triggers movements. This occurs because an increase in pore water pressure leads to a reduction in effective stress and, consequently, in the soil shear strength'[239–241]. According to Berntson & Saèllfors [242], Kenney & Lau [243] and Vaughan [244], seasonal fluctuations in the water table level can cause variations in pore pressure at depths ranging from 5 to 10 m. In the case of slow landslides, processes such as infiltration, deep ground-water circulation patterns, and the resulting increase in hydrostatic levels and/or pore-water pressures - accumulating over long periods before activation - must be considered [245,246 247–252]. Failure conditions arise from a unique combination of all these factors, and the state of the slope system cannot be predicted based on rainfall alone [253]. Following Guzzetti et al. [109], Vallet et al. [254] suggested that it is more appropriate to use “a local threshold that implicitly takes into account the landslide characteristics.”

However, distinguishing between the preparatory and triggering roles of precipitation is often challenging. Typically, the minimum response time of a landslide to rainfall is proportional to the square of its depth (often approximating the saturated thickness) and inversely proportional to hydraulic diffusivity [255]. Deeper landslides generally show more complex behavior and require more time to achieve equilibrium conditions [256]. Several studies have been conducted to understand this response and define the complex relationship between rainfall and landslide kinematics. Vallet et al. [254] stated that, although the destabilization of deep-seated landslides is mainly controlled by a rainfall trigger (short-term component), site-specific time-dependent factors (long-term components), such as creep deformation or modifications in slope groundwater hydraulic connectivity, can also be significant.

Consequently, no general threshold has been proposed in the literature. Rather, three main types of studies can be recognized: the first group aims to define a local window of days or cumulative rainfall to determine a site-specific precipitation threshold, the second group focuses on understanding the role of local groundwater recharge and the third one proposes physically-based models to investigate the hydrological impact on slope stability.

3.3.1. *Cumulative rainfall threshold analysis*

Van Asch et al. [257] argued that a single day of rainfall does not significantly influence deep-seated landslides, while Bonnard and Noverraz [258] and Trigo et al. [259] stated that such movements are usually driven by multiple moderate-intensity storms occurring over weeks or months. Doglioni et al. [260] analyzed precipitation trends related to the reactivation of the Maierato landslide

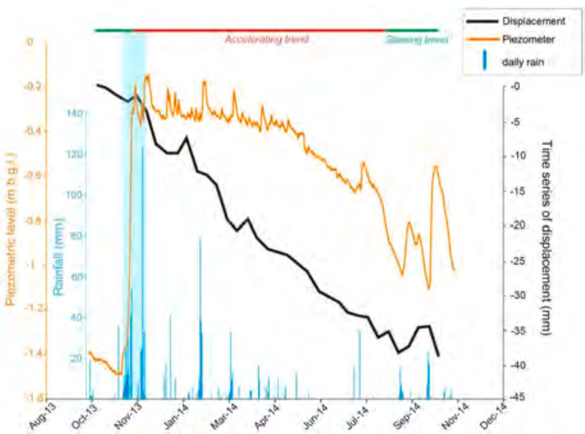

Fig. 6. Comparison between piezometric level and rainfall data of Papanice slow landslide with time series obtained with the CPT-TSC algorithm. The blue shaded column is for the rainy period between November 11, 2013, and December 4, 2013, corresponding to a rapid rise of piezometric level (modified from Ref. [266]).

(Calabria, Italy). By examining cumulative rainfall heights over 5, 10, 15, 20, 30, 45, and 60 days preceding the landslide, the authors identified a peculiar rainfall sequence: a prolonged period of continuous but not intense rainfall, leading to exceptionally high return periods for cumulative rainfall, with a maximum of 105 years. Martelloni et al. [123] suggested that the hydrodynamic response of landslide aquifers is influenced more by antecedent rainfall (multiple rainfall events over a long period) than by a single rainfall event. For this reason, a single and simple rainfall trend alone does not fully explain the behavior of these phenomena [251,261].

Azanon et al. [262] demonstrated that, for the investigated landslides (i.e. Riogordo and Diezma landslides, southeast Spain), the trigger was intense rainfall episodes that occurred after two years with annual rainfall higher than average values. However, if in the case of the Riogordo landslide the relationship between intense rainfall and slope failure is clearly established, in the case of the Diezma landslide, it occurred 20 days after an intense rainfall peak, probably as an effect of the hydrogeologic behavior of the Diezma area. Fiolleau et al. [263] linked a landslide reactivation in the San Francisco Bay Area with an episode of heavy rainfall (about 220 mm in 30 h) following a 7-month drought through the analysis of variations in water table level, soil temperature, soil displacement, seismic wave velocity and the associated correlation coefficient measured in the autumn and in the summer seasons. Jiang et al. [264], using displacement time-series obtained by synthetic aperture radar interferometry (InSAR) technique, observed that the Wadi Landslide (Mao Country, Sichuan Province, China) exhibited a periodic displacement with slight acceleration in 2017 and 2019, because both these years had relatively large rainfall with cumulative annual rainfall exceeding 1200 mm.

3.3.2. Groundwater recharge analysis

Fluctuations in saturation levels within landslide materials, especially loose soils and weathered geological formations, intensify the stress applied to slope materials. These processes contribute to the driving force acting on the slope to exceed the shear strength of the material and, consequently, trigger landslides [265]. A clear correlation between piezometric level and acceleration and deceleration of the Papanice landslide (southern Italy) was found by Confuorto et al. [266], which compare the piezometric level and the rainfall data with the displacement time series derived with the Coherent Pixel Technique-Temporal Sublook Coherence (CPT-TSC) algorithm in the rainy period between November 11, 2013, and December 4, 2013 (Fig. 6).

An attempt to develop a critical piezometric threshold was also carried out by Lissak et al. [267] using long-term continuous single-point time series and shorter, but more spatially distributed, piezometric information. The Authors defined two piezometric thresholds for the landslides that occurred along the Normandy coast (France): the first one based on field surveys (short-term/high resolution) for moderate landslides at 3.50 m depth and a second threshold based on historical data (long-term/low resolution) at −10.35 m depth for the major landslides. Other Authors (i.e. [192,268,269]) also focused on the correlation between groundwater fluctuation connected to rainfall infiltration and recurrent acceleration of landslides. Debevec Jordanova et al. [270] combined and compared interferometric results to the displacements measured by inclinometer to evaluate the rate of displacement of Šumljak landslide and a viaduct, and with a focus on the groundwater level fluctuation in relation to daily rainfall to evaluate its influence on the displacements.

Pepe et al. [271] analyzed the efficiency of the automatic deep-drainage system of the Mendatica landslide (Liguria, Italy) during an extreme rainfall event lasting five days, with a cumulative rainfall of 800.4 mm. The results showed that, despite the Mendatica landslide being affected by the most severe multi-day (5–6 days) rainfall event recorded in the past 75 years [272], the drainage system successfully depressed the local aquifer, preventing the landslide from reactivating. With the aim of developing a regional-scale warning system for landslides, Martelloni et al. [123] developed a prototype algorithm based on the comparison between rainfall recordings and statistically defined thresholds, determined using a single parameter (cumulative rainfall). Based on the landslide inventory of the Emilia-Romagna region, Italy, the authors proposed a variable time-interval cumulative rainfall (up to 240 days) as a threshold for the activation of deep-seated landslides in low-permeability terrains. To identify an alert model based on cumulative rainfall for the Petacciato landslide (Molise, Italy), Doglioni et al. [273] proposed an approach based on the evolutionary polynomial

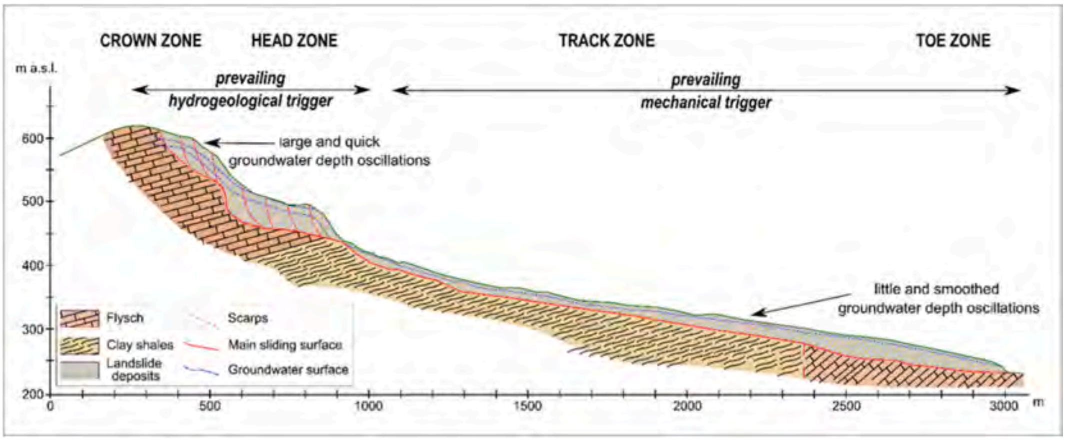

Fig. 7. General cross section of the landslides studied by Ronchetti et al. [251]. The section highlights the hydrological features and triggering mechanisms of the different sectors of the landslides. Modified from Ronchetti et al. [251].

regression technique, which enabled the prediction of landslide reactivation using only cumulative rainfall. The authors obtained promising results by applying two equations: the first one considers long-term cumulative rainfall lagged up to 120 days before the reactivation event, while the second one involves cumulative rainfall up to 90 days, lagged by a maximum of 30 days before the event. Banfi and De Michele [274] attempted to define a correlation between the spatial and temporal characteristics of precipitation clustering over the Italian territory and landslide occurrence (considering different types of phenomena) and, finally, related it to the North Atlantic Oscillation (NAO) and the Mediterranean Oscillation Index (MOI). Using specific statistical thresholds (e.g., excluding exceedances in the 90th percentile series or considering a threshold equal to the 0.7 quantile of daily precipitation, including only wet days), the authors verified the presence of temporal clustering within variable time windows of 15, 30, and 90 days preceding each landslide. They observed that, for all types of landslides except rockfalls, the majority of events were preceded by a temporal clustering of precipitation. This clustering was longer for deep-seated landslides and shorter for debris flows. For the reactivation of the Montaldo di Cosola landslide, Lollino et al. [275] identified a time lag of approximately nine days between the occurrence of a rainfall peak (135.4 mm on November 26, 2002) and the corresponding peak in recorded movements (1.2 mm/day). This specific precipitation value and landslide activation time lag were determined by analyzing two years of precipitation data (May 2002–May 2004) and using the AIS (Automatic Inclinometric System) to quantitatively assess the local relationship between rainfall peaks and slope movement peaks. As the researchers suggested, "the time lag found has to be considered as a 'warning time' for this particular landslide. It means that after a significant rainfall event, particularly in autumn, a peak in landslide movements can be expected around 8–9 days later". Lollino et al. [276] examined the 52-h pluviometric trend preceding the reactivation of the Montescaglioso landslide (Basilicata, Italy) and its impact on the safety factor. The authors noted that "the FS continues to decrease even after the accumulated rainfall reaches a plateau" attributing this to the rapid increase in pore water pressure following the infiltration of an exceptionally large amount of rainfall as the main factor in the reactivation. Ronchetti et al. [251] analyzed the behaviour of four large and deep mass movements involving flysch rock masses and clayey complexes: the Valoria landslide, the Lezza Nuova landslide, the Tolara landslide, and the Ca' Lita landslide, in the Emilia-Romagna region (Fig. 7).

This research reported Groundwater Depth (GWD) monitoring over approximately two years using piezometers equipped with electric transducers. Based on the results of this monitoring, the authors proposed a different response of landslide sectors (crown, head, track, and toe) to rainfall events. In particular, they observed a variable delay ranging from 4 to 15 days between individual rainfall events and GWD variations in the crown area, where flysch rocks remain intact and exhibit limited hydraulic conductivity (ranging from 10^{-5} to 10^{-8} m/s). In the head zone of the landslides, where hydraulic conductivity increases due to the presence of disarranged rock masses and fractures, the delay between rainfall and GWD variation is reduced to 1–8 days, with an almost instantaneous response to single rainfall events during the wet season. For the track and toe zones, which typically contain a chaotic mixture of silt, clay, and blocks, the authors observed a decrease in hydraulic conductivity (around 10^{-8} m/s) but with a very short delay (i.e., hours) and an extremely limited GWD variation (less than 1 m). According to the obtained results, the authors proposed a different triggering mechanism for the crown/head zone, where hydrogeological factors prevail, and for the track/toe zone, where reactivation is primarily driven by mechanical causes. Vallet et al. [254] proposed an approach for determining a statistical rainfall threshold for deep-seated landslides. In particular, the authors combined the Support Vector Machine (SVM) multidimensional rainfall threshold with a semiautomatic event detection method to define an objective and optimal threshold. Their study focused on the Séchilienne landslide (southeast of Grenoble, France), which is monitored by numerous displacement stations using a wide range of techniques, including extensometers, radar, infrared geodesy, inclinometers, and GPS. Displacement and weather data are recorded daily. For training and testing their methods, the authors analyzed both low and high destabilization events, as well as rainfall trends and the recharge of the landslide's perched aquifer. Based on their results, they concluded that using recharge rather than precipitation significantly improved the delineation of a rainfall threshold distinguishing stable from unstable events.

3.3.3. Physically-based models

In the realm of physics-based models, recent scientific literature emphasizes the impact of slope-vegetation-atmosphere interactions on landslide activity, with evidence suggesting these effects may extend to significant depths in natural clay slopes. The

Fig. 8. Evolution of a slope affected first by wildfire and subsequently by rainfall, leading to instability. (a) Pre-fire condition: slope covered by soil and vegetation. (b) Wildfire event with varying burn severity, causing alterations in soil and vegetation. (c) Post-fire rainfall triggering a shallow landslide, with consequent damage to the built environment.

Southern Apennines (Italy), characterized by slopes composed of fissured clays, provide numerous examples of weather-induced deep landslide mechanisms. The interplay between landslide activity and hydro-mechanical processes arising from soil-vegetation-atmosphere interaction has been explored through both uncoupled and coupled two-dimensional hydro-mechanical finite element analyses [277–279]. Pedone et al. [277] demonstrated that net rainfall accumulated over 2 and 6 months serves as effective climatic

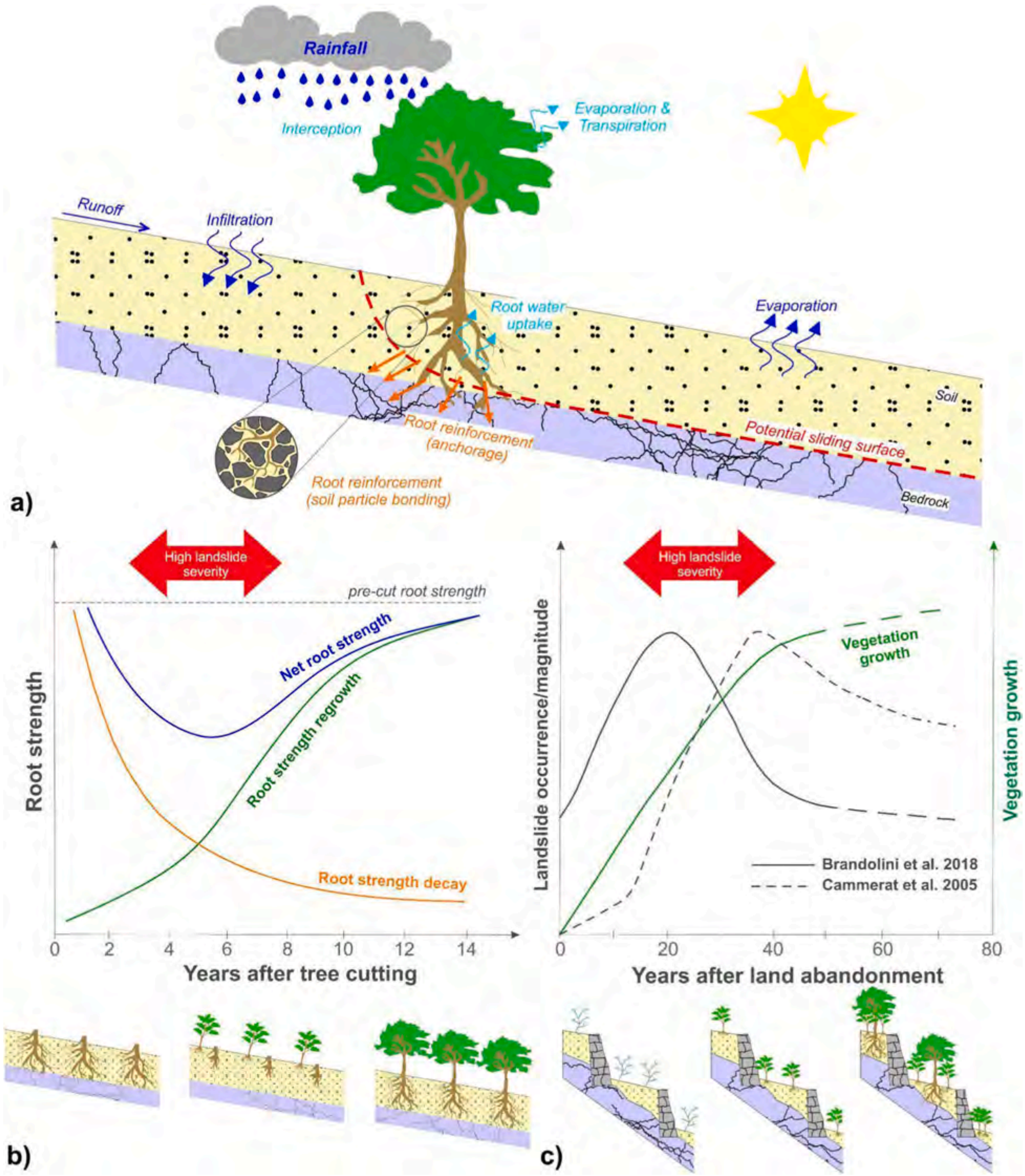

Fig. 9. (a) Illustration of the principal mechanical and hydrological mechanisms provided by vegetation on a slope. (b) Temporal variation of root strength in forested hillslopes after tree logging (redrawn and adapted from Ref. [313]). (c) Relationships between land abandonment, landslide occurrence/magnitude, and vegetation growth in terraced slopes.

threshold variables for landslide bodies at 5 m and 20 m depths, respectively.

However, despite advances in the monitoring and analysis of active slope movements in clay, the pore pressure regime and its relationship with slope movements remain highly complex to understand due to the interaction of numerous phenomena [280–282]. The effects of slope movements further complicate the reliable assessment of the pore pressure regime. Specifically, the low permeability of soil and the non-uniform state of strain and stress induced by movement often lead to the development of excess pore pressures which add to the effects induced by the infiltration of rainwater. Comegna et al. [282], through coupled hydro-mechanical numerical analyses, demonstrated that any redistribution of internal stress associated with the local mobilization of a mudslide body can induce excess pore pressures and subsequent deformation of the landslide. The interplay of movements and associated deformation phenomena results in a continuous alteration of soil properties, thereby affecting the hydrological and mechanical response of the slope. Comegna et al. [283] highlighted the critical role of the shear zone in influencing the groundwater regime, based on data collected during prolonged investigations of slow-active earthflows in the Basento Valley, Southern Italy.

In some cases, even minor slope deformations can significantly alter the pore water pressure regime due to the opening of cracks, closure of fissures, or damming of permeable layers [284]. This issue is particularly relevant for stiff clays, argillaceous rocks, or clayey flysch deposits, which exhibit sharp spatial variations in hydraulic conductivity due to networks of discontinuities and changes in material properties over short distances. These characteristics make modeling the groundwater regime—and particularly the effects of rainfall—a challenging task [285]. Technical literature has increasingly focused on this subject, emphasizing the role of fissures, cracks, and discontinuities [286–288].

In light of this evidence, it is still challenging to accurately characterize the hydraulic and mechanical properties of the landslide body to understand the relationship between hydraulic regime and slope movements.

4. Combination of other hazards with rainfall

The relationship between rainfall intensity, duration, and slope instability has been extensively studied in scientific literature since the late 20th century. However, factors influencing slope stability often evolve, moving rainfall-landslide relationships dynamic and subject to change. Such changes may result from external influences like earthquakes, fires, human activity, climatic oscillations, or even landslide activity itself.

4.1. Wildfire occurrence

Wildfires represent increasingly widespread phenomena that significantly alter the hydro-mechanical properties of soils, creating conditions that enhance susceptibility to natural instabilities such as shallow landslides and debris flows [289–292]. Climate change, modifications in land management and usage, and the accumulation of combustible materials contribute to the increasing frequency and severity of wildfires [293]. The thermal impact of fires causes chemical, physical, and biological changes in soils, with root systems among the most affected components. Vegetation, through its root system, provides cohesion to soils, thus stabilizing slopes. However, wildfires degrade roots to varying extents, depending on factors such as the depth of heat penetration and the temperatures reached ([294] and references therein). The complex interplay between wildfire-induced soil modifications and subsequent hydrological responses significantly amplifies the risk of natural instabilities, making post-fire landscapes highly susceptible to meteorological events over an extended time window [295,296]. In this context, Vahedifard et al. [297] and Melzner et al. [298] report various geohazards influenced by wildfires, including rockfall, debris flows, soil slips, rill and gully erosion, and land subsidence.

The environmental impact of fires can vary in magnitude and persist for years, depending on fire intensity, severity, and frequency (e.g., Ref. [294,296,297]). For instance, Rengers et al. [299] indicate that complete recovery may take 3–5 years, while DeGraff [300] reports 10 years.

Fire intensity refers to the rate of energy released during combustion, whereas fire severity describes the resultant effects on soil physical, chemical, and biological properties. Fire severity correlates with the extent of vegetation combustion and damage, which indirectly affects root degradation and the post-fire vegetation recovery process. The terms fire severity and burn severity are often used interchangeably. Fire severity is predominantly used in classifying and mapping fire events and can be assessed via remote sensing techniques, employing multispectral indices to detect spectral changes in the soil before and after fire occurrences. In situ surveys are frequently conducted for validation, assessing soil alterations such as organic matter loss and vegetation dynamics under post-fire conditions [290,301].

Following wildfires, soil and land cover are immediately impacted. However, the thermal alteration is generally confined to a very thin shallow layer of less than 10 cm [302]. Among the effects of wildfires on slopes, notable consequences include changes in soil water repellency, reductions in hydraulic conductivity, potential formation of hydrophobic layers, degradation of soil structure, and infiltration of ash into soil pores [297]. These phenomena result from the interplay between soil composition, intrinsic soil properties and the thermal regime developed during combustion. DeBano [303] reviewed experimental and field evidence regarding fire-induced water repellency, reporting negligible effects below 175°C, intense water repellency formation between 175 and 200°C, and destruction of hydrophobicity within the 280-400°C range. However, other studies have demonstrated that heating duration also influences these trends (e.g., Ref. [304]). The reduction in hydraulic conductivity is attributed to void collapse following soil and vegetation combustion [305]. Additionally, while some studies suggest that ash layers exhibit hydrophobic behavior, others have linked them to increased infiltration rates and water retention, delaying runoff [306]. Consequently, literature presents discrepancies regarding wildfire effects on slope stability and soil properties.

Beyond the thermo-hydraulic consequences of wildfires, soil mechanical strength may be significantly compromised. Experimental tests assessing soil-root system strength, despite variations in materials, report negligible or poor changes in friction angle but substantial reductions in cohesion (e.g. Ref. [307,308]). Roots decay and tree mortality progressively reduce soil reinforcement, with effects persisting over extended periods. Lei et al. [309] observed a time-dependent reduction in shear strength, with tests conducted on soil samples collected two months, one year and two years post-wildfire.

Rainfall exacerbates post-fire susceptibility by infiltrating fire-affected soils. The combination of reduced mechanical strength and altered hydrological behavior facilitates rapid saturation of shallow soil layers, increasing pore pressure and predisposing slopes to failure. In the initial months following a wildfire, debris flows are among the most frequent geohazards, triggered by two primary processes: erosion and material entrainment due to surface runoff, and infiltration-induced shallow landslides [189]. The first process occurs immediately following significant rainfall events, whereas the second is linked to delayed root and tree mortality (Fig. 8). Although the probability of geohazard occurrence endures for extended periods after a wildfire, it gradually reduces over time [310].

The assessment of rainfall-induced landslide initiation generally involves defining intensity-duration thresholds (see above). However, post-fire conditions significantly alter these thresholds, necessitating site-specific re-evaluations. Approaches for analyzing post-fire instability triggering include empirical, statistical and physically-based theoretical models. Empirical and statistical models rely on historical data, with statistical methodologies encompassing logistic regression and machine learning techniques. However, to use such methodologies, a comprehensive inventory of post-wildfire landslides is required, which is currently lacking globally. More recently, physically-based models have been introduced. Although these approaches are often computationally expensive and need site-specific geotechnical data, they are a valid tool to account for wildfire effects, considering the variations in root reinforcement and hydraulic conditions of the unsaturated soil covers potentially unstable [291,296]. Observations indicate that post-fire shallow landslides evolving in floods and debris flows are predominantly triggered by short-duration and high-frequency rainfall events [311]. Rainfall thresholds in burned areas are markedly lower than those in unburned areas. Despite significant advancements in wildfire and rainfall-induced geohazard research, critical knowledge gaps persist. Data on soil recovery trajectories and the evolution of post-fire geohazard susceptibility remain limited [297]. Given the current context of climate change and increasing wildfire frequency, advancing research to enhance understanding, prevention, and prediction of post-fire disasters is both a scientific and socio-economic priority.

4.2. *Vegetation alteration (natural and anthropogenic)*

Slope instability processes driven by rainfall can be highly influenced by the presence of vegetation cover, especially in hilly and mountainous environments susceptible to rapid mass movements, such as shallow landslides. It is widely recognized that vegetation promotes slope stability through hydro-mechanical mechanisms that contribute to increasing the resisting forces acting along slopes [312–314]. Among these mechanisms, mechanical root reinforcement is generally considered the most important (Fig. 9a).

The reinforcement provided by plant roots can be twofold depending on root diameter and spatial density [315,316]. On the one hand, single large (diameter >2 mm) woody roots penetrate soil layers in different directions to reach stiffer and more resistant soil horizons or the underlying bedrock, thus working as basal or lateral soil anchoring systems that exploit root tensile strength (Fig. 9a). On the other hand, the dense network of fine roots (diameter <2 mm) growing between soil granules produces more compact soil aggregates, resulting in higher overall cohesion (Fig. 9a). In contrast, the hydrological reinforcement functions of vegetation are mainly attributed to processes that contribute to reducing soil moisture in the vadose zone, thus counteracting the negative role of pore water pressures [317–319]. These include the action of interception by plant canopies, which reduces the amount of effective rainfall reaching the ground, combined with evapotranspiration processes, which enable soil desaturation and suction development, thereby increasing soil shear strength and enhancing slope stability (Fig. 9a). Root water uptake influences soil water retention capacity, causing vegetated soils to reach drier states than bare soils, thereby increasing the contrast between wet and dry conditions and enabling greater water storage while preventing the onset of critical instability hydrological thresholds [319]. Roots exert a complex and variable influence on both saturated and unsaturated hydraulic conductivity by modifying soil structure, pore size distribution and

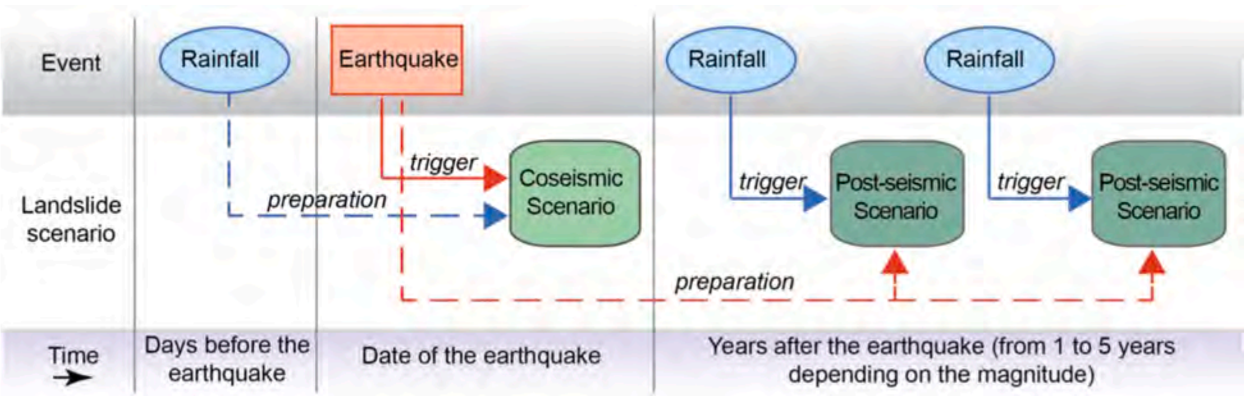

Fig. 10. Role of antecedent rainfall in the earthquake-triggered shallow landslides involving unsaturated slope covers.

their connections. Processes like root growth and penetration, shrinkage-swelling cycles, and root decay tend to increase permeability through the formation of macropores and preferential flow paths, whereas pore clogging, soil compaction around roots, and the release of organic exudates may reduce hydraulic conductivity ([319–322]). These changes affect slope stability by controlling infiltration rates, pore-water pressure development, and suction dynamics, with either potentially stabilizing or destabilizing effects depending on multiple interacting factors (e.g., plant species and age, root architecture and density, slope morphological features, climatic conditions).

However, the beneficial contributions of vegetation-related hydro-mechanical functions to slope stability can be negatively affected by both natural (e.g., insect pests, diseases, wildfires) and anthropic (e.g., deforestation, timber harvesting, land use and land cover (LULC) changes) causes [314,323,324]. One of the most documented adverse effects of vegetation degradation on slope stability is the progressive decay of root strength following tree logging (Fig. 9b). Root decay is usually accompanied by the formation of soil piping that can act as preferential flow circuits for rainwater infiltrating from the ground, causing an increase in pore water pressure, especially during intense rainfall events [325]. Several experimental and modelling studies revealed consistent temporal patterns of root reinforcement reduction after plant removal [326–329], indicating that roots become almost completely degraded approximately 15-20 years after cutting, with the highest rates of decay recorded around 10 years [318]. This resulted in a simultaneous increase in landslide magnitude and intensity (by a factor of 2 to 10) until vegetation cover is fully re-established, and pre-logging conditions are restored [330–333] (Fig. 9b). Similar temporal patterns of the severity of rainfall-induced mass movements were found in hilly-mountainous slopes following farmland abandonment. For example, Brandolini et al. [334] suggested that, in terraced landscapes, the period between the cessation of farming activities and the considerable spread of natural vegetation (<25-30 years) could represent the most hazardous scenario. Similarly, studies in different morphological, and LULC contexts indicated that the slope stabilization promoted by the progressive growth of natural vegetation can require up to 30-40 years, depending on vegetation species, the dynamics of forest regeneration, as well as land management practices and policies [335–337] (Fig. 9c).

These findings highlight a significant time-dependent nature of the effects of vegetation changes on the occurrence of rainfall-induced shallow landslides, emphasizing their preparatory role. Therefore, as claimed by some authors [318,338], in order to capture reliable future landslide hazard and risk scenarios, it will be extremely important to implement the dynamic role of hydro-mechanical vegetation effects in slope stability modelling. Recently, other authors have shown that wildfire-driven vegetation alteration in Mediterranean landscapes can be effectively analyzed through multi-criteria, landscape-based approaches. The FIRE project on Ischia Island is a notable example, integrating geomorphological, ecological and LULC factors to model spatial wildfire-risk scenarios [339]. These research directions will be crucial in light of changing climate conditions, since it can be reasonably expected that harsher weather patterns will affect both agricultural and forest ecosystems, thus altering their protective hydro-mechanical functions [340]. For example, the occurrence of prolonged periods of drought punctuated by intense or extreme rainstorms may lead to a deterioration of root mechanical reinforcement [341], which in turn can further exacerbate the severity of slope instability processes. Furthermore, new climate scenarios can also have social and economic impacts leading to climate- and economically dependent LULC change [342] that can modify over time the response of slopes prone to landslides driven by rainfall.

4.3. Earthquakes and rainfall

The simultaneous occurrence of seismic ground motion and other destabilizing factors, such as soil saturation from rainfall (Fig. 10), plays a crucial role in assessing landslide hazards and the associated risks to settlements and infrastructure [343–347]. Recent studies further highlight how rainfall-earthquake interactions may intensify under evolving climatic conditions. He et al. [348] demonstrated that nonstationary rainfall, when combined with seismic shaking, can significantly increase long-term landslide probabilities, while Bohnhoff et al. [349] showed that climate-driven sea-level rise and extreme weather can modify crustal stress conditions, potentially amplifying cascading hazards such as earthquake-induced landslides. Martino et al. [350] conducted a comprehensive quantitative analysis to evaluate changes in landslide activity at the basin scale following a 5.1 Mw earthquake in Central Italy's Molise region in August 2018. The study combined direct field observations with Differential SAR Interferometry (DInSAR) analysis over a three-year period, spanning two years before and one year after the earthquake. This approach identified both first-time and reactivated landslides within a region of high landslide susceptibility, characterized by lithologies such as marly clays and flysch. Findings revealed that seasonal rainfall interacting with slopes destabilized by the earthquake triggered a significantly higher number of landslides compared to previous years under similar rainfall conditions. Notably, the number of reactivation events increased by approximately 118%, during one year after the low-magnitude earthquake. This increase in activity was observed in both first-time and reactivated landslides, marked by shorter periods of inactivity and prolonged periods of sustained activity. Martino et al. [351] investigated the 2016-2017 earthquake-induced landslide scenarios for seismic microzonation in the Accumoli area (central Italy). Since the seismic sequence exacerbated the region's vulnerability to landslides, this study focused on the triggering of slow landslides, such as earthflows and planar or rotational slides, in this highly susceptible area following a low-magnitude (5.1 Mw) earthquake. Through field surveys conducted immediately after the event, the authors documented the distribution of seismically induced effects, particularly landslides in cohesive soils and structural collapses. They analyzed how the spatial distribution of these phenomena correlated with seismic and rainfall intensities. The intense rainfall, delivering approximately 120 mm over three days before and during the earthquake, significantly worsened slope stability: the soil saturation during seismic shaking played a critical role, influencing both the extent of induced effects and their spatial concentration relative to epicentral distance and earthquake magnitude. This led to a more severe landslide scenario than would typically be expected for an earthquake of such low magnitude. Specifically, the affected area extended far beyond the traditional Keefer radius [352] of approximately 2 km, reaching distances up to 20 km, indicating that saturated soil conditions dramatically amplify the impact of seismic activity on slope stability. This phenomenon

Table 2
Overview of observational datasets, remote sensing products, and climate model outputs relevant to the Mediterranean and Italian regions for climate and landslide-related applications. Products are categorized as observational (OBS), remote sensing (RS), reanalyses (RE), hindcasts (HI), and climate simulations (CS). The ENEA-5km and ICTP-Reg_CM5 products are driven by CMIP6 models, while the other CS products are driven by CMIP5 models. For each product, the table reports the acronym, institution responsible, temporal coverage, use of data assimilation, convection-permitting (CP) status, horizontal (HR) and temporal (TR) resolution, spatial domain, and reference. When information was unavailable or not consistently identifiable, the corresponding entry is left blank.

Acronym	Institution	Product	Start date	End date	Data assim	CP	HR	TR	Domain	Reference
E-Obs	COPERNICUS	OBS	1950	2024			0.1°	d	Europe	[358]
CRU	East Anglia U	OBS	1901	2018			0.5°	m	global	[359]
GRIPHO	ICTP	OBS	2001	2016			3 km	h	Italy	[360],
ARCIS	ARPAs	OBS	1961	2015			5 km	d	C-N Italy	[361]
SCIA	ISPRA	OBS							Italy	[362]
EURO4M		OBS	1971	2019			5 km	d	Alps	[363]
ESA - CCI	ESA	RS data					0.25°	d, m	global	[364]
ERA5	ECMWF	RE	1940	2022	yes	no	31 km	h	global	[365]
ERA5-Land	ECMWF	RE	1950	present	indirect	NA	0.1°	h	global	[366]
UERRA	COPERNICUS	RE	1961	2019	yes	no	11,1	6h	Europe	UERRA home page
SPHERA	ARPAE	RE	1995	2020	yes	yes	2.2 km	h	Italy	[367]:
MERIDA	RSE	RE			yes	no	7 km	h	Italy	[368]
MERIDA-HRES	RSE	RE			yes	yes	4 km	h	Italy	[369]
VHR-REA_IT	CMCC	HI	1989	2020	no	yes	2.2 km	h	Italy	[370]:
COSMO-REA6	DWD	RE	2008	2018	no	no	6 km		Europe	[371]
COSMO-REA2	DWD	RE	2008	2018	yes	yes	2 km		Central Europe	[371]
CERRA	COPERNICUS	RE	1984	2021	yes	no	5 km		Europe	[372]
MERRA2	NASA	RE	1980	2024	Yes	No	0.5°	3h	global	[373]
CHAPTER	CIMA	HI	1981	2020	no	yes	3 km		Europe	Bernini et al., submitted
VHR-PRO_IT	CMCC	CS	2006	2070	no	yes	2.2 km	h	Italy	[93]
ENEA-5km	ENEA	HI	1980	2023	no	no	5 km	h	Italy and West Med	[95]
		CS	2015	2100						
ICTP-Reg_CM5	ICTP	CS	1995	2021	no	yes	3 km	h	Europe	-
			2021	2042						
			2048	2067						
			2067	2086						
FPS Convection	CORDEX Team	CS	1996 2041 2090	2005	no	yes	3 km	h	ALP-3	[374]
				2050						
				2099						

does not extend to disrupted or rapid landslides, such as collapses or fast flows [353]. Beyond the Italian case studies, the scientific literature offers a range of approaches to study multi-hazard landslide scenarios. Sassa et al. [354] emphasized that the combined effect of earthquakes and rainfall can trigger landslides even under conditions that would not be critical if considered separately. Faris & Wang [355] used stochastic analysis to evaluate the impact of rainfall on earthquake-induced landslides in Indonesia, showing that variability in the hydraulic response of slopes significantly modifies risk scenarios. More recently, Nguyen & Kim [356] applied Monte Carlo simulations to predict rainfall–earthquake-induced landslides in Seoul, South Korea, demonstrating the effectiveness of probabilistic approaches.

5. Discussions

The previous sections have reviewed the current knowledge of the role of rainfall in the preparation and triggering of both slow and rapid shallow landslides. This comprehensive overview of the state of the art provides the basis for integrating projected climate data, under different climate change scenarios, into operational modelling toolchains. In doing so, the objective of the research is extended towards the development of an integrated, national-scale framework for analysing the influence of rainfall on landslide dynamics, that can be extended to a variety of case studies.

This integration will, in future developments, allow the use of climate projections to simulate and generate ground instability scenarios driven by evolving climatic conditions. Considering the project's focus, the proposed toolchains are primarily designed to address shallow landslides, where rainfall-induced processes can be more directly associated with climatic forcing. The following discussion therefore explores the available climate projections and the modelling frameworks that support this integration, highlighting their potential and limitations within the broader context of landslide hazard assessment under climate change.

5.1. Climate information

Given that the availability of validated observational datasets, extensive in time and space, is an indispensable prerequisite for any impact study, climate models can anyway offer insights into climate variables of interest for the recent past and not only for future scenarios. In particular, reanalyses, which, through a process of assimilation of observed data, make it possible to reconstruct with reasonable fidelity the weather and climate situations of just past decades. In addition to these, there are also products called "hindcasts," which are based on dynamic downscaling of the reanalyses themselves, making it possible to locally increase the resolution of the data by simulating physical phenomena at the most resolved scales and not by mere interpolation.

Model studies indicate the Mediterranean region as a climate change hotspot, prone to the impacts of local scale and severe weather [82,357]. Because of the complex morphology (semi-closed basin with high and complex surroundings), the Mediterranean region and the Italian territory need to rely on high-resolution information to deal and manage the impacts of weather extremes, both for current and future climate. Among the most relevant climatic variables for landslide applications, precipitation is undoubtedly the most critical, alongside other surface variables, such as temperature, humidity and soil moisture. Table 2 summarizes a non-exhaustive set of databases and research groups currently providing up to date and ready-to-use climate scenarios and benchmark products, that can be used in applications such the one presented in this paper. The table reports both observational products that refer to time series of in situ measurements, as well as interpolated products on regular grids. In the latter case, the nominal resolution depends greatly on the spatial extent of the database and the number of stations used. A detailed evaluation of the characteristics of individual products is beyond the scope of this discussion, and readers are referred to the relevant literature for further information.

In the table, products are differentiated according to their type: observational (OBS), remote sensing data (RS), and climate models. Among the latter there are: Reanalyses (RE), hindcast simulation (HI), climate simulation (CS). The table also contains the name of the product, the institution that developed/maintains it, whether data-assimilation has been used or not, whether CP scheme is active or not, the Horizontal Resolution in km or degrees (HR), the time resolution (m-monthly, d-daily, h-hourly), the domain covered, and the reference paper if any. In case the information was not available or not easily identifiable for the whole dataset, we leave a blank entry.

All the datasets listed in Table 2 refer to atmospheric variables except ERA5-Land which is a reanalysis achieved through global high-resolution numerical integrations of the ECMWF land surface model driven by the downscaled meteorological forcing from the ERA5 climate reanalysis and contains land and soil variables.

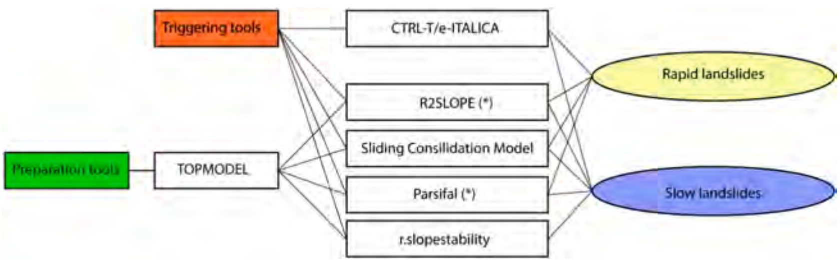

Fig. 11. Inventory of tools compiled for modeling rainfall-induced preparation and triggering of ground instabilities. (*) These tools also support seismic forcing, potentially enabling multi-hazard scenario assessment.

Beside the specific products listed in the table it is worth to mention also the dataset stemming from intercomparison experiments, such as CORDEX (https://cordex.org/) which covers the European domain both with the EURO-CORDEX and the MED-CORDEX initiative.

In particular, we report that the CORDEX initiative dedicated a Flagship Pilot Study to convection (CORDEX-FPSCONV) whose major protocol and potentiality are described in Coppola et al. [375], while preliminary results over climate scale for precipitation are presented in Ban et al. [89] and Pichelli et al. [90].

In the framework of the RETURN project, several activities have generated new convection-permitting scales climate model runs. The ensemble runs from CORDEX Flagship Pilot Study on Convective Phenomena over Europe and the Mediterranean have been remapped to a common resolution and benchmarked in some areas using ground-observed extremes [91,376]. A national scale benchmark based observed extremes is being produced using a regionalized formulation of the Metastatistical Extreme Value Distribution [377]. New convection-permitting model runs have been completed over Italy (and including most of Europe) at 3 km and 1 h scale by ICTP-Trieste, forced by EC-Earth3-Veg GCM, according to CMIP6 scenarios (see Table 2). A regional downscaling of CMIP6 global climate projections to local scales for the Mediterranean and Italian regions has been performed, aiming to produce high-resolution climate information for the assessment of climate change signals, with a focus on precipitation extreme events (also reported in Table 2). The experiments cover hindcast (i.e. ERA5-driven) and historical simulations (driven by theMPI-ESM1-2-HR model) to simulate the present (1980-2014) and future (2015-2100) climate under three different emission scenarios (SSP1-2.6, SSP2-4.5, SSP5-8.5) [95], and results have been already summarized in Section 2. In the context of the application proposed in this article, all datasets can be used to characterize the spatio-temporal variability of precipitation as the main driver of landslide phenomena linked to climate change, both in terms of predisposing and triggering factors. Comparing the present and future climate can help identify any changes in the risk of certain events, as well as provide indications of the expected effects in various scenarios and understand whether and how different climate mitigation strategies could have qualitatively and quantitatively assessable effects.

5.2. Toolchains framework for modelling the rainfall role in landslide preparation and triggering

Operational toolchains are defined as sequences of computational and analytical tools designed to produce scenarios of ground instability effects linked to specific types of preparation processes and triggering actions, characterized by a given intensity.

Based on the principle of leveraging existing knowledge, we first focused on the identification and rationalization of computational tools useful for constructing these logical-operational analysis flows, characterizing each operational tool according to various criteria and initially designing their interconnection.

The resulting toolchains (Fig. 11) specifically address rainfall-induced shallow landslides commonly observed in mountainous and hilly environments (Table 1). They are designed to model and simulate the role of rainfall in both the preparation (time-dependent processes) and triggering (transient processes) of slope failures. Accordingly, tools dedicated to susceptibility or predisposing factor analysis (e.g., SZplugin, [378,379]) and those developed for run-out modelling (e.g., QPROTO, [380]; STONE, [381]; RASH3D, [382]) are not included in the present framework. The compiled toolchains (Fig. 11) can thus address, with varying levels of detail, the following types of shallow landslides commonly observed in Italian mountainous and hilly environments:

- Rapid-kinematics phenomena: rockfalls/topples and debris/mud flows.
- Slow-kinematics phenomena: shallow planar slides and roto-translational landslides.

5.2.1. Tools for the evaluation of preparatory conditions

- TOPMODEL

TOPMODEL (TOPography-based hydrological MODEL) is derived from the seminal work of Beven et al. [383] and critically reviewed in Beven [384]. Its core concept is the topographic index, defined as the ratio of upslope contributing area to the local slope angle. This index provides a measure of hydrological similarity, under the assumption that locations with equal values respond in comparable ways to rainfall and groundwater dynamics. Areas with higher index values are expected to saturate first and thus contribute more readily to surface and subsurface runoff.

To capture the complexity of catchment hydrology in a simplified manner, TOPMODEL assumes that subsurface runoff is generated uniformly within zones sharing the same index, that the hydraulic gradient of the water table parallels the land surface slope, and that soil transmissivity declines exponentially with depth. These simplifying assumptions allow the model to be implemented effectively with digital terrain data and GIS.

By simulating water table fluctuations in shallow soil deposits following rainfall events, provided the relevant hydro-mechanical parameters are available, TOPMODEL outputs can be used for two key purposes:

i) to assess how rainfall intensifies pre-existing slope instability conditions, and
ii) to generate input data for quantitative slope stability analyses in soil-mantled terrains, particularly with respect to shallow translational and, to a lesser degree, rotational–translational failure mechanisms.

5.2.2. Tools for the evaluation of triggering effects

- e-ITALICA-CTRL-T

The empirical rainfall threshold approach emerges as the key methodological tool for assessing rainfall-triggered slope instabilities, as it provides a unified framework applicable to different landslide kinematics. In particular, e-ITALICA (enhanced ITAlian rainfall-induced LandslIdes CAtalogue; [13]) is a comprehensive Italian landslide catalogue that documents 6312 rainfall-induced landslides recorded between 1996 and 2021. These events, originally listed in the ITALICA catalogue [385], are now enriched with detailed information on their rainfall triggering conditions, expressed in terms of rainfall duration D (hours) and cumulative event rainfall E (mm). The triggering conditions were derived from hourly rainfall measurements collected at 4033 gauges and processed using a rigorous and reproducible methodology. In addition to rainfall information, the catalogue also includes topographic and land cover attributes, making it a valuable dataset for analyzing rainfall conditions capable of triggering landslides, calibrating and validating physically-based prediction models, and defining empirical rainfall thresholds from local to national scales, thereby contributing to landslide risk reduction in Italy. To process these data, the CTRL-T tool (Calculation of Thresholds for Rainfall-induced Landslides–Tool; [386]) was applied. Developed in R, CTRL-T automatically reconstructs rainfall events from standard rainfall series and landslide records, identifies multiple rainfall conditions responsible for slope failures, and defines frequentist rainfall thresholds for different non-exceedance probabilities. The tool further incorporates machine learning algorithms to refine empirical rainfall thresholds by correlating the spatial and temporal occurrence of landslides with their triggering rainfall. When historical rainfall series are available, these thresholds can also be characterized in terms of hazard.

Although e-ITALICA produces binary forecasts (landslide/no landslide) without pinpointing exact locations, these can be linked to inventoried landslides (reactivations) or to highly susceptible areas (potential first-time activations). The catalogue supports analysis of rainfall conditions that trigger landslides, calibration and validation of physically-based prediction models, and the definition of empirical rainfall thresholds across Italy, contributing to landslide risk reduction. It is applicable to all types of landslides, from rapid to slow-moving.

- R2SLOPE

The R2SLOPE tool [387] is a GIS-based probabilistic model designed for the regional assessment of slope stability under both rainfall and seismic forcing. For rainfall-induced shallow landslides in soil, it couples a hydrological framework (TOPMODEL), with the infinite slope stability equation to simulate how infiltration raises pore-water pressures and lowers the factor of safety, allowing different rainfall scenarios to be translated into probabilities of failure. For earthquake-induced instability, it uses semi-empirical relationships to estimate expected co-seismic displacements for both rock sliding, including planar and wedge mechanisms, and shallow soil landslides. These displacements are computed from peak ground acceleration and peak ground velocity values in combination with the yield coefficient *Ky*. By linking distributed hydrological response to slope failure thresholds and integrating seismic predictive relationships, R2SLOPE can be applied to both rapid and slow landslides, offering a versatile framework for assessing multi-hazard scenarios.

- Sliding-Consolidation Model

The Sliding-Consolidation Model [388] is a hydro-mechanical framework developed to estimate deformations in slopes caused by changes in pore water pressure, particularly those induced by rainfall. It is designed to capture the complex interplay between infiltration-driven pore pressure build-up, consolidation processes, and shear deformation within the basal shear zone, thereby providing a mechanistic understanding of how hydrologic forcing translates into deformation velocity and the potential evolution of shallow failures into either rapid or slow-moving landslides. By linking hydrological inputs from models such as TOPMODEL, the Sliding-Consolidation Model can account for the preparatory effects of rainfall, including spatially variable infiltration and soil saturation, allowing for a more realistic representation of rainfall-triggered instability.

The model is applicable to a wide range of landslide types, from slow, creeping slopes to fast, catastrophic failures, making it a versatile tool for both research and practical hazard assessment. Its strength lies in its ability to connect pore water pressure dynamics with slope mechanical behavior over both short- and long-time scales, offering insight into long-term slope dynamics, deformation velocities, and the conditions under which shallow landslides may accelerate. However, the model is limited in its scope as it does not include the effects of seismic triggers or other rapid-loading mechanisms, which constrains its applicability in multi-hazard scenarios where rainfall and earthquakes might act in combination. Despite this limitation, the Sliding-Consolidation Model remains a powerful framework for understanding rainfall-driven landslide processes and for predicting the potential timing, magnitude, and evolution of slope failures under varying hydrological conditions.

- PARSIFAL

The PARSIFAL (Probabilistic Approach to pRovide Scenarios of earthquake-Induced slope FAiLures) framework was developed as an integrated computational tool for the prediction of slope-failure scenarios induced by seismic loading, under predefined hydraulic conditions of the slopes, and with reference to failure mechanisms related to rock-block instabilities (planar, wedge, and toppling failures) and shallow translational soil slides [351,389,390]. The analysis follows a stepwise procedure that, with specific reference to first-time failures, can be summarized as follows:

i) assessment of static stability conditions for different hydraulic states (expressed in terms of joint saturation percentage for rock masses, and pore pressure ratio – *Ru* – for shallow soil slides);
ii) definition of the critical acceleration coefficient (*Ky*) and pseudo-static stability analysis for given PGA values and hydraulic conditions;
iii) estimation of coseismic displacement approach and related exceedance probability of a given critical displacement threshold using a pseudo-dynamic method.

The implemented analytical solutions are based on the global limit equilibrium approach (static and pseudo-static stability analysis) and the Newmark rigid-block method (pseudo-dynamic analysis).

Originally conceived as a modular collection of computational tools, the PARSIFAL framework has been specifically updated and integrated to meet the requirements of the project's Proof of Concept (PoC). In particular, to enhance its performance, two distinct processing chains were developed: one dedicated to rock-mass instabilities (PARSIFAL-R) and the other to shallow soil instabilities (PARSIFAL-T), depending also on the nature of the required input data. Both PARSIFAL-R and PARSIFAL-T include a final module that allows for the estimation of coseismic displacement as a function of *Ky* based on a semi-empirical relation [391], without requiring the use of spectrum-compatible accelerograms needed for the Newmark analysis.

Furthermore, regarding hydraulic conditions – crucial for assessing the effects of meteorological and climatic forcings independently from multi-hazard interactions – while no computational tool is currently available for rock masses to transform rainfall input into hydraulic head along the joint network, for soil translational slides the TOPMODEL hydrological model [383] has been integrated by means of a dedicated script providing an estimation of the water table depth - and, thus, the *Ru* factor – following a given rainfall. Although simplified, this model enables the evaluation of the preparatory and/or triggering effects of rainfall events.

● r.slopestability

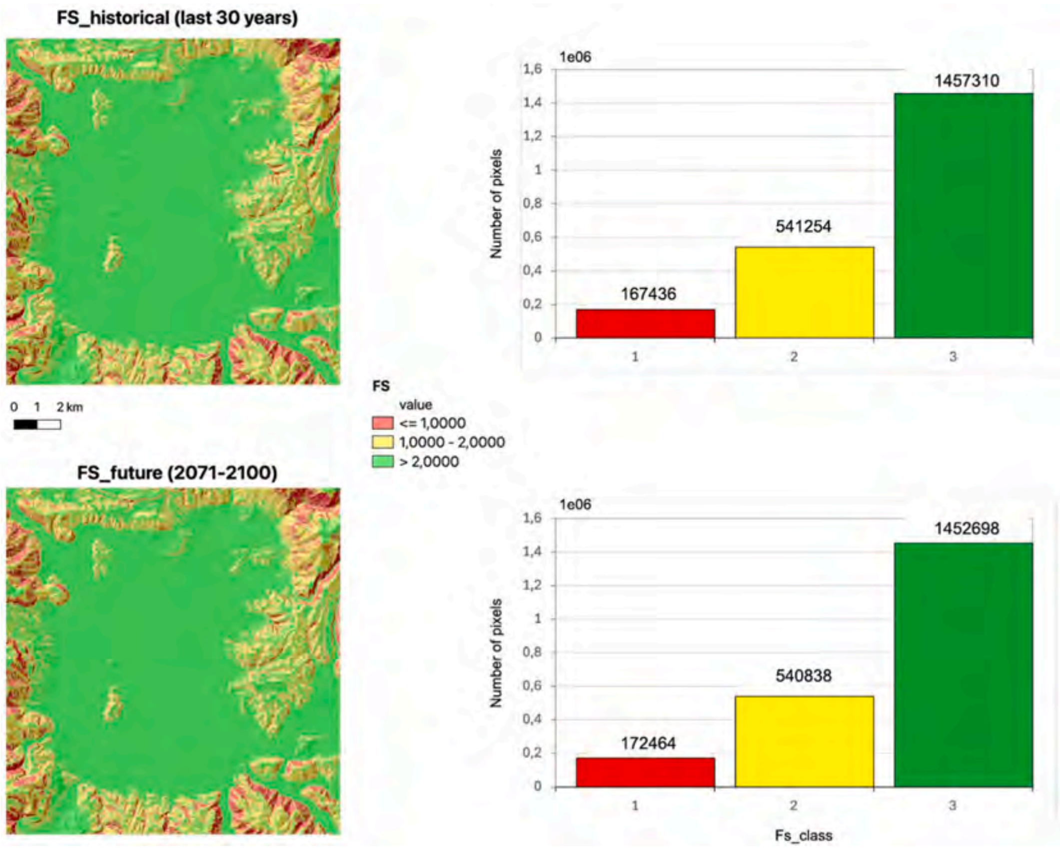

Fig. 12. Landslide scenarios (Safety Factor FS ≤ 1,3) for the Inland environment of RETURNLAND, computed by running the VS2 toolchains with 1-h precipitation extremes with a 100-year return period for both historical conditions and end-century climate projections, under the worst emission scenario (SSP5-8.5).

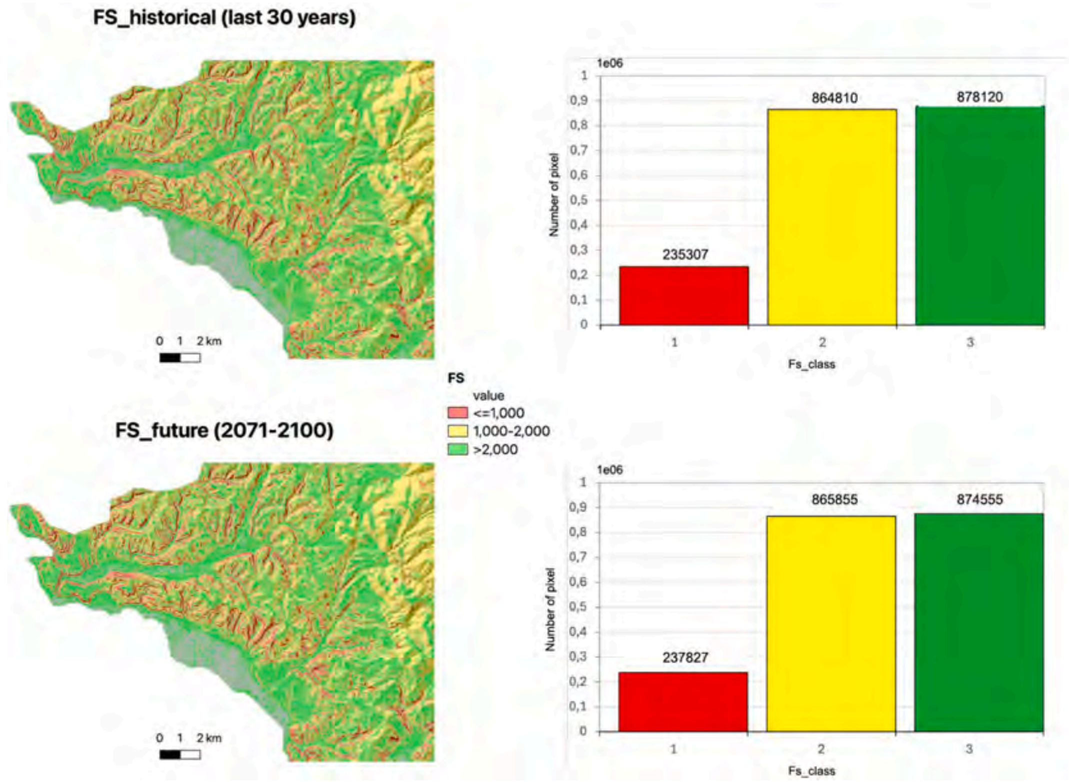

Fig. 13. Landslide scenarios (Safety Factor FS ≤ 1) for the Coastal environment of RETURNLAND, computed by running the VS2 toolchains with 1-h precipitation extremes with a 100-year return period for both historical conditions and end-century climate projections, under the worst emission scenario (SSP5-8.5).

r.slopestability is a spatially distributed, physically-based model for landslide susceptibility analysis. It is open-source and was developed by Mergili et al. [392] as a C- and Python-based raster module of the GRASS GIS software package. Its application ranges from shallow soil slips to deep-seated mass movements in geologically complex areas, being suitable for large areas, including tens to hundreds of square kilometres or more appropriately accounting for the natural variability of the governing parameters.

It offers five modes of physically-based slope stability simulations. Four are based on randomly located and sized ellipsoidal slip surfaces, and one employs the infinite slope stability model. The ellipsoidal approaches allow the user to consider either only the ellipsoid bottom or also the bottoms of soil layers intersecting the ellipsoid. In addition, the tool can be run with a single ellipsoid of fixed parameters for targeted analysis. The model requires as inputs a digital elevation model (DEM), the saturated water content (via TOPMODEL), ranges of geotechnical parameter values derived from laboratory tests, and estimates of soil depth obtained in the field. Each soil class or layer must be associated with geometric and geotechnical properties such as thickness, cohesion, friction angle, and bulk density.

The model calculates the factor of safety (FoS) and the probability of slope failure (P_f) for each surface. Probability density functions are exploited to assign P_f to each ellipsoid. The minimum value of FoS and the maximum value of P_f recorded for each pixel are then taken as indicators of slope instability. The final output consists of raster maps of FoS and P_f, providing spatially distributed estimates of slope stability conditions and allowing identification of areas with higher landslide susceptibility.

5.3. Virtual test bed toolchain validation

The virtual test bed (VTB) environment provides an integrated analytical environment for simulating multi-hazard and multi-risk scenarios under changing climatic conditions [393]. Within this framework, selected modelling toolchains described before have been applied to evaluate how different hazard processes may interact and affect synthetic territorial settings. Two representative virtual domains, an “Inland” and a “Coastal” environment, were defined to explore the response of geomorphological systems and built areas to sequences of hazardous events.

In this study, we simulated shallow-landslide scenarios under varying rainfall regimes in both environments. These simulations allowed the toolchains to be tested in a controlled yet geomorphologically realistic context, supporting the assessment of their performance under diverse climatic forcing. Extended results and full-resolution outputs from these simulations are openly available on Zenodo (https://zenodo.org/records/18987490).

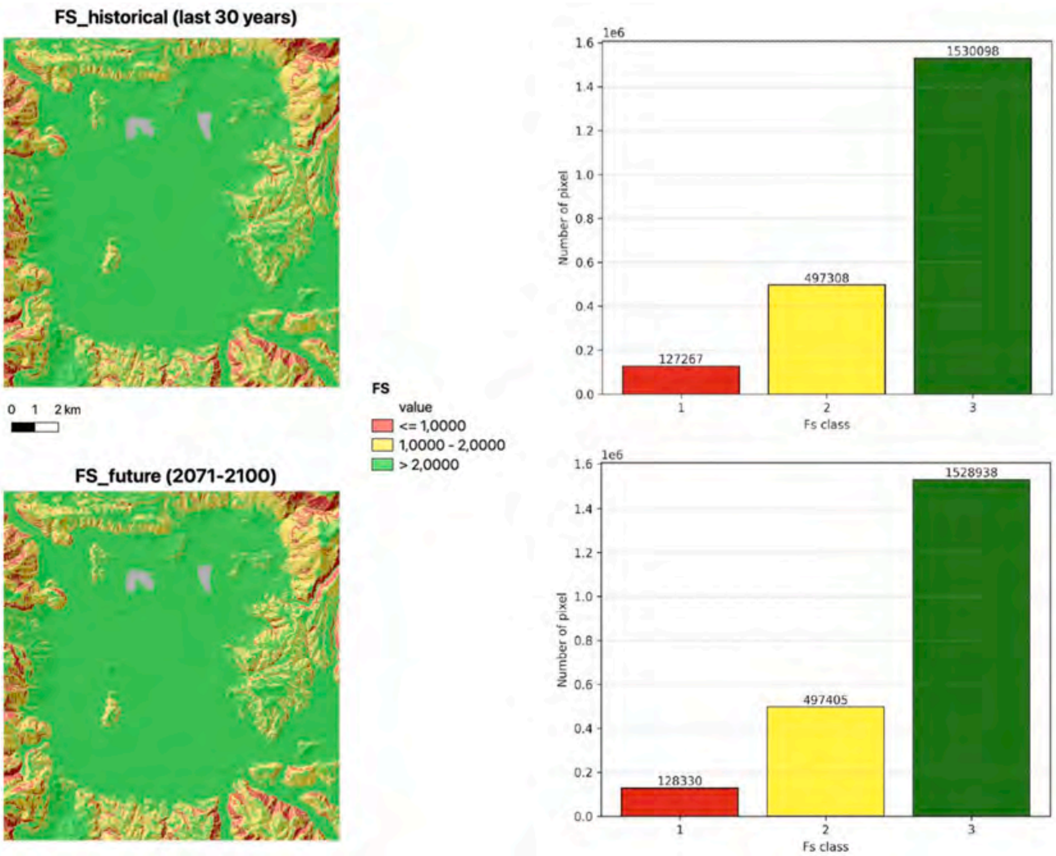

Fig. 14. Landslide scenarios for the RETURNLAND Virtual Test Bed Inland area (Safety Factor FS ≤ 1) computed by running the VS2 toolchains with 1-h precipitation extremes with a 2-year return periods for both historical conditions and end-century climate projections, under the worst emission scenario (SSP5-8.5). Plots indicate the frequency distribution of FS values for both the historical and future landslide scenarios.

5.3.1. Precipitation modelling

This study exploits two extremely different duration/return period settings of rainfall: 1-h precipitation extremes with a 100-year and 2-years return periods for both historical conditions and end-century climate projections. The analysis integrates kilometer-scale CPMs with the SMEV (Simplified Metastatistical Extreme Value) framework. The model approach builds on metastatistical extreme value theory introduced by Marani and collaborators and further advanced for practical hydrometeorological use by Marra et al. [394, 395]. SMEV models the distribution of all ordinary rainfall events rather than relying exclusively on annual maxima or threshold exceedances, making it well suited to relatively short yet information-dense CPM outputs. Using this methodology, we estimated historical and future 100-year quantiles and produced spatial maps describing their geographic variability [91,92]. These products support the evaluation of how hourly extremes may intensify under climate change and form a robust basis for shallow landslide hazard assessment for climate-adaptation planning. Foundational research that informs this workflow includes Ban et al. [396], Prein et al. [86], Fosser et al. [374], for CPMs, alongside Marani & Ignaccolo [397], Marra et al. [91,92,394,395], Correa-Sánchez et al. [376], and Lompi et al. [94] for SMEV and the integration of CPM and SMEV.

5.3.2. Landslide scenarios

Fig. 12 shows the results of the computational run performed with the VS2 toolchain in the RETURN-Land Inland environment, using 1-h precipitation extremes with a 100-year return period, for both historical conditions and end-century climate projections. The results obtained for the two different climatic scenarios do not show significant increment of landslide areas in the worst future scenario since, given the very long return period, quite severe landslide scenarios are predicted also for historical conditions. Similar results have been obtained for the RETURN-Land Coastal environment (Fig. 13), suggesting the need to increase the simulations with different duration/return period under different emission scenarios, also taking into account the landslide preparatory condition variables.

In light of the preliminary analyses outlined above, a new run of the toolchains has been carried out for the VTB Inland area, using historical (last 30 years; average intensity: 24 mm/h for the Inland area and 21 mm/h for the Coastal area) and projected data (2071-2100; average intensity: 27 mm/h for the Inland area and 25 mm/h for the Coastal area) with 1h duration and 2-years return periods. Figs. 14 and 15 show the results of the computational run performed with the toolchain in both the VTB Inland and Coastal areas,

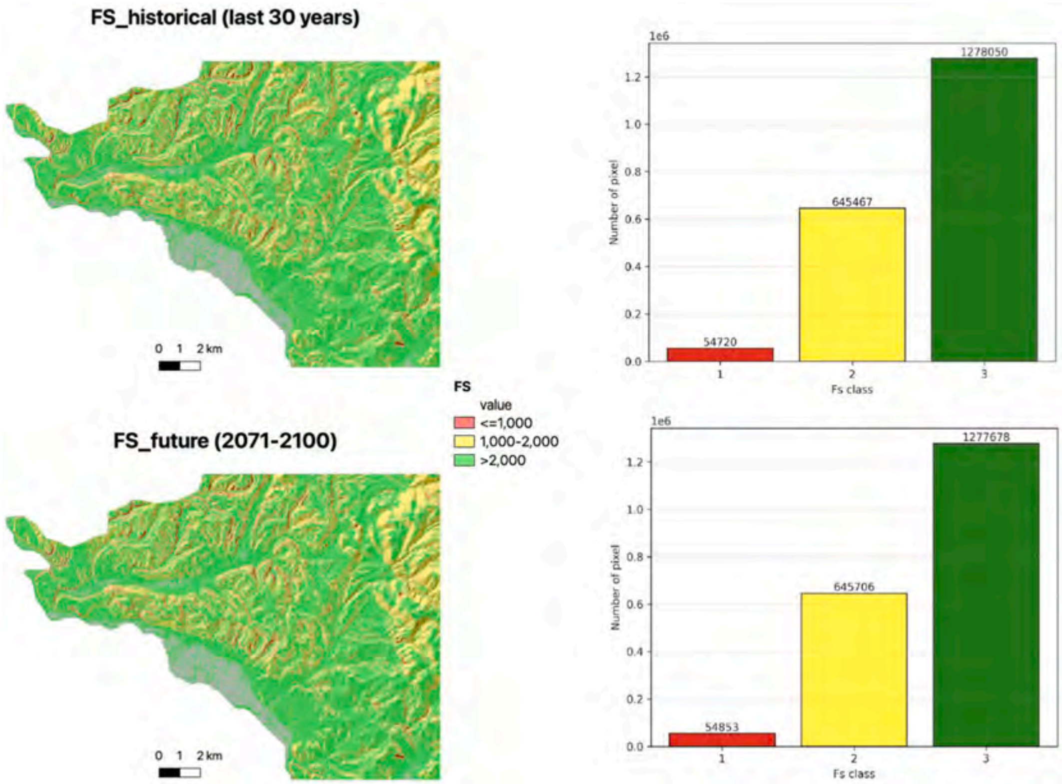

Fig. 15. Landslide scenarios for the RETURNLAND Virtual Test Bed Coastal area (Safety Factor FS ≤ 1) computed by running the VS2 toolchains with 1-h precipitation extremes with a 2-year return periods for both historical conditions and end-century climate projections, under the worst emission scenario (SSP5-8.5). Plots indicate the frequency distribution of FS values for both the historical and future landslide scenarios.

exploiting 1-h precipitation extremes with a 2-years return period, calculated both for the present time and for the 2071-2100 projections, under the worst emission scenario (SSP5-8.5).

The results obtained in the two different climatic scenarios again do not show significant increment of landslide areas in the worst future scenario. Such an unexpected result could be biased by the different space and time resolution and uncertainty of rainfall and other input parameters data related mainly to soil properties.

Therefore, the outcomes suggest the need of deeper sensitivity analyses on the toolchain with respect to the input parameters. Furthermore, deepening the analysis of the preparatory role of rainfall, by analysing soil moisture data derived by climate models (both historical and end-century projection), despite the uncertainty linked to these estimates, would be very useful to have impact scenarios that also account for soil moisture (and, more importantly, for its changes between historical and future conditions, rather than for absolute values). This will allow us to refine the parameter configuration for the proper functioning of the toolchains.

6. Conclusions

This study demonstrates that rainfall is a key climate-sensitive driver of slope instability in Italy, influencing landslide dynamics through both preparatory and triggering mechanisms. The review of current knowledge shows that shallow landslides respond rapidly to short-duration, high-intensity storms, while prolonged rainfall episodes progressively weaken slopes through cumulative wetting and hydrological preconditioning. The observed spatio-temporal variability of landslide occurrence therefore represents a meaningful indicator of climate-change impacts.

By synthesizing existing literature, this work develops a national-scale conceptual framework supported by modular toolchains designed to integrate rainfall information into landslide modelling. The use of virtual test beds provides a controlled yet geomorphologically realistic environment for exploring multi-hazard interactions and assessing the internal coherence of modelling workflows. This conceptual validation highlights both the potential of the proposed approach and the main structural weakness of current methodologies, such as the difficulty of translating rainfall data into soil-moisture and pore-pressure conditions, which remains the most critical step for reliably modelling preparatory processes.

Concluding, the framework presented here offers a foundation for future operational developments and identifies priority areas for research. Advancing climate-driven landslide modelling will require:

(i) improving the representation and validation of hydrological responses to rainfall, particularly soil-moisture and pore-pressure dynamics;
(ii) expanding and intercomparing convection-permitting climate model ensembles to better capture extreme precipitation; and
(iii) strengthening predictive and early-warning capabilities to support adaptive land-management and resilience strategies in Italy's most vulnerable landscapes.

Open research

The present work is intended as a review where no reprocessing of previously published data or application of software tools was undertaken.

CRediT authorship contribution statement

M. Delchiaro: Conceptualization, Data curation, Investigation, Visualization, Writing – original draft, Writing – review & editing. **V. Ruscitto:** Conceptualization, Data curation, Investigation, Visualization, Writing – original draft, Writing – review & editing. **G. Iacobucci:** Conceptualization, Data curation, Investigation, Visualization, Writing – original draft, Writing – review & editing. **D. Piacentini:** Conceptualization, Data curation, Investigation, Supervision, Writing – review & editing. **F. Troiani:** Conceptualization, Data curation, Investigation, Supervision, Writing – review & editing. **E. Dallan:** Data curation, Investigation, Visualization, Writing – original draft, Writing – review & editing. **M. Borga:** Data curation, Investigation, Supervision, Writing – review & editing. **M.V. Struglia:** Data curation, Investigation, Supervision, Visualization, Writing – original draft, Writing – review & editing. **A. Montanari:** Data curation, Investigation, Supervision, Writing – review & editing. **M. Marani:** Data curation, Investigation, Supervision, Writing – review & editing. **S. Silvestri:** Data curation, Investigation, Supervision, Writing – review & editing. **C. Puglisi:** Writing – original draft, Writing – review & editing. **L.M. Falconi:** Writing – original draft, Writing – review & editing. **G. Righini:** Writing – original draft, Writing – review & editing. **S. Segoni:** Writing – original draft, Writing – review & editing. **M. Pirone:** Writing – original draft, Writing – review & editing. **R. Tufano:** Writing – original draft, Writing – review & editing. **R. Narcisi:** Writing – original draft, Writing – review & editing. **F. Vagnon:** Writing – original draft, Writing – review & editing. **G. Taddia:** Writing – original draft, Writing – review & editing. **P. Mazzoglio:** Visualization, Writing – original draft, Writing – review & editing. **P. Claps:** Supervision, Writing – review & editing. **C. Martinello:** Writing – original draft, Writing – review & editing. **E. Rotigliano:** Supervision, Writing – original draft, Writing – review & editing. **G. La Porta:** Visualization, Writing – original draft, Writing – review & editing. **M. Ferrarotti:** Visualization, Writing – original draft, Writing – review & editing. **M. Pirulli:** Visualization, Writing – original draft, Writing – review & editing. **G. Pepe:** Writing – original draft, Writing – review & editing. **B. Antonielli:** Visualization, Writing – original draft, Writing – review & editing. **L.M. Giannini:** Data curation, Investigation, Writing – review & editing. **C. Esposito:** Data curation, Investigation, Writing – review & editing. **S. Martino:** Funding acquisition, Supervision, Writing – review & editing. **F. Bozzano:** Funding acquisition, Supervision, Writing – review & editing. **D. Calcaterra:** Funding acquisition, Supervision, Writing – original draft, Writing – review & editing. **D. Di Martire:** Funding acquisition, Writing – review & editing. **M. Della Seta:** Conceptualization, Data curation, Investigation, Supervision, Writing – review & editing.

Declaration of competing interest

The authors declare that they have no known competing financial interests or personal relationships that could have appeared to influence the work reported in this paper.

Acknowledgments

This study was carried out within the RETURN Extended Partnership and received funding from the European Union Next-GenerationEU (National Recovery and Resilience Plan—NRRP, Mission 4, Component 2, Investment 1.3—D.D. 1243 2/8/2022, PE0000005). We sincerely thank the editor and the four anonymous reviewers for their insightful comments, which have greatly strengthened the quality of the manuscript.

Data availability

Data will be made available on request.

References

[1] J.D. Hays, J. Imbrie, N.J. Shackleton, Variations in the earth's orbit: pacemaker of the ice ages: for 500,000 years, major climatic changes have followed variations in obliquity and precession, Science 194 (4270) (1976) 1121–1132, https://doi.org/10.1126/science.194.4270.1121.
[2] M. Lynas, B.Z. Houlton, S. Perry, Greater than 99% consensus on human caused climate change in the peer-reviewed scientific literature, Environ. Res. Lett. 16 (11) (2021) 114005, https://doi.org/10.1088/1748-9326/ac2966.
[3] IPCC, Summary for policymakers, in: H. Lee, J. Romero (Eds.), Climate Change 2023: Synthesis Report. Contribution of Working Groups I, II and III to the Sixth Assessment Report of the Intergovernmental Panel on Climate Change, IPCC, Geneva, Switzerland, 2023, pp. 1–34, https://doi.org/10.59327/IPCC/AR6-9789291691647.001.

[4] P. Friedlingstein, M.W. Jones, M. O'Sullivan, R.M. Andrew, D.C. Bakker, J. Hauck, J. Zeng, Global carbon budget 2021, Earth Syst. Sci. Data 14 (4) (2022) 1917–2005, https://doi.org/10.5194/essd-14-1917-2022.

[5] I.M. Held, B.J. Soden, Robust responses of the hydrological cycle to global warming, J. Clim. 19 (21) (2006) 5686–5699, https://doi.org/10.1175/JCLI3990.1.

[6] IPCC, Climate Change 2021: the Physical Science Basis. Contribution of Working Group I to the Sixth Assessment Report of the IPCC, Cambridge University Press, 2021. Chapter 11 "Weather and Climate Extreme Events in a Changing Climate".

[7] F.E. Otto, Attribution of extreme events to climate change, Annu. Rev. Environ. Resour. 48 (1) (2023) 813–828, https://doi.org/10.1146/annurev-environ-112621-083538.

[8] F.E. Otto, Attribution of extreme events to climate change, Annu. Rev. Environ. Resour. 48 (1) (2023) 813–828, https://doi.org/10.1146/annurev-environ-112621-083538.

[9] P. Mazzoglio, A. Viglione, D. Ganora, P. Claps, Mapping the uneven temporal changes in ordinary and extraordinary rainfall extremes in Italy, J. Hydrol.: Reg. Stud. 58 (2025) 102287, https://doi.org/10.1016/j.ejrh.2025.102287.

[10] EM-DAT, CRED/UCLouvain, Brussels, Belgium - Www.Emdat.Be.

[11] S.A. Benz, P. Blum, Global detection of rainfall-triggered landslide clusters, Nat. Hazards Earth Syst. Sci. 19 (7) (2019) 1433–1444, https://doi.org/10.5194/nhess-19-1433-2019.

[12] R. Emberson, D. Kirschbaum, T. Stanley, Global connections between El nino and landslide impacts, Nat. Commun. 12 (1) (2021) 2262, https://doi.org/10.1038/s41467-021-22398-4.

[13] M.T. Brunetti, S.L. Gariano, M. Melillo, M. Rossi, S. Peruccacci, An enhanced rainfall-induced landslide catalogue in Italy, Sci. Data 12 (1) (2025) 216, https://doi.org/10.1038/s41597-025-04551-6.

[14] S.L. Gariano, G. Rianna, How will the projected climate change influence rainfall-induced landslides in Europe? A review of modelling approaches, Landslides 22 (2025) 3011–3027, https://doi.org/10.1007/s10346-025-02550-7, 2025.

[15] S. Clò, F. David, S. Segoni, The impact of hydrogeological events on firms: evidence from Italy, J. Environ. Econ. Manag. 124 (2024) 102942, https://doi.org/10.1016/j.jeem.2024.102942.

[16] J.A. Rutllant, F. Matus, V. Rudloff, R. Rondanelli, The role of atmospheric rivers in rainfall-induced landslides: a study from the Elqui valley, J. Arid Environ. 216 (2023) 105016, https://doi.org/10.1016/j.jaridenv.2023.105016.

[17] Y. Zhu, R.E. Newell, A proposed algorithm for moisture fluxes from atmospheric rivers, Mon. Weather Rev. 126 (3) (1998) 725–735, https://doi.org/10.1175/1520-0493(1998)126%3C0725:APAFMF%3E2.0.CO;2.

[18] L. Zhao, M. Liu, Z. Song, S. Wang, Z. Zhao, S. Zuo, Regional-scale modeling of rainfall-induced landslides under random rainfall patterns, Environ. Model. Software 155 (2022) 105454, https://doi.org/10.1016/j.envsoft.2022.105454.

[19] S. Chelli, C. Wellstein, G. Campetella, R. Canullo, R. Tonin, S. Zerbe, R. Gerdol, Climate change response of vegetation across climatic zones in Italy, Clim. Res. 71 (2017) 249–262, https://doi.org/10.3354/cr01443.

[20] M.T. Löbmann, C. Geitner, C. Wellstein, S. Zerbe, The influence of herbaceous vegetation on slope stability–a review, Earth Sci. Rev. 209 (2020) 103328, https://doi.org/10.1016/j.earscirev.2020.103328.

[21] Sistema Nazionale Protezione Ambiente (SNPA), Il Clima in Italia Nel 2023, Report Ambientali SNPA, 2023, 42/2024 ISBN 978-88-448-1217-1 © Report ambientali SNPA, 42/2024, https://www.snpambiente.it/notizie/snpa/il-clima-in-italia-nel-2023/.

[22] L. Schilirò, A. Bosman, G.M. Caielli, A. Corazza, S. Crema, C. Di Salvo, P. Tommasi, The May 2023 rainstorm-induced landslides in the Emilia-Romagna region (Northern Italy): considerations from UAV investigations under emergency conditions, Geosciences 15 (3) (2025) 101, https://doi.org/10.3390/geosciences15030101.

[23] A. Biondi, L. Facheris, F. Argenti, F. Cuccoli, Comparison of different quantitative precipitation estimation methods based on a severe rainfall event in tuscany, Italy, November 2023, Remote Sens. 16 (21) (2024) 3985, https://doi.org/10.3390/rs16213985.

[24] M. Berti, M. Pizziolo, M. Scaroni, M. Generali, V. Critelli, M. Mulas, A. Corsini, RER2023: the landslide inventory dataset of the May 2023 Emilia-Romagna meteorological event, Earth Syst. Sci. Data 17 (3) (2025) 1055–1074, https://doi.org/10.5194/essd-17-1055-2025.

[25] ARPAE Agenzia regionale prevenzione ambiente Energia Emilia-Romagna (ARPAE) - https://www.arpae.it/it/notizie/alluvione-19-20-ottobre-un-analisi-preliminare (Accessed 15/July/2025).

[26] E. Flaounas, S. Davolio, S. Raveh-Rubin, F. Pantillon, M.M. Miglietta, M.A. Gaertner, D. Ricard, Mediterranean cyclones: current knowledge and open questions on dynamics, prediction, climatology and impacts, Weather Clim. Dyn. 3 (1) (2022) 173–208, https://doi.org/10.5194/wcd-3-173-2022.

[27] C.V. Makris, K. Tolika, V.N. Baltikas, K. Velikou, Y.N. Krestenitis, The impact of climate change on the storm surges of the Mediterranean Sea: coastal sea level responses to deep depression atmospheric systems, Ocean Model. 181 (2023) 102149, https://doi.org/10.1016/j.ocemod.2022.102149.

[28] H.C. Bloomfield, J. Hillier, A. Griffin, A.L. Kay, L.C. Shaffrey, F. Pianosi, P.D. Bates, Co-occurring wintertime flooding and extreme wind over Europe, from daily to seasonal timescales, Weather Clim. Extrem. 39 (2023) 100550, https://doi.org/10.1016/j.wace.2023.100550.

[29] ARPAL Agenzia Regionale per la Protezione Dell'Ambiente Ligure (ARPAL) -https://www.arpal.liguria.it/home-page/notizie-tematiche/item/ciaran-e-vaia-nel-video-le-mareggiate-a-confronto.html (accessed 15/July/2025).

[30] ARPA-FVG Agenzia Regionale per la Protezione Dell'Ambiente del Friuli Venezia Giulia (ARPA-FVG) - https://www.meteo.fvg.it/clima/clima_fvg/03_cambiamenti_climatici/07_GRUPPO_DI_LAVORO_CLIMA_FVG_e_Segnali_dal_Clima/SegnaliDalClimaFVG2024.pdf (accessed 15/July/2025).

[31] A. Sharma, H. Sajjad, Roshani, M.H. Rahaman, A systematic review for assessing the impact of climate change on landslides: research gaps and directions for future research, Spatial Inf. Res. 32 (2) (2023) 165–185, https://doi.org/10.1007/s41324-023-00551-z.

[32] M. Delchiaro, M. Della Seta, S. Martino, M. Dehbozorgi, R. Nozaem, Reconstruction of river valley evolution before and after the emplacement of the giant Seymareh rock avalanche (Zagros Mts., Iran), Earth Surf. Dyn. 7 (4) (2019) 929–947, https://doi.org/10.5194/esurf-7-929-2019.

[33] M. Delchiaro, M. Della Seta, S. Martino, M. Moumeni, R. Nozaem, G.M. Marmoni, C. Esposito, The role of long-term preparatory factors in mass rock creep deforming slopes: insights from the Zagros Mts. belt (Iran), Landslides (2024) 1–21, https://doi.org/10.1007/s10346-024-02252-6.

[34] P. Reichenbach, M. Rossi, B.D. Malamud, M. Mihir, F. Guzzetti, A review of statistically-based landslide susceptibility models, Earth Sci. Rev. 180 (2018) 60–91, https://doi.org/10.1016/j.earscirev.2018.03.001.

[35] E. Conte, L. Pugliese, A. Troncone, A simple method for predicting rainfall-induced shallow landslides, J. Geotech. Geoenviron. Eng. 148 (10) (2022) 04022079, https://doi.org/10.1061/(ASCE)GT.1943-5606.0002877.

[36] A.C. Mondini, F. Guzzetti, M. Melillo, Deep learning forecast of rainfall-induced shallow landslides, Nat. Commun. 14 (1) (2023) 2466, https://doi.org/10.1038/s41467-023-38135-y.

[37] F. Guzzetti, M. Melillo, A.C. Mondini, Landslide predictions through combined rainfall threshold models, Landslides 22 (1) (2025) 137–147, https://doi.org/10.1007/s10346-024-02340-7.

[38] M. Delchiaro, J. Rouhi, M. Valiante, M. Della Seta, C. Esposito, et al., Bivariate landslide susceptibility analysis in the Lorestan Arc (Zagros Mountains, Iran), Italian Journal of Engineering Geology and Environment (2021) 53–66, https://doi.org/10.4408/IJEGE.2021-01.S-05.

[39] G.B. Crosta, P.J.N.H. Frattini, Distributed modelling of shallow landslides triggered by intense rainfall, Nat. Hazards Earth Syst. Sci. 3 (1/2) (2003) 81–93, https://doi.org/10.5194/nhess-3-81-2003.

[40] Q. Ran, Y. Hong, W. Li, J. Gao, A modelling study of rainfall-induced shallow landslide mechanisms under different rainfall characteristics, J. Hydrol. 563 (2018) 790–791, https://doi.org/10.1016/j.jhydrol.2018.06.040.

[41] Y. Liu, Z. Deng, X. Wang, The effects of rainfall, soil type and slope on the processes and mechanisms of rainfall-induced shallow landslides, Appl. Sci. 11 (24) (2021) 11652, https://doi.org/10.3390/app112411652.

[42] J. Mathew, D.G. Babu, S. Kundu, C.C. Pant, K.V. Kumar, Integrating intensity–duration-based rainfall threshold and antecedent rainfall-based probability estimate towards generating early warning for rainfall-induced landslides in parts of the Garhwal Himalaya, India, Landslides 11 (2014) 575–588, https://doi.org/10.1007/s10346-013-0408-2.

[43] S.W. Kim, K.W. Chun, M. Kim, F. Catani, B. Choi, J.I. Seo, Effect of antecedent rainfall conditions and their variations on shallow landslide-triggering rainfall thresholds in South Korea, Landslides 18 (2) (2021) 569–582, https://doi.org/10.1007/s10346-020-01505-4.
[44] M. Zocchi, M. Delchiaro, F. Troiani, G. Scarascia Mugnozza, P. Mazzanti, PS-InSAR post-processing for assessing the spatio-temporal differential kinematics of complex landslide systems: a case study of DeBeque Canyon Landslide (Colorado, USA), Earth Surf. Process. Landf. 49 (14) (2024) 4862–4880, https://doi.org/10.1002/esp.6002.
[45] M. Bittelli, R. Valentino, F. Salvatorelli, P.R. Pisa, Monitoring soil-water and displacement conditions leading to landslide occurrence in partially saturated clays, Geomorphology 173 (2012) 161–173, https://doi.org/10.1016/j.geomorph.2012.06.006.
[46] T.A. Bogaard, R. Greco, Landslide hydrology: from hydrology to pore pressure, Wiley Interdiscip. Rev.: Water 3 (3) (2016) 439–459, https://doi.org/10.1002/wat2.1126.
[47] T. Bogaard, R. Greco, Invited perspectives: hydrological perspectives on precipitation intensity–duration thresholds for landslide initiation: proposing hydro-meteorological thresholds, Nat. Hazards Earth Syst. Sci. 18 (1) (2018) 31–39, https://doi.org/10.5194/nhess-18-31-2018.
[48] A. Wicki, P. Lehmann, C. Hauck, S.I. Seneviratne, P. Waldner, M. Stähli, Assessing the potential of soil moisture measurements for regional landslide early warning, Landslides 17 (8) (2020) 1881–1896, https://doi.org/10.1007/s10346-020-01400-y.
[49] M. Delchiaro, F. Vergari, C. Esposito, M. Del Monte, The influence of anthropogenic topographic changes on geomorphological processes in the city of Rome (Italy): a case study of the Malagrotta area, Earth Surf. Process. Landf. 50 (3) (2025) e70033, https://doi.org/10.1002/esp.70033.
[50] M.J. Crozier, Deciphering the effect of climate change on landslide activity: a review, Geomorphology 124 (3–4) (2010) 260–267, https://doi.org/10.1016/j.geomorph.2010.04.009.
[51] S.L. Gariano, F. Guzzetti, Landslides in a changing climate, Earth Sci. Rev. 162 (2016) 227–252, https://doi.org/10.1016/j.earscirev.2016.08.011.
[52] J.L. Wong, M.L. Lee, F.Y. Teo, K.W. Liew, A review of impacts of climate change on slope stability, in: S. Kolathayar, A. Mondal, S.C. Chian (Eds.), Climate Change and Water Security, Lecture Notes in Civil Engineering, 178, Springer, Singapore, 2021, https://doi.org/10.1007/978-981-16-5501-2_13.
[53] M. Delchiaro, G. Iacobucci, M. Della Seta, N. Gribenski, D. Piacentini, V. Ruscitto, F. Troiani, A fluvial record of late Quaternary climate changes and tectonic uplift along the Marche Piedmont zone of the Apennines: new insights from the Tesino River (Italy), Geomorphology 445 (2024) 108971, https://doi.org/10.1016/j.geomorph.2023.108971.
[54] M. Delchiaro, V. Ruscitto, W. Schwanghart, E. Brignone, D. Piacentini, F. Troiani, BankfullMapper: a semi-automated MATLAB tool on high-resolution digital terrain models for spatio-temporal monitoring of bankfull geometry and discharge, Comput. Geosci. (2025) 106001, https://doi.org/10.1016/j.cageo.2025.106001.
[55] G. Iacobucci, M. Delchiaro, F. Troiani, D. Nadali, Land-surface quantitative analysis for mapping and deciphering the construction processes of piedmont alluvial fans in the Anti-Lebanon Mountains, Geomorphology 453 (2024) 109148, https://doi.org/10.1016/j.geomorph.2024.109148.
[56] G. Iacobucci, V. Ruscitto, M. Delchiaro, F. Troiani, M. Della Seta, D. Piacentini, The contribution of geomorphology on climate services: recent developments on the assessment of climate-impact indicators in the frame of the PNRR RETURN project, Geogr. Fis. Din. Quaternaria 48 (1–2) (2025) 59–71, https://doi.org/10.4454/fgrt74jk.
[57] V. Ruscitto, M. Delchiaro, M. Richard, G. Iacobucci, D. Piacentini, F. Troiani, M. Della Seta, Quaternary landscape evolution of Apennines peri adriatic belt: insights from climate and tectonics, Sci. Adv. (2026), https://doi.org/10.1126/sciadv.aec5376.
[58] M.E. Discenza, C. Esposito, E. Di Luzio, M. Delchiaro, D. Di Martire, M. Minnillo, G.S. Mugnozza, Deep-seated gravitational slope deformations in Molise region (Italy): novel inventory and main geomorphological features, J. Maps 19 (1) (2023) 2163198, https://doi.org/10.1080/17445647.2022.2163198.
[59] F. Avanzi, C. De Michele, S. Gabriele, A. Ghezzi, R. Rosso, Orographic signature on extreme precipitation of short durations, J. Hydrometeorol. 16 (1) (2015) 278–294, https://doi.org/10.1175/JHM-D-14-0063.1.
[60] P. Mazzoglio, I. Butera, M. Alvioli, P. Claps, The role of morphology in the spatial distribution of short-duration rainfall extremes in Italy, Hydrol. Earth Syst. Sci. 26 (2022) 1659–1672, https://doi.org/10.5194/hess-26-1659-2022.
[61] P. Mazzoglio, I. Butera, P. Claps, A local regression approach to analyze the orographic effect on the spatial variability of sub-daily rainfall annual maxima, Geomat. Nat. Hazards Risk 14 (1) (2023) 2205000, https://doi.org/10.1080/19475705.2023.2205000.
[62] A. Buzzi, N. Tartaglione, P. Malguzzi, Numerical simulations of the 1994 Piedmont flood: role of orography and moist processes, Mon. Wea. Rev. 126 (1998) 2369–2383, https://doi.org/10.1175/1520-0493(1998)126,2369:NSOTPF.2.0.CO;2.
[63] R. Rudari, D. Entekhabi, G. Roth, Large-scale atmospheric patterns associated with mesoscale features leading to extreme precipitation events in northwestern Italy, Adv. Water Resour. 28 (2005) 601–614, https://doi.org/10.1016/j.advwatres.2004.10.017.
[64] I.F. Trigo, T.D. Davies, G.R. Bigg, Objective climatology of cyclones in the mediterranean region, J. Clim. 12 (1999) 1685–1696, https://doi.org/10.1175/1520-0442(1999)012<1685:OCOCIT>2.0.CO;2.
[65] M. Brunetti, G. Lentini, M. Maugeri, T. Nanni, I. Auer, R. Böhm, W. Schöner, Climate variability and change in the greater alpine region over the last two centuries based on multi-variable analysis, Int. J. Climatol. 29 (15) (2009) 2197–2225, https://doi.org/10.1002/joc.1857.
[66] A. Crespi, M. Brunetti, G. Lentini, M. Maugeri, 1961–1990 high-resolution monthly precipitation climatologies for Italy, Int. J. Climatol. 3 (2018) 878–895, https://doi.org/10.1002/joc.5217.
[67] C. Frei, C. Schär, A precipitation climatology of the Alps from high-resolution rain-gauge observations, Int. J. Climatol. 18 (1998) 873–900, https://doi.org/10.1002/(SICI)1097-0088(19980630)18:8%3C873::AID-JOC255%3E3.0.CO;2-9.
[68] M. Cannarozzo, L. Noto, F. Viola, Spatial distribution of rainfall trends in Sicily (1921–2000), Phys. Chem. Earth 31 (2006) 1201–1211, https://doi.org/10.1016/j.pce.2006.03.022.
[69] E. Caporali, M. Lompi, T. Pacetti, V. Chiarello, S. Fatichi, A review of studies on observed precipitation trends in Italy, Int. J. Climatol. 41 (1) (2021) E1–E25, https://doi.org/10.1002/joc.6741.
[70] S.M. Vicente-Serrano, Y. Tramblay, F. Reig, et al., High temporal variability not trend dominates mediterranean precipitation, Nature 639 (2025) 658–666, https://doi.org/10.1038/s41586-024-08576-6.
[71] A. Crisci, B. Gozzini, F. Meneguzzo, S. Pagliara, G. Maracchi, Extreme rainfall in a changing climate: regional analysis and hydrological implications in Tuscany, Hydrol. Process. 16 (6) (2002) 1261–1274, https://doi.org/10.1002/hyp.1061.
[72] B. Bonaccorso, A. Cancelliere, G. Rossi, Detecting trends of extreme rainfall series in Sicily, Adv. Geosci. 2 (2005) 7–11, https://doi.org/10.5194/adgeo-2-7-2005.
[73] E. Arnone, D. Pumo, F. Viola, L.V. Noto, G. La Loggia, Rainfall statistics changes in Sicily, Hydrol. Earth Syst. Sci. 17 (7) (2013) 2449–2458, https://doi.org/10.5194/hess-17-2449-2013.
[74] S. Persiano, E. Ferri, G. Antolini, A. Domeneghetti, V. Pavan, A. Castellarin, Changes in seasonality and magnitude of sub-daily rainfall extremes in Emilia-Romagna (Italy) and potential influence on regional rainfall frequency estimation, J. Hydrol.: Reg. Stud. 32 (2020) 100751, https://doi.org/10.1016/j.ejrh.2020.100751.
[75] A. Avino, L. Cimorelli, P. Furcolo, L.V. Noto, A. Pelosi, D. Pianese, S. Manfreda, Are rainfall extremes increasing in southern Italy? J. Hydrol. 631 (2024) 130684 https://doi.org/10.1016/j.jhydrol.2024.130684.
[76] D. Treppiedi, G. Cipolla, A. Francipane, L.V. Noto, Detecting precipitation trend using a multiscale approach based on quantile regression over a Mediterranean area, Int. J. Clim. 41 (2021) 5938–5955, https://doi.org/10.1002/joc.7161.
[77] R. Roseto, P. Dellino, D. Capolongo, Spatial distribution and trend analysis of extreme rainfall time series in Apulia region (Italy), Phys. Geogr. Quat. Dyn 46 (2024) 163–177, https://doi.org/10.4454/jt76er4b.
[78] A. Libertino, D. Ganora, P. Claps, Evidence for increasing rainfall extremes remains elusive at large spatial scales: the case of Italy, Geophys. Res. Lett. 46 (13) (2019) 7437–7446, https://doi.org/10.1029/2019GL083371.
[79] H. Ayat, J.P. Evans, S.C. Sherwood, J. Soderholm, Intensification of subhourly heavy rainfall, Science 378 (6620) (2022) 655–659, https://doi.org/10.1126/science.abn8657.

[80] M. Kendon, M. McCarthy, S. Jevrejeva, A. Matthews, T. Legg, State of the UK climate 2018, Int. J. Climatol. 39 (Suppl. 1) (2019) 1–55, https://doi.org/10.1002/joc.6213.
[81] E. Dallan, M. Borga, M. Zaramella, F. Marra, Enhanced summer convection explains observed trends in extreme subdaily precip-itation in the Eastern Italian alps, Geophys. Res. Lett. 49 (5) (2022), https://doi.org/10.1029/2021GL096727 e2021GL096727.
[82] F. Giorgi, Climate change hot-spots, Geophys. Res. Lett. 33 (8) (2006), https://doi.org/10.1029/2006GL025734.
[83] F. Giorgi, C. Jones, G. Asrar, Addressing climate information needs at the regional level: the CORDEX framework, WMO Bull 58 (3) (2009) 175–183. https://public.wmo.int/media/magazine-article/addressing-climate-information-needs-regional-level-cordex-framework.
[84] D. Maraun, M. Widmann, Statistical Downscaling and Bias Correction for Climate Research, Cambridge University Press, Cambridge, 2018, https://doi.org/10.1017/9781107588783.
[85] P.M. Ruti, S. Somot, F. Giorgi, C. Dubois, E. Flaounas, A. Obermann, V. Vervatis, MED-CORDEX initiative for Mediterranean climate studies, Bull. Am. Meteorol. Soc. 97 (7) (2016) 1187–1208, https://doi.org/10.1175/BAMS-D-14-00176.1.
[86] A.F. Prein, W. Langhans, G. Fosser, A. Ferrone, N. Ban, K. Goergen, et al., A review on regional convection-permitting climate modeling: demonstrations, prospects, and challenges, Rev. Geophys. 53 (2) (2015) 323–361, https://doi.org/10.1002/2014RG000475.
[87] P. Lucas-Picher, D. Argüeso, E. Brisson, Y. Tramblay, P. Berg, A. Lemonsu, S. Kotlarski, C. Caillaud, Convection-permitting modeling with regional climate models: latest developments and next steps, Wiley Interdiscip. Rev. Clim. Change 12 (6) (2021) e731, https://doi.org/10.1002/wcc.731.
[88] E. Dallan, F. Marra, G. Fosser, M. Marani, G. Formetta, C. Schär, M. Borga, How well does a convection-permitting regional climate model represent the reverse orographic effect of extreme hourly precipitation? Hydrol. Earth Syst. Sci. 27 (5) (2023) 1133–1149, https://doi.org/10.5194/hess-27-1133-2023.
[89] N. Ban, C. Caillaud, E. Coppola, E. Pichelli, S. Sobolowski, M. Adinolfi, B. Ahrens, A. Alias, I. Anders, S. Bastin, D. Belušić, S. Berthou, E. Brisson, R.M. Cardoso, S.C. Chan, O.B. Christensen, J. Fernández, L. Fita, T. Frisius, G. Gasparac, F. Giorgi, K. Goergen, J.E. Haugen, Ø. Hodnebrog, S. Kartsios, E. Katragkou, E. J. Kendon, K. Keuler, A. Lavin-Gullon, G. Lenderink, D. Leutwyler, T. Lorenz, D. Maraun, P. Mercogliano, J. Milovac, H.-J. Panitz, M. Raffa, A. Reca Remedio, C. Schär, P.M.M. Soares, L. Srnec, B.M. Steensen, P. Stocchi, M.H. Tolle, H. Truhetz, J. Vergara- Temprado, M.H. de Vries, K. Warrach-Sagi, V. Wulfmeyer, M. J. Zander, The first multi-model ensemble of regional climate simulations at kilometer-scale resolution, part I: evaluation of precipitation, Clim. Dyn. 57 (1) (2021) 275–302, https://doi.org/10.1007/s00382-021-05708-w.
[90] E. Pichelli, E. Coppola, S. Sobolowski, N. Ban, F. Giorgi, P. Stocchi, J. Vergara-Temprado, The first multi-model ensemble of regional climate simulations at kilometer-scale resolution part 2: historical and future simulations of precipitation, Clim. Dyn. 56 (11) (2021) 3581–3602, https://doi.org/10.1007/s00382-021-05657-4.
[91] E. Dallan, M. Borga, G. Fosser, A. Canale, B. Roghani, M. Marani, F. Marra, A method to assess and explain changes in sub-daily precipitation return levels from convection-permitting simulations, Water Resour. Res. 60 (5) (2024) e2023WR035969, https://doi.org/10.1029/2023WR035969.
[92] E. Dallan, F. Marra, G. Fosser, M. Marani, M. Borga, Dynamical factors heavily modulate the future increase of sub-daily extreme precipitation in the alpine-mediterranean region, Earths Future 12 (2024), https://doi.org/10.1029/2024EF005185 e2024EF005185.
[93] M. Raffa, M. Adinolfi, A. Reder, G.F. Marras, M. Mancini, G. Scipione, P. Mercogliano, Very high resolution projections over Italy under different CMIP5 IPCC scenarios, Sci. Data 10 (1) (2023) 238, https://doi.org/10.1038/s41597-023-02144-9.
[94] M. Lompi, F. Marra, R. Deidda, E. Caporali, M. Borga, E. Dallan, Non-stationary frequency analysis of long-term Convection Permitting simulations reveals sub-daily extreme precipitation changes in central-southern Europe, Adv. Water Resour. (2025) 105071, https://doi.org/10.1016/j.advwatres.2025.105071.
[95] M.V. Struglia, A. Anav, M. Antonelli, S. Calmanti, F. Catalano, A. Dell'Aquila, E. Pichelli, G. Pisacane, Impact of spatial resolution on multi-scenario WRF-ARW simulations driven by the CMIP6 MPI-ESM1-2-HR global model: a focus on precipitation distribution over Italy, Geosci. Model Dev. 18 (2025) 6095–6116, https://doi.org/10.5194/gmd-18-6095-2025.
[96] N. Ban, J. Rajczak, J. Schmidli, C. Schär, Analysis of Alpine precipitation extremes using generalized extreme value theory in convection-resolving climate simulations, Clim. Dyn. 55 (1–2) (2020) 61–75, https://doi.org/10.1007/s00382-018-4339-4.
[97] P. Mazzoglio, M. Lompi, F. Marra, E. Dallan, R. Deidda, P. Claps, S. Manfreda, L.V. Noto, A. Viglione, M. Raffa, P. Mercogliano, M. Marani, E. Caporali, M. Borga, Orographic and land-sea contrast effects in convection-permitting simulations of extreme sub-daily precipitation, Weather Clim. Extrem. (2025) 100798, https://doi.org/10.1016/j.wace.2025.100798.
[98] F. Marra, E. Dallan, M. Borga, R. Greco, T. Bogaard, Brief communication: threshold not probability. The conceptual difference between ID thresholds for landslide initiation and IDF curves, EGUsphere (2025), https://doi.org/10.5194/egusphere-2025-3378 [preprint].
[99] A. Collison, S. Wade, J. Griffiths, M. Dehn, Modelling the impact of predicted climate change on landslide frequency and magnitude in SE England, Eng. Geol. 55 (3) (2000) 205–218, https://doi.org/10.1016/S0013-7952(99)00121-0.
[100] M. Dehn, G. Bürger, J. Buma, P. Gasparetto, Impact of climate change on slope stability using expanded downscaling, Eng. Geol. 55 (3) (2000) 193–204, https://doi.org/10.1016/S0013-7952(99)00123-4.
[101] N. Dixon, E. Brook, Impact of predicted climate change on landslide reactivation: case study of Mam Tor, UK, Landslides 4 (2) (2007) 137–147, https://doi.org/10.1007/s10346-006-0071-y.
[102] M. Jakob, S. Lambert, Climate change effects on landslides along the southwest coast of British Columbia, Geomorphology 107 (3–4) (2009) 275–284, https://doi.org/10.1016/j.geomorph.2008.12.009.
[103] M. Jakob, T. Owen, Projected effects of climate change on shallow landslides, North Shore Mountains, Vancouver, Canada, Geomorphology 393 (2021) 107921, https://doi.org/10.1016/j.geomorph.2021.107921.
[104] V. Jomelli, D. Brunstein, M. Déqué, M. Vrac, D. Grancher, Impacts of future climatic change (2070–2099) on the potential occurrence of debris flows: a case study in the Massif des Ecrins (French Alps), Clim. Change 97 (1–2) (2009) 171–191, https://doi.org/10.1007/s10584-009-9616-0.
[105] M. Schmidt, T. Glade, Linking global circulation model outputs to regional geomorphic models: a case study of landslide activity in New Zealand, Clim. Res. 25 (2003) 135–152, https://doi.org/10.3354/cr025135.
[106] M. Stoffel, T. Mendlik, M. Schneuwly-Bollschweiler, A. Gobiet, Possible impacts of climate change on debris-flow activity in the Swiss Alps, Clim. Change 122 (1–2) (2014) 141–155, https://doi.org/10.1007/s10584-013-0993-z.
[107] J.L. Zêzere, R.M. Trigo, I.F. Trigo, Shallow and deep landslides induced by rainfall in the Lisbon region (Portugal): assessment of relationships with the North Atlantic Oscillation, Nat. Hazards Earth Syst. Sci. 5 (3) (2005) 331–344, https://doi.org/10.5194/nhess-5-331-2005.
[108] N. Caine, The rainfall intensity-duration control of shallow landslides and debris flows, Geogr. Ann. Phys. Geogr. 62 (1–2) (1980) 23–27.
[109] F. Guzzetti, S. Peruccacci, M. Rossi, C.P. Stark, The rainfall intensity-duration control of shallow landslides and debris flows: an update, Landslides 5 (1) (2008) 3–17, https://doi.org/10.1007/s10346-007-0112-1.
[110] F. Guzzetti, S. Peruccacci, M. Rossi, C.P. Stark, Rainfall thresholds for the initiation of landslides in central and southern Europe, Meteorol. Atmos. Phys. 98 (3) (2007) 239–267, https://doi.org/10.1007/s00703-007-0262-7.
[111] S. Segoni, L. Piciullo, S.L. Gariano, A review of the recent literature on rainfall thresholds for landslide occurrence, Landslides 15 (8) (2018) 1483–1501, https://doi.org/10.1007/s10346-018-0966-4.
[112] Stefano Luigi Gariano, Massimo Melillo, Silvia Peruccacci, Maria Teresa Brunetti, How much does the rainfall temporal resolution affect rainfall thresholds for landslide triggering? Natural Hazards 100 (2) (2019) 655–670, https://doi.org/10.1007/s11069-019-03830-x. (Accessed 31 December 2019).
[113] M.T. Abraham, N. Satyam, S. Kushal, A. Rosi, B. Pradhan, S. Segoni, Rainfall threshold estimation and landslide forecasting for Kalimpong, India using SIGMA model, Water 12 (4) (2020) 1195, https://doi.org/10.3390/w12041195.
[114] Bui D. Tien, B. Pradhan, O. Lofman, I. Revhaug, Ø.B. Dick, Regional prediction of landslide hazard using probability analysis of intense rainfall in the Hoa Binh province, Vietnam, Nat. Hazards 66 (2) (2013) 707–730, https://doi.org/10.1007/s11069-012-0510-0.
[115] Nader Saadatkhah, Azman Kassim, Lee Min Lee, Hulu Kelang, Malaysia regional mapping of rainfall-induced landslides using TRIGRS model, Arabian Journal of Geosciences 8 (5) (2014) 3183–3194, https://doi.org/10.1007/s12517-014-1410-2. (Accessed 22 April 2014).
[116] S. Lee, J.S. Won, S.W. Jeon, I. Park, M.J. Lee, Spatial landslide hazard prediction using rainfall probability and a logistic regression model, Math. Geosci. 47 (5) (2015) 565–589, https://doi.org/10.1007/s11004-014-9560-z.

[117] P. Jaiswal, C.J. van Westen, Estimating temporal probability for landslide initiation along transportation routes based on rainfall thresholds, Geomorphology 112 (2009) 96–105, https://doi.org/10.1016/j.geomorph.2009.05.008.

[118] M.L. Lee, K.Y. Ng, Y.F. Huang, W.C. Li, Rainfall-induced landslides in Hulu Kelang area, Malaysia, Nat. Hazards 70 (2014) 353–375, https://doi.org/10.1007/s11069-013-0814-8.

[119] T. Ma, C. Li, Z. Lu, B. Wang, An effective antecedent precipitation model derived from the power-law relationship between landslide occurrence and rainfall level, Geomorphology 216 (2014) 187–192, https://doi.org/10.1016/j.geomorph.2014.03.033.

[120] C. Kanjanakul, T. Chub-Uppakarn, T. Chalermyanont, Rainfall thresholds for landslide early warning system in Nakhon Si Thammarat, Arab J Geosci 9 (2016) 584, https://doi.org/10.1007/s12517-016-2614-4.

[121] S. Liu, J. Du, K. Yin, C. Zhou, C. Huang, J. Jiang, J. Yu, Regional early warning model for rainfall induced landslide based on slope unit in Chongqing, China, Eng. Geol. 333 (2024) 107464, https://doi.org/10.1016/j.enggeo.2024.107464.

[122] X. Liang, S. Segoni, W. Fan, K. Yin, L. Deng, T. Xiao, N. Casagli, Integration of effective antecedent rainfall to improve the performance of rainfall thresholds for landslide early warning in Wanzhou District, China, Int. J. Disaster Risk Reduct. 119 (2025) 105317, https://doi.org/10.1016/j.ijdrr.2025.105317.

[123] G. Martelloni, S. Segoni, R. Fanti, F. Catani, Rainfall thresholds for the forecasting of landslide occurrence at regional scale, Landslides 9 (4) (2012) 485–495, https://doi.org/10.1007/s10346-011-0308-2.

[124] R. Greco, M. Giorgio, G. Capparelli, P. Versace, Early warning of rainfall-induced landslides based on empirical mobility function predictor, Eng. Geol. 153 (2013) 68–79, https://doi.org/10.1016/j.enggeo.2012.11.009.

[125] A. Rosi, S. Segoni, V. Canavesi, A. Monni, A. Gallucci, N. Casagli, Definition of 3D rainfall thresholds to increase operative landslide early warning system performances, Landslides 18 (3) (2021) 1045–1057, https://doi.org/10.1007/s10346-020-01523-2.

[126] N. Nocentini, C. Medici, F. Barbadori, A. Gatto, R. Franceschini, M. del Soldato, S. Segoni, Optimization of rainfall thresholds for landslide early warning through false alarm reduction and a multi-source validation, Landslides 21 (3) (2024) 557–571, https://doi.org/10.1007/s10346-023-02176-7.

[127] P. Marino, D.J. Peres, A. Cancelliere, R. Greco, T.A. Bogaard, Soil moisture information can improve shallow landslide forecasting using the hydrometeorological threshold approach, Landslides 17 (9) (2020) 2041–2054, https://doi.org/10.1007/s10346-020-01420-8.

[128] T. Halter, P. Lehmann, A. Wicki, J. Aaron, M. Stähli, Optimising landslide initiation modelling with high-resolution saturation prediction based on soil moisture monitoring data, Landslides (2024) 1–18, https://doi.org/10.1007/s10346-024-02304-x.

[129] S. Zhang, M. Calvello, G. Pecoraro, Integrating rainfall severity and soil saturation indices to define hydro-meteorological thresholds for landslides, J. Hydrol. 654 (2025) 130211, https://doi.org/10.1016/j.jhydrol.2025.132873.

[130] B.B. Mirus, M.D. Morphew, J.B. Smith, Developing hydro-meteorological thresholds for shallow landslide initiation and early warning, Water 10 (9) (2018) 1274, https://doi.org/10.3390/w10091274.

[131] J.L. Conrad, M.D. Morphew, R.L. Baum, B.B. Mirus, HydroMet: a new code for automated objective optimization of hydrometeorological thresholds for landslide initiation, Water 13 (13) (2021) 1752, https://doi.org/10.3390/w13131752.

[132] R.M. Palau, M. Berenguer, M. Hürlimann, D. Sempere-Torres, Implementation of hydrometeorological thresholds for regional landslide warning in Catalonia (NE Spain), Landslides 20 (10) (2023) 2039–2054, https://doi.org/10.1007/s10346-023-02094-8.

[133] C.W.W. Ng, B. Yang, Z.Q. Liu, J.S.H. Kwan, L. Chen, Spatiotemporal modelling of rainfall-induced landslides using machine learning, Landslides 18 (2021) 2499–2514, https://doi.org/10.1007/s10346-021-01662-0.

[134] Z. Liu, G. Gilbert, J.M. Cepeda, A.O.K. Lysdahl, L. Piciullo, H. Hefre, S. Lacasse, Modelling of shallow landslides with machine learning algorithms, Geosci. Front. 12 (2021) 385–393, https://doi.org/10.1016/j.gsf.2020.04.014.

[135] T.A. Stanley, D.B. Kirschbaum, G. Benz, R.A. Emberson, P.M. Amatya, W. Medwedeff, M.K. Clark, Data-driven landslide nowcasting at the global scale, Front. Earth Sci. 9 (2021), https://doi.org/10.3389/feart.2021.640043.

[136] P. Distefano, D.J. Peres, P. Scandura, A. Cancelliere, Brief communication: introducing rainfall thresholds for landslide triggering based on artificial neural networks, Nat. Hazards 22 (2022) 1151–1157, https://doi.org/10.5194/nhess-22-1151-2022.

[137] N. Nocentini, A. Rosi, S. Segoni, R. Fanti, Towards landslide space-time forecasting through machine learning: the influence of rainfall parameters and model setting, Front. Earth Sci. 11 (2023) 1152130, https://doi.org/10.3389/feart.2023.1152130.

[138] N. Nocentini, A. Rosi, L. Piciullo, Z. Liu, S. Segoni, R. Fanti, Regional-scale spatiotemporal landslide probability assessment through machine learning and potential applications for operational warning systems: a case study in Kvam (Norway), Landslides 21 (10) (2024) 2369–2387, https://doi.org/10.1007/s10346-024-02287-9.

[139] F.S. Tehrani, M. Calvello, Z. Liu, L. Zhang, S. Lacasse, Machine learning and landslide studies: recent advances and applications, Nat. Hazards (2022), https://doi.org/10.1007/s11069-022-05423-7.

[140] B. Jin, S. Liu, T. Zeng, Y. Li, T. Wang, L. Gui, K. Yin, Spatio-temporal forecasting of landslide hazard in Chongqing National Transmission Protection Regions, China, Int. J. Digit. Earth 17 (1) (2024) 2392843, https://doi.org/10.1080/17538947.2024.2392843.

[141] F. Cantonati, G. Lissari, F. Vagnon, et al., From Alpine catchment classification to debris flow monitoring, GeoHazards 6 (2025) 15, https://doi.org/10.3390/geohazards6010015.

[142] D. Vianello, F. Vagnon, S. Bonetto, et al., Debris flow susceptibility mapping using the rock engineering system (RES) method: a case study, Landslides 20 (2023) 735–756, https://doi.org/10.1007/s10346-022-01985-6.

[143] S. Segoni, R.S. Ajin, N. Nocentini, R. Fanti, Insights gained from the review of landslide susceptibility assessment studies in Italy, Remote Sens. 16 (2024) 1–31, https://doi.org/10.3390/rs16234491.

[144] H.R. Pourghasemi, Z. Teimoori Yansari, P. Panagos, B. Pradhan, Analysis and evaluation of landslide susceptibility: a review on articles published during 2005–2016 (periods of 2005–2012 and 2013–2016), Arabian J. Geosci. 11 (9) (2018) 193, https://doi.org/10.1007/s12517-018-3531-5.

[145] F. Catani, D. Lagomarsino, S. Segoni, V. Tofani, Landslide susceptibility estimation by random forests technique: sensitivity and scaling issues, Nat. Hazards Earth Syst. Sci. 13 (11) (2013) 2815–2831, https://doi.org/10.5194/nhess-13-2815-2013.

[146] Odin Marc, Marielle Gosset, Hitoshi Saito, Taro Uchida, Jean-Philippe Malet, Spatial Patterns of Storm-Induced Landslides and Their Relation to Rainfall Anomaly Maps, Geophysical Research Letters 46 (20) (2019) 11167–11177, https://doi.org/10.1029/2019gl083173. (Accessed 28 October 2019).

[147] F. Caleca, P. Confuorto, F. Raspini, S. Segoni, V. Tofani, N. Casagli, S. Moretti, Shifting from traditional landslide occurrence modeling to scenario estimation with a "glass-box" machine learning, Sci. Total Environ. 950 (2024) 175277, https://doi.org/10.1016/j.scitotenv.2024.175277.

[148] G.F. Wieczorek, T. Glade, Climatic factors influencing occurrence of debris flows, in: M. Jakob, O. Hungr (Eds.), Debris Flow Hazards and Related Phenomena, Springer, Berlin Heidelberg, 2005, pp. 325–362, https://doi.org/10.1007/3-540-27129-5_14.

[149] Tongsan Lann, Han Bao, Hengxing Lan, Han Zheng, Changgen Yan, et al., Hydro-mechanical effects of vegetation on slope stability: A review, Science of The Total Environment 926 (2024) 171691, https://doi.org/10.1016/j.scitotenv.2024.171691.

[150] F. Ponziani, C. Pandolfo, M. Stelluti, et al., Assessment of rainfall thresholds and soil moisture modeling for operational hydrogeological risk prevention in the Umbria region (Central Italy), Landslides 9 (2012) 229–237, https://doi.org/10.1007/s10346-011-0287-3.

[151] D.B. Kirschbaum, R. Adler, Y. Hong, A. Lerner-Lam, Evaluation of a preliminary satellite-based landslide hazard algorithm using global landslide inventories, Nat. Hazards Earth Syst. Sci. 9 (2009) 673–686, https://doi.org/10.5194/nhess-9-673-2009.

[152] D.B. Kirschbaum, R. Adler, Y. Hong, et al., Advances in landslide nowcasting: evaluation of a global and regional modeling approach, Environ. Earth Sci. 66 (2012) 1683–1696, https://doi.org/10.1007/s12665-011-0990-3.

[153] A. Fares, M. Temimi, K. Morgan, T.J. Kelleners, In-situ and remote soil moisture sensing technologies for vadose zone hydrology, Vadose Zone J. 12 (2) (2013) 1–3, https://doi.org/10.2136/vzj2013.03.0058.

[154] A. Gemitzi, M. Kofidou, G. Falalakis, B. Fang, V. Lakshmi, Estimating high-resolution soil moisture by combining data from a sparse network of soil moisture sensors and remotely sensed MODIS LST information, Hydrol. Res. 55 (9) (2024) 905–920, https://doi.org/10.2166/nh.2024.043.

[155] J. Peng, A. Loew, Recent advances in soil moisture estimation from remote sensing, Water 9 (7) (2017) 530, https://doi.org/10.3390/w9070530.

[156] G.P. Petropoulos, G. Ireland, B. Barrett, Surface soil moisture retrievals from remote sensing: current status, products & future trends, Phys. Chem. Earth, Parts A/B/C 83–84 (2015) 36–56, https://doi.org/10.1016/j.pce.2015.02.009.
[157] J.-Y. Dai, S.-T. Cheng, Modeling shallow soil moisture dynamics in mountainous landslide active regions, Front. Environ. Sci. 10 (2022) 913059, https://doi.org/10.3389/fenvs.2022.913059.
[158] J.D. Galvincio, R. De Queiroga Miranda, G.G. Da Luz, Use of soil moisture as an indicator of climate change in the SUPer system, Hydrology 11 (5) (2024) 65, https://doi.org/10.3390/hydrology11050066.
[159] D. Calcaterra, M. Parise, B. Palma, L. Pelella, The influence of meteoric events in triggering shallow landslides in pyroclastic deposits of Campania, Italy, in: E. Bromhead, N. Dixon, M.L. Ibsen (Eds.), Landslides in Research, Theory and Practice: Proceedings of the 8th International Symposium on Landslides, A. A. Balkema, 2000, pp. 209–214, https://doi.org/10.1680/lirtapv1.34617.0035.
[160] Tuhua Ma, Changjiang Li, Zhiming Lu, Qiyun Bao, Rainfall intensity–duration thresholds for the initiation of landslides in Zhejiang Province, China, Geomorphology 245 (2015) 193–206, https://doi.org/10.1016/j.geomorph.2015.05.016.
[161] C. Millán-Arancibia, W. Lavado-Casimiro, Rainfall thresholds estimation for shallow landslides in Peru from gridded daily data, Nat. Hazards Earth Syst. Sci. 23 (3) (2023) 1191–1206, https://doi.org/10.5194/nhess-23-1191-2023.
[162] A.R. Roul, S.P. Pradhan, S.D. Panda, The relation between rainfall and landslides in India: an empirical approach for prediction of landslide, J. Earth Syst. Sci. 134 (2025) 97, https://doi.org/10.1007/s12040-025-02551-z.
[163] A. Rosi, S. Segoni, F. Catani, N. Casagli, Statistical and environmental analyses for the definition of a regional rainfall threshold system for landslide triggering in Tuscany (Italy), J. Geogr. Sci. 22 (4) (2012) 617–629, https://doi.org/10.1007/s11442-012-0951-0.
[164] G.T. Harilal, D. Madhu, M.V. Ramesh, K.V. Kumar, S. Anbazhagan, Towards establishing rainfall thresholds for a real-time landslide early warning system in Sikkim, India, Landslides 16 (2019) 2395–2408, https://doi.org/10.1007/s10346-019-01244-1.
[165] S. Barthélemy, S. Bernardie, G. Grandjean, Assessing rainfall threshold for shallow landslides triggering: a case study in the Alpes Maritimes region, France, Nat. Hazards 121 (2025) 4023–4049, https://doi.org/10.1007/s11069-024-06941-2.
[166] M. Moser, F. Hohensinn, Geotechnical aspects of soil slips in Alpine regions, Eng. Geol. 19 (3) (1983) 185–211, https://doi.org/10.1016/0013-7952(83)90003-0.
[167] A. Cancelli, R. Nova, Landslides in soil debris cover triggered by rainstorms in Valtellina (central Alps – italy), in: Proc. IV International Conference and Field Workshop on Landslides, 1985, pp. 267–272. Tokyo, August 1985.
[168] S.H. Cannon, Rainfall conditions for abundant debris avalanches, San Francisco Bay region, California, Geology 38 (1985) 267–272.
[169] G.F. Wieczorek, Effect of rainfall intensity and duration on debris flows in central Santa Cruz Mountains, California, in: J.E. Costa, G.F. Wieczorek (Eds.), Debris Flow=Avalanches: Process, Recognition, and Mitigation, 7, Geological Society of America, Reviews in Engineering Geology, 1987, pp. 93–104, https://doi.org/10.1130/REG7-p93.
[170] R.W. Jibson, Debris flows in southern Puerto Rico, Geol. Soc. Am. (1989) 29–55, https://doi.org/10.1130/SPE236-p29, special paper 236.
[171] F.M. Guadagno, Debris flows in the Campanian volcaniclastic soils, in: Slope Stability Engineering, 125, Developments and Applications, 1991, https://doi.org/10.1680/ssedaa.16606.0021.
[172] K.S. Rodolfo, A.T. Arguden, Rain-lahar generation and sediment-delivery systems at Mayon Volcano, Philippines, in: R.V. Fisher, G.A. Smith (Eds.), Sedimentation in Volcanic Settings, 45, Society of Economic Paleontologists and Mineralogists, special publication, 1991, pp. 71–88, https://doi.org/10.2110/pec.91.45.0071.
[173] M. Ceriani, Rainfall and landslides in the Alpine area of Lombardia Region, central Alps, Italy, Proceedings, Interpraevent Int. Symp, Bern 2 (1992) 9–20.
[174] M.C. Larsen, A. Simon, A rainfall intensity-duration threshold for landslides in a humid-tropical environment, Puerto Rico, Geogr. Ann. Phys. Geogr. 75 (1–2) (1993) 13–23, https://doi.org/10.1080/04353676.1993.11880379.
[175] R.A. Arboleda, M. Martinez, 1992 lahars in the Pasig-Potrero River system, in: Fire and Mud: Eruptions and Lahars of Mount Pinatubo, Quezon City and University of Washington Press, Seattle, 1996, p. 1126. https://pubs.usgs.gov/pinatubo/arboleda/.
[176] M. Clarizia, G. Gullà, G. Sorbino, Sui meccanismi di innesco dei soil slip, Int. Conf. Prev. Hydrogeol. Hazards: Sci. Res. 1 (1996) 585–597. https://www.researchgate.net/publication/284773248_Sui_meccanismi_di_innesco_dei_soil_slip.
[177] N.M. Tuñgol, M.T.M. Regalado, Rainfall, acoustic flow monitor records, and observed lahars of the Sacobia River in 1992. In: fire and mud: eruptions and lahars of Mount Pinatubo, in: C.G. Newhall, R.S. Punongbayan (Eds.), Philippine Institute of Volcanology and Seismology, Quezon City and University of Washington Press, Seattle, 1996, p. 1126. https://pubs.usgs.gov/pinatubo/tungol/.
[178] M. Zimmermann, P. Mani, P. Gamma, P. Gsteiger, O. Heiniger, G. Hunziker, Murganggefahr und Klimänderungein GIS-basierter Ansatz, in: Schlussbericht des Nationalen Forschungsprogrammes, NFP 31, vdf Hochschulverlag AG, Zürich, 1997, p. 161. https://boris-portal.unibe.ch/handle/20.500.12422/198072.
[179] P. Paronuzzi, A. Coccolo, G. Garlatti, Eventi meteorici critici e debris flows nei bacini montani del Friuli, L'Acqua, Sezione I/Memorie 6 (1998) 39–50. http://www.gruppocp.it/download/articoli/ACQUA_1998_debris_flows.pdf.
[180] D.R. Montgomery, K.M. Schmidt, H.M. Greenberg, W.E. Dietrich, Forest clearing and regional landsliding, Geology 28 (4) (2000) 311–314, https://doi.org/10.1130/0091-7613(2000)28%3C311:FCARL%3E2.0.CO;2.
[181] G.F. Wieczorek, B.A. Morgan, R.H. Campbell, Debris-flow hazards in the Blue Ridge of central Virginia, Environ. Eng. Geosci. 6 (1) (2000) 3–23, https://doi.org/10.2113/gseegeosci.6.1.3.
[182] G.B. Crosta, P. Frattini, Rainfall thresholds for triggering soil slips and debris flow, in: Proc. of the 2nd EGS Plinius Conference on Mediterranean Storms, 2547, Publication CNR GNDCI, 2001, October, pp. 463–487. https://www.researchgate.net/publication/285298340_Rainfall_thresholds_for_triggering_soil_slips_and_debris_flow.
[183] L. Marchi, M. Arattano, A.M. Deganutti, Ten years of debris-flow monitoring in the Moscardo Torrent (Italian Alps), Geomorphology 46 (1–2) (2002) 1–17, https://doi.org/10.1016/S0169-555X(01)00162-3.
[184] R. Ahmad, Developing early warning systems in Jamaica: rainfall thresholds for hydrogeological hazards, in: National Disaster Management Conference. Ocho Rios: UDS, 2003, 2003. https://www.mona.uwi.edu/uds/rainhazards_files/frame.htm.
[185] M. Jakob, H. Weatherly, A hydroclimatic threshold for landslide initiation on the North Shore Mountains of Vancouver, British Columbia, Geomorphology 54 (3–4) (2003) 137–156, https://doi.org/10.1016/S0169-555X(02)00339-2.
[186] P. Aleotti, A warning system for rainfall-induced shallow failures, Eng. Geol. 73 (3–4) (2004) 247–265, https://doi.org/10.1016/j.enggeo.2004.01.007.
[187] M. Floris, M. Mari, R.W. Romeo, U. Gori, Modelling of landslide-triggering factors-A case study in the northern Apennines, Italy, in: Engineering Geology for Infrastructure Planning in Europe: a European Perspective, Springer Berlin Heidelberg, Berlin, Heidelberg, 2004, pp. 745–753, https://doi.org/10.1007/978-3-540-39918-6_82.
[188] R.L. Baum, J.W. Godt, E.L. Harp, J.P. McKenna, S.R. McMullen, Early warning of landslides for rail traffic between Seattle and Everett, Washington, USA, in: Landslide Risk Management, CRC Press, 2005, pp. 741–750, https://doi.org/10.1201/9781439833711.
[189] S.H. Cannon, J.E. Gartner, Wildfire-related debris flow from a hazards perspective, in: M. Jakub, O. Hungr (Eds.), Debris-Flow Hazards and Related Phenomena, 2005, pp. 363–385, https://doi.org/10.1007/3-540-27129-5_15.
[190] C. Chien-Yuan, C. Tien-Chien, Y. Fan-Chieh, Y. Wen-Hui, T. Chun-Chieh, Rainfall duration and debris-flow initiated studies for real-time monitoring, Environ. Geol. 47 (5) (2005) 715–724, https://doi.org/10.1007/s00254-004-1203-0.
[191] J. Corominas, F.J. Ayala, A. Cendrero, J. Chacón, J.R. Díaz de Terán, A. Gonzáles, J. Moja, J.M. Vilaplana, Impacts on natural hazard of climatic origin. ECCE final report: a preliminary assessment of the impacts in Spain due to the effects of climate change, Ministerio de Medio Ambiente 12 (2005) 529–557. https://www.researchgate.net/publication/283920868_Impacts_on_natural_hazards_of_climatic_origin_A_Flood_risk.
[192] J. Corominas, J. Moya, A. Ledesma, A. Lloret, J.A. Gili, Prediction of ground displacements and velocities from groundwater level changes at the Vallcebre landslide (Eastern Pyrenees, Spain), Landslides 2 (2) (2005) 83–96, https://doi.org/10.1007/s10346-005-0049-1.
[193] Y. Hong, H. Hiura, K. Shino, K. Sassa, A. Suemine, H. Fukuoka, G. Wang, The influence of intense rainfall on the activity of large-scale crystalline schist landslides in Shikoku Island, Japan, Landslides 2 (2) (2005) 97–105, https://doi.org/10.1007/s10346-004-0043-z.

[194] R.K. Dahal, S. Hasegawa, Representative rainfall thresholds for landslides in the Nepal Himalaya, Geomorphology 100 (3–4) (2008) 429–443, https://doi.org/10.1016/j.geomorph.2008.01.014.
[195] D.P. Kanungo, S. Sharma, Rainfall thresholds for prediction of shallow landslides around Chamoli-Joshimath region, Garhwal Himalayas, India, Landslides 11 (4) (2014) 629–638, https://doi.org/10.1007/s10346-013-0438-9.
[196] W. Zhou, C. Tang, Rainfall thresholds for debris flow initiation in the Wenchuan earthquake-stricken area, Southwestern China, Landslides 11 (5) (2014) 877–887, https://doi.org/10.1007/s10346-013-0421-5.
[197] M. Hong, J. Kim, S. Jeong, Rainfall intensity–duration thresholds for landslide prediction in South Korea by considering the effects of antecedent rainfall, Landslides 15 (2018) 523–534, https://doi.org/10.1007/s10346-017-0892-x.
[198] L. Piciullo, S.L. Gariano, M. Melillo, M.T. Brunetti, S. Peruccacci, F. Guzzetti, M. Calvello, Definition and performance of a threshold-based regional early warning model for rainfall-induced landslides, Landslides 14 (3) (2017) 995–1008, https://doi.org/10.1007/s10346-016-0750-2.
[199] M.T. Brunetti, S. Peruccacci, M. Rossi, S. Luciani, D. Valigi, F. Guzzetti, Rainfall thresholds for the possible occurrence of landslides in Italy, Nat. Hazards Earth Syst. Sci. 10 (3) (2010) 447–458, https://doi.org/10.5194/nhess-10-447-2010.
[200] S.L. Gariano, M.T. Brunetti, G. Iovine, M. Melillo, S. Peruccacci, O. Terranova, C. Vennari, F. Guzzetti, Calibration and validation of rainfall thresholds for shallow landslide forecasting in Sicily, southern Italy, Geomorphology 228 (2015) 653–665, https://doi.org/10.1016/j.geomorph.2014.10.019.
[201] K.J. Beven, M.J. Kirkby, A physically based, variable contributing area model of basin hydrology, Hydrol. Sci. J. 24 (1) (1979) 43–69, https://doi.org/10.1080/02626667909491834.
[202] E.M. O'Loughlin, Prediction of surface saturation zones in natural catchments by topographic analysis, Water Resour. Res. 22 (5) (1986) 794–804, https://doi.org/10.1029/WR022i005p00794.
[203] R. Vertessy, E. O'Loughlin, E. Beverly, T. Butt, Australian experiences with the CSIRO Topog model in land and water resources management, in: Water Resources Planning in a Changing World: Proceedings of the UNESCO International Symposium, 1994, pp. 135–144. http://hdl.handle.net/102.100.100/238914?index=1.
[204] C. Hammond, D. Hall, S. Miller, P. Swetik, Level I Stability Analysis (LISA) Documentation for Version 2.0 (General Technical Report INT-285), U.S. Department of Agriculture, Forest Service, 1992. https://forest.moscowfsl.wsu.edu/cgi-bin/engr/library/searchpub.pl?pub=1992a.
[205] R.T. Pack, D.G. Tarboton, C.N. Goodwin, The SINMAP approach to terrain stability mapping, in: Proceedings of the 8th International Congress of the International Association of Engineering Geology and the Environment 2, A. A. Balkema, 1998, pp. 1157–1165, in: https://www.researchgate.net/publication/285009111_The_SINMAP_approach_to_terrain_stability_mapping_Procedeengs_of_the_8th_congress_of_the_international_association_of_engineering_geology_Vancouver_British_Columbia.
[206] D.R. Montgomery, W.E. Dietrich, A physically based model for the topographic control on shallow landsliding, Water Resour. Res. 30 (4) (1994) 1153–1171, https://doi.org/10.1029/93WR02979.
[207] W. Wu, R.C. Sidle, A distributed slope stability model for steep forested hillslopes, Water Resour. Res. 31 (8) (1995) 2097–2110, https://doi.org/10.1029/95WR01136.
[208] R.L. Baum, W.Z. Savage, J.W. Godt, TRIGRS—A FORTRAN Program for Transient Rainfall Infiltration and Grid-based Regional slope-stability Analysis (U.S. Geological Survey Open-File Report 02-0424), U.S. Geological Survey, 2002. http://pubsdata.usgs.gov/pubs/of/2008/1159/index.html.
[209] G. Rossi, F. Catani, L. Leoni, S. Segoni, V. Tofani, HIRESSS: a physically based slope stability simulator for HPC applications, Nat. Hazards Earth Syst. Sci. 13 (1) (2013) 151–166, https://doi.org/10.5194/nhess-13-151-2013.
[210] L.A. Richards, Capillary conduction of liquids through porous mediums, Physics 1 (5) (1931) 318–333, https://doi.org/10.1063/1.1745010.
[211] R.M. Iverson, Landslide triggering by rain infiltration, Water Resour. Res. 36 (7) (2000) 1897–1910, https://doi.org/10.1029/2000WR900090.
[212] R. Rigon, G. Bertoldi, T.M. Over, GEOtop: a distributed hydrological model with coupled water and energy budgets, J. Hydrometeorol. 7 (3) (2006) 371–388, https://doi.org/10.1175/JHM497.1.
[213] B.B. Mirus, B.A. Ebel, K. Loague, B.C. Wemple, Simulated effect of a forest road on near-surface hydrologic response, Earth Surf. Process. Landf. 32 (1) (2007) 126–142, https://doi.org/10.1002/esp.1387.
[214] G. Formetta, M. Bancheri, O. David, R. Rigon, Performance of site-specific parameterizations of longwave radiation, Hydrol. Earth Syst. Sci. 20 (11) (2016) 4641–4654, https://doi.org/10.5194/hess-20-4641-2016.
[215] R. Tufano, G. Formetta, D. Calcaterra, P. De Vita, Hydrological control of soil thickness spatial variability on the initiation of rainfall-induced shallow landslides using a three-dimensional model, Landslides 18 (10) (2021) 3367–3380, https://doi.org/10.1007/s10346-021-01723-5.
[216] S. Simoni, F. Zanotti, G. Bertoldi, R. Rigon, Modelling the probability of occurrence of shallow landslides and channelized debris flows using GEOtop-FS, Hydrol. Process. 22 (4) (2008) 532–545, https://doi.org/10.1002/hyp.6886.
[217] G. Formetta, V. Rago, G. Capparelli, R. Rigon, F. Muto, P. Versace, Integrated physically based system for modeling landslide susceptibility, Procedia Earth Planet. Sci. 9 (2014) 74–82, https://doi.org/10.1016/j.proeps.2014.06.016.
[218] G. Capparelli, P. Versace, FLaIR and SUSHI: two mathematical models for early warning of landslides induced by rainfall, Landslides 8 (1) (2011) 67–79, https://doi.org/10.1007/s10346-010-0228-6.
[219] D. Salciarini, C. Tamagnini, P. Conversini, S. Rapinesi, Spatially distributed rainfall thresholds for the initiation of shallow landslides, Nat. Hazards 61 (1) (2012) 229–245, https://doi.org/10.1007/s11069-011-9739-2.
[220] T. Salvatici, V. Tofani, G. Rossi, M. D'Ambrosio, C. Tacconi Stefanelli, E.B. Masi, A. Rosi, V. Pazzi, P. Vannocci, M. Petrolo, F. Catani, S. Ratto, H. Stevenin, N. Casagli, Application of a physically based model to forecast shallow landslides at a regional scale, Nat. Hazards Earth Syst. Sci. 18 (7) (2018) 1919–1935, https://doi.org/10.5194/nhess-18-1919-2018.
[221] M.A. Thomas, B.B. Mirus, B.D. Collins, Identifying physics-based thresholds for rainfall-induced landsliding, Geophys. Res. Lett. 45 (18) (2018) 9651–9661, https://doi.org/10.1029/2018GL079662.
[222] Z. Liao, Y. Hong, J. Wang, H. Fukuoka, K. Sassa, D. Karnawati, T.F. Fathani, Prototyping an experimental early warning system for rainfall-induced landslides in Indonesia using satellite remote sensing and geospatial datasets, Landslides 7 (3) (2010) 317–324, https://doi.org/10.1007/s10346-010-0219-7.
[223] Y. Wu, H. Lan, X. Gao, L. Li, Z. Yang, A simplified physically based coupled rainfall threshold model for triggering landslides, Eng. Geol. 195 (2015) 63–69, https://doi.org/10.1016/j.enggeo.2015.05.022.
[224] G. Grelle, M. Soriano, P. Revellino, L. Guerriero, F.M. Guadagno, Space–time prediction of rainfall-induced shallow landslides through a combined probabilistic/deterministic approach, optimized for initial water table conditions, Bull. Eng. Geol. Environ. 73 (2014) 877–890, https://doi.org/10.1007/s10064-013-0546-8.
[225] R.J. Marin, Physically based and distributed rainfall intensity and duration thresholds for shallow landslides, Landslides 17 (2020) 2907–2917, https://doi.org/10.1007/s10346-020-01481-9.
[226] L. Montrasio, R. Valentino, A model for triggering mechanisms of shallow landslides, Nat. Hazards Earth Syst. Sci. 8 (5) (2008) 1149–1159, https://doi.org/10.5194/nhess-8-1149-2008.
[227] P. De Vita, E. Napolitano, J.W. Godt, R.L. Baum, V. Allocca, Deterministic estimation of hydrological thresholds for shallow landslide initiation and slope stability models: case study from the Somma-Vesuvius area of southern Italy, Landslides 10 (6) (2013) 713–728, https://doi.org/10.1007/s10346-012-0348-2.
[228] E. Napolitano, F. Fusco, R.L. Baum, J.W. Godt, P. De Vita, Effect of antecedent-hydrological conditions on rainfall triggering of debris flows in ash-fall pyroclastic mantled slopes of Campania (southern Italy), Landslides 13 (2016) 967–983, https://doi.org/10.1007/s10346-015-0647-5.
[229] F. Fusco, P. De Vita, B.B. Mirus, R.L. Baum, V. Allocca, R. Tufano, E. Di Clemente, D. Calcaterra, Physically based estimation of rainfall thresholds triggering shallow landslides in volcanic slopes of southern Italy, Water 11 (9) (2019) 1915, https://doi.org/10.3390/w11091915.
[230] L. Raimondi, G. Pepe, M. Firpo, D. Calcaterra, A. Cevasco, An open-source and QGIS-integrated physically based model for spatial prediction of rainfall-induced shallow landslides (SPRIn-SL), Environ. Model. Software 160 (2023) 105587, https://doi.org/10.1016/j.envsoft.2022.105587.

[231] S. Guglielmi, M. Pirone, A.S. Dias, F. Cotecchia, G. Urciuoli, Thermohydraulic numerical modeling of slope–vegetation–atmosphere interaction: case study of the pyroclastic slope cover at Monte Faito, Italy, J. Geotech. Geoenviron. Eng. 149 (11) (2023) 05023005, https://doi.org/10.1061/(ASCE)GT.1943-5606.0002960.

[232] G. Rianna, A. Reder, L. Pagano, From empirically to physically based early warning predictions of rainfall induced landslides in silty volcanic soils: the Lattari Mountains case study, Bull. Eng. Geol. Environ. 82 (2023) 223, https://doi.org/10.1007/s10064-023-03228-x.

[233] M. Pirone, G. Forte, A. Santo, G. Urciuoli, Novel rainfall thresholds for shallow slip prediction based on field monitoring: case study of the Lattari Mountains, Italy, J. Geotech. Geoenviron. Eng. 151 (3) (2025) 04025016, https://doi.org/10.1061/JGGEFK.GTENG-12797.

[234] M. Bordoni, B. Corradini, L. Lucchelli, R. Valentino, M. Bittelli, V. Vivaldi, C. Meisina, Empirical and physically based thresholds for the occurrence of shallow landslides in a prone area of northern Italian Apennines, Water 11 (12) (2019) 2653, https://doi.org/10.3390/w11122653.

[235] R. Narcisi, S.E. Pappalardo, G. Taddia, M. De Marchi, Assessing climate impacts on slow-moving landslides in the western Alps of Piemonte: integration of monitoring techniques for detecting displacements, Front. Earth Sci. 12 (2024) 1365469, https://doi.org/10.3389/feart.2024.1365469.

[236] T. Sato, Y. Shuin, Rainfall characteristics and magnitude control the volume of shallow and deep-seated landslides: inferences from analyses using a simple runoff model, Geomorphology 466 (2024) 109453, https://doi.org/10.1016/j.geomorph.2024.109453.

[237] J.L. Zêzere, T. Vaz, S. Pereira, et al., Rainfall thresholds for landslide activity in Portugal: a state of the art, Environ. Earth Sci. 73 (2015) 2917–2936, https://doi.org/10.1007/s12665-014-3672-0.

[238] S. Leroueil, R.J. Chandler, Natural slopes and cuts: movement and failure mechanisms, Geotechnique 51 (3) (2001) 197–243, https://doi.org/10.1680/geot.2001.51.3.197.

[239] K. Terzaghi, Mechanism of landslides, in: Application of Geology to Engineering Practice, Geological Society of America, Boulder, CO, 1950, https://doi.org/10.1130/Berkey.1950.83.

[240] T. Glade, M.J. Crozier, The nature of landslide hazard and impact, in: T. Glade, M.G. Anderson, M.J. Crozier (Eds.), Landslide Hazard and Risk, Wiley, Chichester, 2005, pp. 43–74, https://doi.org/10.1002/9780470012659.ch2.

[241] M.T.J. Terlien, The determination of statistical and deterministic hydrological landslide triggering thresholds, Environ. Geol. 35 (2–3) (1998) 124–130, https://doi.org/10.1007/s002540050299.

[242] J.A. Berntson, G.B. Saèllfors, Pore pressure variations in marine clay deposits, Proc. 4th Int. Symp. Landslides, Toronto 1 (1984) 363–366. https://www.cabidigitallibrary.org/doi/full/10.5555/19861906697.

[243] T.C. Kenney, K.C. Lau, Temporal changes of groundwater pressure in a natural slope of nonfissured clay, Can. Geotech. J. 21 (1) (1984) 138–146, https://doi.org/10.1139/t84-011.

[244] P.R. Vaughan, Assumption, prediction and reality in geotechnical engineering, Geotechnique 44 (4) (1994) 573–609, https://doi.org/10.1680/geot.1994.44.4.573.

[245] J.N. Hutchinson, A coastal mudflow on the London Clay cliffs at Beltinge, North Kent, Geotechnique 20 (4) (1970) 412–438, https://doi.org/10.1680/geot.1970.20.4.412.

[246] R.M. Iverson, J.J. Major, Rainfall, groundwater flow, and seasonal motion at minor creek landslide, northwestern California: physical interpretation of empirical relations, Geol. Soc. Am. Bull. 99 (1987) 579–594, https://doi.org/10.1130/0016-7606(1987)99<0579:RGFASM>2.0.CO;2.

[247] Y. Guglielmi, J.M. Vengeon, C. Bertrand, et al., Hydrogeochemistry: an investigation tool to evaluate infiltration into large moving rock masses (case studies of La Clapière and Séchilienne alpine landslides), Bull. Eng. Geol. Environ. 61 (2002) 311–324, https://doi.org/10.1007/s10064-002-0163-4.

[248] F. Cappa, Y. Guglielmi, V.M. Soukatchoff, et al., Hydromechanical modeling of a large moving rock slope inferred from slope levelling coupled to spring long-term hydrochemical monitoring: example of the La Clapière landslide (Southern Alps, France), J. Hydrol. 291 (2004) 67–90, https://doi.org/10.1016/j.jhydrol.2003.12.013.

[249] V. de Montety, V. Marc, C. Emblanch, J.P. Malet, C. Bertrand, O. Maquaire, T.A. Bogaard, Identifying the origin of groundwater and flow processes in complex landslides affecting black marls: insights from a hydrochemical survey, Earth Surf. Process. Landf. 32 (2007) 32–48, https://doi.org/10.1002/esp.1370.

[250] S. Matsuura, S. Asano, T. Okamoto, Relationship between rain and/or meltwater, pore-water pressure and displacement of a reactivated landslide, Eng. Geol. 101 (1–2) (2008) 49–59, https://doi.org/10.1016/j.enggeo.2008.03.007.

[251] F. Ronchetti, L. Borgatti, F. Cervi, A. Corsini, Hydro-mechanical features of landslide reactivation in weak clayey rock masses, Bull. Eng. Geol. Environ. 69 (2) (2010) 267–274, https://doi.org/10.1007/s10064-009-0249-3.

[252] M. Valiante, F. Bozzano, D. Guida, The Sant'Andrea-Molinello landslide system (Mt. Pruno, Roscigno, Italy), Rendiconti Online della Società Geologica Italiana 41 (2016) 214–217, https://doi.org/10.3301/ROL.2016.132.

[253] M. Berti, M.L.V. Martina, S. Franceschini, S. Pignone, A. Simoni, M. Pizziolo, Probabilistic rainfall thresholds for landslide occurrence using a Bayesian approach, J. Geophys. Res. Earth Surf. 117 (4) (2012), https://doi.org/10.1029/2012JF002367.

[254] A. Vallet, D. Varron, C. Bertrand, O. Fabbri, J. Mudry, A multi-dimensional statistical rainfall threshold for deep landslides based on groundwater recharge and support vector machines, Nat. Hazards 84 (2) (2016) 821–849, https://doi.org/10.1007/s11069-016-2453-3.

[255] A.L. Handwerger, J.J. Roering, D.A. Schmidt, Controls on the seasonal deformation of slow-moving landslides, Earth Planet Sci. Lett. 377 (2013) 239–247, https://doi.org/10.1016/j.epsl.2013.06.047.

[256] R. Vassallo, G.M. Grimaldi, C. Di Maio, Pore water pressures induced by historical rain series in a clayey landslide: 3D modeling, Landslides 12 (2015) 731–744, https://doi.org/10.1007/s10346-014-0508-7.

[257] T.W.J. Van Asch, L.P.H. van Beek, R.T. van Balen, A view on some hydrological triggering systems in landslides, Geomorphology 30 (1–2) (1999) 25–32, https://doi.org/10.1016/S0169-555X(99)00055-0.

[258] C.H. Bonnard, F. Noverraz, Influence of climate change on large landslides: assessment of long-term movements and trends, in: Proceedings of the International Conference on Landslides Causes, Impact and Countermeasures, 2001, pp. 121–138. https://infoscience.epfl.ch/handle/20.500.14299/235574.

[259] R.M. Trigo, M.N. Lorenzo, I.F. Trigo, C.C. DaCamara, The influence of the North Atlantic Oscillation on rainfall triggering of landslides near Lisbon, Nat. Hazards 36 (2005) 331–354, https://doi.org/10.1007/s11069-004-4548-x.

[260] A. Doglioni, P. Di Bari, M. Ponte, V. Simeone, Analysis of the rainfall preceding the activation of the large Maierato landslide in 2010, in: C. Margottini, P. Canuti, K. Sassa (Eds.), Landslide Science and Practice: Volume 4 – Global Environmental Change, Springer, Berlin, Heidelberg, 2011, pp. 107–114, https://doi.org/10.1007/978-3-642-31337-0_14.

[261] F. Noverraz, C. Bonnard, H. Dupraz, L. Huguenin, Grands glissements de versants et climat – VERSINCLIM: comportement passé, présent et futur des grands versants instables subactifs en fonction de l'évolution climatique, et évolution en continu des mouvements en profondeur, in: Rapport Final PNR 31, Hochschulverlag AG an der ETH Zurich, 1998, p. 314.

[262] J.M. Azañón, A. Azor, J. Yesares, M. Tsige, R.M. Mateos, F. Nieto, J. Delgado, M. Lòpez-Chicano, W. Martìn, J. Rodríguez-Fernández, Regional-scale high-plasticity clay-bearing formation as controlling factor on landslides in Southeast Spain, Geomorphology 120 (1–2) (2010) 26–37, https://doi.org/10.1016/j.geomorph.2009.09.012.

[263] S. Fiolleau, S. Uhlemann, S. Wielandt, B. Dafflon, Understanding slow-moving landslide triggering processes using low-cost passive seismic and inclinometer monitoring, J. Appl. Geophys. 215 (2023) 105090, https://doi.org/10.1016/j.jappgeo.2023.105090.

[264] M. Jiang, X. Zhao, X. Shi, Kinematic behavior analysis of the wadi landslide from time-series sentinel-1 data, IEEE J. Sel. Top. Appl. Earth Obs. Remote Sens. 15 (2021) 127–135, https://doi.org/10.1109/JSTARS.2021.3134177.

[265] E. Gebremichael, R. Hernandez, H. Alsleben, M. Ahmed, R. Denne, O. Harvey, Kinematics and controlling factors of slow-moving landslides in central Texas: a multisource data fusion approach, Geosciences 14 (5) (2024) 133, https://doi.org/10.3390/geosciences14050133.

[266] P. Confuorto, D. Di Martire, G. Centolanza, R. Iglesias, J.J. Mallorqui, A. Novellino, S. Plank, M. Ramondini, K. Thuro, D. Calcaterra, Post-failure evolution analysis of a rainfall-triggered landslide by multi-temporal interferometry SAR approaches integrated with geotechnical analysis, Rem. Sens. Environ. 188 (2017) 51–72, https://doi.org/10.1016/j.rse.2016.11.002.

[267] C. Lissak, O. Maquaire, R. Davidson, J.P. Malet, Piezometric thresholds for triggering landslides along the Normandy coast, France, Géomorphol. Relief, Process. Environ. 20 (2) (2014) 145–158, https://doi.org/10.4000/geomorphologie.10607.
[268] A. Urgilez Vinueza, J. Robles, M. Bakker, P. Guzman, T. Bogaard, Characterization and hydrological analysis of the guarumales deep-seated landslide in the tropical ecuadorian andes, Geosciences 10 (7) (2020) 267, https://doi.org/10.3390/geosciences10070267.
[269] N. Losacco, O. Bottiglieri, F. Santaloia, C. Vitone, F. Cotecchia, The geo-hydro-mechanical properties of a turbiditic formation as internal factors of slope failure processes, Geosciences 11 (10) (2021) 429, https://doi.org/10.3390/geosciences11100429.
[270] G. Debevec Jordanova, Z. Popović, P.E. Yastika, et al., SBAS DInSAR and in situ monitoring of the Šumljak landslide (SW Slovenia) dynamics driven by rainfall and piezometric-level fluctuation, Landslides 22 (2025) 1397–1411, https://doi.org/10.1007/s10346-024-02408-4.
[271] G. Pepe, A. Cevasco, M. Piazza, R. Macciò, F. Arrighetti, N. Casagli, On the efficiency and effectiveness of automatic deep drainage systems during an extreme rainfall event: the Mendatica landslide case study (western Liguria, Italy), Landslides 18 (12) (2021) 3799–3820, https://doi.org/10.1007/s10346-021-01740-3.
[272] D. Notti, A. Wrzesniak, N. Dematteis, P. Lollino, N.L. Fazio, F. Zucca, D. Giordan, A multidisciplinary investigation of deep-seated landslide reactivation triggered by an extreme rainfall event: the Monesi di Mendatica landslide, Ligurian Alps, Landslides 18 (7) (2021) 2341–2365, https://doi.org/10.1007/s10346-021-01651-3.
[273] A. Doglioni, F. Fiorillo, F.M. Guadagno, V. Simeone, Evolutionary polynomial regression to alert rainfall-triggered landslide reactivation, Landslides 9 (1) (2012) 53–62, https://doi.org/10.1007/s10346-011-0274-8.
[274] F. Banfi, C. De Michele, Temporal clustering of precipitation driving landslides over the Italian territory, Earths Future 12 (5) (2024), https://doi.org/10.1029/2023EF003885.
[275] G. Lollino, M. Arattano, P. Allasia, D. Giordan, Time response of a landslide to meteorological events, Nat. Hazards Earth Syst. Sci. 6 (2007) 179–184, https://doi.org/10.5194/nhess-6-179-2006.
[276] P. Lollino, A. Ugenti, D. de Lucia, M. Parise, C. Vennari, P. Allasia, N.L. Fazio, Failure mechanism of a rainfall-triggered landslide in clay slopes, Geosciences 13 (4) (2023), https://doi.org/10.3390/geosciences13040125.
[277] G. Pedone, G. Ruggieri, R. Trizzino, Characterisation of climatic variables used to identify instability thresholds in clay slopes, Géotech. Lett. 8 (3) (2018) 231–239, https://doi.org/10.1680/jgele.18.00020.
[278] F. Cotecchia, V. Tagarelli, G. Pedone, G. Ruggieri, S. Guglielmi, F. Santaloia, Analysis of climate-driven processes in clayey slopes for early warning system design, Proc. Inst. Civ. Eng. Geotech. Eng. 172 (6) (2019) 465–480, https://doi.org/10.1680/jgeen.18.00217.
[279] Annamaria di Lernia, Federica Cotecchia, Gaetano Elia, Vito Tagarelli, Francesca Santaloia, et al., Assessing the influence of the hydraulic boundary conditions on clay slope stability: The Fontana Monte case study, Engineering Geology 297 (2022) 106509, https://doi.org/10.1016/j.enggeo.2021.106509.
[280] A. Pellegrino, L. Picarelli, G. Urciuoli, Experiences of mudslides in Italy (general report), Occurrence and mechanisms of flow-like landslides in natural slopes and earthfills 1 (2004) 191–206, http://hdl.handle.net/11588/120945.
[281] L. Picarelli, G. Urciuoli, M. Ramondini, L. Comegna, Main features of mudslides in tectonised highly fissured clay shales, Landslides 2 (1) (2005) 15–30, https://doi.org/10.1007/s10346-004-0040-2.
[282] L. Comegna, L. Picarelli, G. Urciuoli, The mechanics of mudslides as a cyclic undrained–drained process, Landslides 4 (3) (2007) 217–232, https://doi.org/10.1007/s10346-007-0083-2.
[283] L. Comegna, L. Picarelli, G. Urciuoli, Effects of slope movements on soil structure and hydrological response, Geotech. Geol. Eng. 38 (5) (2020) 5633–5647, https://doi.org/10.1007/s10706-020-01341-2.
[284] B.C. Vieira, N.F. Fernandes, Landslides in Rio de Janeiro: the role played by variations in soil hydraulic conductivity, Hydrol. Process. 18 (4) (2004) 791–805, https://doi.org/10.1002/hyp.1363.
[285] L. Picarelli, C. Di Maio, P. Tommasi, G. Urciuoli, L. Comegna, Pore water pressure measuring and modeling in stiff clays and clayey flysch deposits: a challenging problem, Eng. Geol. 296 (2022) 106442, https://doi.org/10.1016/j.enggeo.2021.106442.
[286] F. Cotecchia, C. Vitone, F. Santaloia, G. Pedone, O. Bottiglieri, Slope instability processes in intensely fissured clays: case histories in the Southern Apennines, Landslides 12 (5) (2015) 877–893, https://doi.org/10.1007/s10346-014-0516-7.
[287] W. Shao, T.A. Bogaard, M. Bakker, R. Greco, Quantification of the influence of preferential flow on slope stability using a numerical modelling approach, Hydrol. Earth Syst. Sci. 19 (2015) 2197–2212, https://doi.org/10.5194/hess-19-2197-2015.
[288] C. Di Maio, J. De Rosa, R. Vassallo, Pore water pressures and hydraulic conductivity in the slip zone of a clayey earthflow: experimentation and modelling, Eng. Geol. 292 (2021) 106263, https://doi.org/10.1016/j.enggeo.2021.106263.
[289] H. Tang, L.A. McGuire, F.K. Rengers, J.W. Kean, D.M. Staley, J.B. Smith, Evolution of debris-flow initiation mechanisms and sediment sources during a sequence of postwildfire rainstorms, J. Geophys. Res. Earth Surf. 124 (6) (2019) 1572–1595, https://doi.org/10.1029/2018JF004837.
[290] A. Parsons, P.R. Robichaud, S.A. Lewis, C. Napper, J.T. Clark, Field Guide for Mapping Post-fire Soil Burn Severity (No. RMRS-GTR-243, U.S. Department of Agriculture, Forest Service, Rocky Mountain Research Station, 2010, https://doi.org/10.2737/RMRS-GTR-243. RMRS-GTR-243).
[291] M. Abdollahi, F. Vahedifard, B.A. Leshchinsky, Hydromechanical modeling of evolving post-wildfire regional-scale landslide susceptibility, Eng. Geol. 335 (2024) 107538, https://doi.org/10.1016/j.enggeo.2024.107538.
[292] G. La Porta, A. Leonardi, S. La Ferlita, M. Pirulli, Post-wildfire debris flow in the Northwestern Italian alps: description and numerical analysis of the June 2018 Bussoleno event, Landslides 22 (2025) 3625–3640, https://doi.org/10.1007/s10346-025-02605-9, 2025.
[293] M. Parise, S.H. Cannon, Wildfire impacts on the processes that generate debris flows in burned watersheds, Nat. Hazards 61 (2012) 217–227, https://doi.org/10.1007/s11069-011-9769-9.
[294] A. Farid, M.K. Alam, V.S.N.S. Goli, I.D. Akin, T. Akinleye, X. Chen, Q. Cheng, P. Cleall, S. Cuomo, V. Foresta, S. Ge, L. Iervolino, P. Iradukunda, C.H. Luce, E. Koda, S.B. Mickovski, B.C. O'Kelly, E.K. Paleologos, D. Peduto, J. Winkler, A review of the occurrence and causes for wildfires and their impacts on the geoenvironment, Fire 7 (8) (2024) 295, https://doi.org/10.3390/fire7080295.
[295] J.C. Gill, B.D. Malamud, Reviewing and visualizing the interactions of natural hazards, Rev. Geophys. 52 (4) (2014) 680–722, https://doi.org/10.1002/2013RG000445.
[296] M. Abdollahi, F. Vahedifard, F.T. Tracy, Post-wildfire stability of unsaturated hillslopes against rainfall-triggered landslides, Earths Future 11 (3) (2023), https://doi.org/10.1029/2022EF003213.
[297] F. Vahedifard, M. Abdollahi, B.A. Leshchinsky, T.D. Stark, M. Sadegh, A. AghaKouchak, Interdependencies between wildfire-induced alterations in soil properties, near-surface processes, and geohazards, Earth Space Sci. 11 (2) (2024), https://doi.org/10.1029/2023EA003498.
[298] S. Melzner, D. Peduto, J. Hübl, F. Fiorucci, C. Phillips, Wildfire-induced geohydrological risk in the Alps, Landslides 22 (2025) 3989–4011, https://doi.org/10.1007/s10346-025-02581-0.
[299] F.K. Rengers, L.A. McGuire, N.S. Oakley, J.W. Kean, D.M. Staley, H. Tang, Landslides after wildfire: initiation, magnitude, and mobility, Landslides 17 (11) (2020) 2631–2641, https://doi.org/10.1007/s10346-020-01506-3.
[300] J. DeGraff, Geologic Investigation of the Pilot Ridge Debris Flow, Groveland Ranger District, Stanislaus National Forest, United States Department of Agriculture Forest, 1997. Service FS-6200-7 (10/73).
[301] J.E. Keeley, Fire intensity, fire severity and burn severity: a brief review and suggested usage, Int. J. Wildland Fire 18 (1) (2009) 116–126, https://doi.org/10.1071/WF07049.
[302] J.M. Chicco, G. Mandrone, D. Vacha, Effects of wildfire on soils: field studies and modelling on induced underground temperature variations, Front. Earth Sci. 11 (2023), https://doi.org/10.3389/feart.2023.1307569.
[303] L.F. DeBano, The role of fire and soil heating on water repellency in wildland environments: a review, J. Hydrol. 231 (2000) 195–206, https://doi.org/10.1016/S0022-1694(00)00194-3.
[304] S.H. Doerr, W.H. Blake, R.A. Shakesby, F. Stagnitti, S.H. Vuurens, G.S. Humphreys, P. Wallbrink, Heating effects on water repellency in Australian eucalypt forest soils and their value in estimating wildfire soil temperatures, Int. J. Wildland Fire 13 (2) (2004) 157–163, https://doi.org/10.1071/WF03051.

[305] B.A. Ebel, J.A. Moody, Parameter estimation for multiple post-wildfire hydrologic models, Hydrol. Process. 34 (21) (2020) 4049–4066, https://doi.org/10.1002/hyp.13865.

[306] B.A. Ebel, J.A. Moody, D.A. Martin, Hydrologic conditions controlling runoff generation immediately after wildfire, Water Resour. Res. 48 (3) (2012), https://doi.org/10.1029/2011WR011470.

[307] R. Secci, S.V. Calcina, G. Ranieri, G. Uras, Analysis of the stability variation of a slope crossed by forest fire, Int. J. Civ. Eng. 3 (1) (2014) 41–50. https://www.researchgate.net/publication/261809203_Analysis_of_the_stability_variation_of_a_slope_crossed_by_forest_fire.

[308] D. Peduto, L. Iervolino, V. Foresta, Experimental analysis of the fire-induced effects on the physical, mechanical, and hydraulic properties of sloping pyroclastic soils, Geosciences 12 (5) (2022) 198, https://doi.org/10.3390/geosciences12050198.

[309] Mingyu Lei, Yifei Cui, Junjun Ni, Guotao Zhang, Yao Li, et al., Temporal evolution of the hydromechanical properties of soil-root systems in a forest fire in China, Science of The Total Environment 809 (2022) 151165, https://doi.org/10.1016/j.scitotenv.2021.151165, 151165.

[310] M.A. Thomas, F.K. Rengers, J.W. Kean, L.A. McGuire, D.M. Staley, K.R. Barnhart, B.A. Ebel, Postwildfire soil-hydraulic recovery and the persistence of debris flow hazards, J. Geophys. Res. Earth Surf. 126 (6) (2021), https://doi.org/10.1029/2021JF006091.

[311] J.A. Moody, R.A. Shakesby, P.R. Robichaud, S.H. Cannon, D.A. Martin, Current research issues related to post-wildfire runoff and erosion processes, Earth Sci. Rev. 122 (2013) 10–37, https://doi.org/10.1016/j.earscirev.2013.03.004.

[312] D.R. Greenway, Vegetation and slope stability, in: M.G. Anderson, K.S. Richards (Eds.), Slope Stability, Geotechnical Engineering and Geomorphology, John Wiley & Sons, Chichester, UK, 1987, pp. 187–230.

[313] R.C. Sidle, H. Ochiai, Landslides: Processes, Prediction and Land Use, 18, American Geophysical Union (AGU), 2000 Florida Avenue N.W., Washington, D.C. 20009-1277, USA. Water Resources Monograph, 2006, p. 312, https://doi.org/10.1007/s10346-008-0119-2.

[314] C. Phillips, T. Hales, H. Smith, L. Basher, Shallow landslides and vegetation at the catchment scale: a perspective, Ecol. Eng. 173 (2021) 106436, https://doi.org/10.1016/j.ecoleng.2021.106436.

[315] A. Stokes, C. Atger, A.G. Bengough, T. Fourcaud, R.C. Sidle, Desirable plant root traits for protecting natural and engineered slopes against landslides, Plant Soil 324 (2009) 1–30, https://doi.org/10.1007/s11104-009-0159-y.

[316] M. Schwarz, D. Cohen, D. Or, Root-soil mechanical interactions during pullout and failure of root bundles, J. Geophys. Res. 115 (2010) F04035, https://doi.org/10.1029/2009JF001603.

[317] R.C. Sidle, T.A. Bogaard, Dynamic earth system and ecological controls of rainfall-initiated landslides, Earth Sci. Rev. 159 (2016) 275–291, https://doi.org/10.1016/j.earscirev.2016.05.013.

[318] C. Vergani, F. Giadrossich, P. Buckley, M. Conedera, M. Pividori, F. Salbitano, M. Schwarz, Root reinforcement dynamics of European coppice woodlands and their effect on shallow landslides: a review, Earth Sci. Rev. 167 (2017) 88–102, https://doi.org/10.1016/j.earscirev.2017.02.002.

[319] M. Cecconi, V. Tagarelli, F. Cotecchia, V. Pane, F. Anselmucci, I. Bertolini, G. Biondi, D. Boldrin, V. Capobianco, G. Cardile, S. Cuomo, P. De Vita, A. Fraccica, G. Meijer, L. Pagano, M. Pirone, M. Schwarz, A. Tarantino, J. Vaunat, A. Yildiz, Soil-vegetation-atmosphere interaction for engineering applications: recent multi-scale and multi-disciplinary insights, Geomech. Energy Environ. (2025) 100723, https://doi.org/10.1016/j.gete.2025.100723.

[320] M. Ghestem, R.C. Sidle, A. Stokes, The influence of plant root systems on subsurface flow: implications for slope stability, Bioscience 61 (2011) 869–879, https://doi.org/10.1525/bio.2011.61.11.6.

[321] J.J. Ni, A.K. Leung, C.W.W. Ng, Modelling effects of root growth and decay on soil water retention and permeability, Can. Geotech. J. 56 (7) (2019) 1049–1055, https://doi.org/10.1139/cgj-2018-0402.

[322] W. Shao, T. Bogaard, M. Bakker, M. Berti, The influence of preferential flow on pressure propagation and landslide triggering of the Rocca Pitigliana landslide, J. Hydrol. 543 (2016) 360–372, https://doi.org/10.1016/j.jhydrol.2016.10.015.

[323] M. Conedera, P. Larissa, P. Marxer, F. Forster, D. Rickenmann, L. Re, Consequences of forest fires on the hydrogeological response of mountain catchments: a case study of the Riale Buffaga, Ticino, Switzerland, Earth Surf. Process. Landf. 28 (2003) 117–129, https://doi.org/10.1002/esp.425.

[324] J. Maringer, D. Ascoli, L. Dorren, P. Bebi, M. Conedera, Temporal trends in the protective capacity of burnt beech forests (Fagus sylvatica L.) against rockfall, Eur. J. For. Res. 135 (4) (2016) 657–673, https://doi.org/10.1007/s10342-016-0962-y.

[325] T. Uchida, K. Kosugi, T. Mizuyama, Effects of pipeflow on hydrological process and its relation to landslide: a review of pipeflow studies in forested headwater catchments, Hydrol. Process. 15 (2001) 2151–2174, https://doi.org/10.1002/hyp.281.

[326] M. Ammann, A. Böll, C. Rickli, T. Speck, O. Holdenrieder, Significance of tree root decomposition for shallow landslides, For. Snow Landsc. Res. 82 (79–94) (2009) 79. https://www.researchgate.net/publication/228708326_Significance_of_tree_root_decomposition_for_shallow_landslides.

[327] A.C. Johnson, P. Wilcock, Association between cedar decline and hillslope stability in mountainous regions of southeast Alaska, Geomorphology 46 (2002) 129–142, https://doi.org/10.1016/S0169-555X(02)00059-4.

[328] F. Preti, Forest protection and protection forest: tree root degra- dation over hydrological shallow landslides triggering, Ecol. Eng. (2012), https://doi.org/10.1016/j.ecoleng.2012.11.009.

[329] A. Watson, C. Phillips, M. Marden, Roost strength, growth, and rates of decay: root reinforcement changes of two three species and their contribution to slope stability, Plant Soil 217 (1999) 39–47, https://doi.org/10.1023/A:1004682509514.

[330] C.L. O'Loughlin, A.J. Pearce, Influence of Cenozoic geology on mass movement and sediment yield response to forest removal, North Westland, New Zealand, Bull. Int. Assoc. Eng. Geol. 13 (1) (1976) 41–46, https://doi.org/10.1007/BF02634757.

[331] R.C. Sidle, W. Wu, Simulating effects of timber harvesting on the temporal and spatial distribution of shallow landslides, Z. Geomorphol. N.F. 43 (1999) 185–201, https://doi.org/10.1127/zfg/43/1999/185.

[332] A.S. Dhakal, R.C. Sidle, Long-term modeling of landslides for different forest management practices, Earth Surf. Process. Landf. 28 (2003) 853–868, https://doi.org/10.1002/esp.499.

[333] F. Imaizumi, R.C. Sidle, Effect of forest harvesting on hydrogeomorphic processes in steep terrain of central Japan, Geomorphology 169–170 (2012) 109–122, https://doi.org/10.1016/j.geomorph.2012.04.017.

[334] P. Brandolini, A. Cevasco, D. Capolongo, G. Pepe, F. Lovergine, M. Del Monte, Response of terraced slopes to a very intense rainfall event and relationships with land abandonment: a case study from Cinque Terre (Italy), Land Degrad. Dev. 29 (3) (2018) 630–642, https://doi.org/10.1002/ldr.2672.

[335] E. Cammeraat, R. van Beek, A. Kooijman, Vegetation succession and its consequences for slope stability in SE Spain, Plant Soil 278 (2005) 135–147, https://doi.org/10.1007/s11104-005-5893-1.

[336] A. Latocha, Geomorphic connectivity within abandoned small catchments (Stołowe Mts, SW Poland), Geomorphology 212 (2014) 4–15, https://doi.org/10.1016/j.geomorph.2013.04.030.

[337] C. Moos, A. Stritih, M. Teich, B. Alessandra, Mountain protective forests under threat? An in-depth review of global change impacts on their protective effect against natural hazards, Front. For. Glob. Change 6 (2023) 1223934, https://doi.org/10.3389/ffgc.2023.1223934.

[338] A. DiBiagio, V. Capobianco, A. Oen, L.M. Tallaksen, State-of-the-art: parametrization of hydrological and mechanical reinforcement effects of vegetation in slope stability models for shallow landslides, Landslides 21 (10) (2024) 2417–2446, https://doi.org/10.1007/s10346-024-02300-1.

[339] A. Lei, M. Ferrarotti, G.M. Marmoni, M. Fiorucci, S. Martino, The FIRE research project: landscape architecture's role in modelling multi-criteria risk scenarios in Ischia, J. Landsc. Architect. 20 (1–2) (2025) 104–123, https://doi.org/10.1080/18626033.2025.2480920.

[340] S. Li, Z. Wang, H.H. Stutz, State-of-the-art review on plant-based solutions for soil improvement, Biogeotechnics (2023), https://doi.org/10.1016/j.bgtech.2023.100035.

[341] Q. Ma, N. Wu, H. Xiao, Z. Li, W. Li, Effect of Bermuda grass root on mechanical properties of soil under dry–wet cycles, Bull. Eng. Geol. Environ. 80 (9) (2021) 7083–7097, https://doi.org/10.1007/s10064-021-02369-1.

[342] S. Briner, C. Elkin, R. Huber, Evaluating the relative impact of climate and economic changes on forest and agricultural ecosystem services in mountain regions, J. Environ. Manag. 129 (2013) 414–422, https://doi.org/10.1016/j.jenvman.2013.07.018.

[343] J.F. Bird, J.J. Bommer, Earthquake losses due to ground failure, Eng. Geol. 75 (2) (2004) 147–179, https://doi.org/10.1016/j.enggeo.2004.05.006.

[344] Y. Li, G. Chen, C. Tang, G. Zhou, L. Zheng, Rainfall and earthquake-induced landslide susceptibility assessment using GIS and artificial neural network, Nat. Hazards Earth Syst. Sci. 12 (8) (2012) 2719–2729, https://doi.org/10.5194/nhess-12-2719-2012.
[345] P. Ruggeri, V.M. Fruzzetti, A. Ferretti, G. Scarpelli, Seismic and rainfall induced displacements of an existing landslide: findings from the continuous monitoring, Geosciences 10 (3) (2020) 90, https://doi.org/10.3390/geosciences10030090.
[346] V. Kumar, L. Cauchie, A.S. Mreyen, M. Micu, H.B. Havenith, Evaluating landslide response in a seismic and rainfall regime: a case study from the SE Carpathians, Romania, Nat. Hazards Earth Syst. Sci. 21 (12) (2021) 3767–3788, https://doi.org/10.5194/nhess-21-3767-2021.
[347] P. Khadka, O. Kolawole, A.C. Amenuvor, M.L. Ankah, Coupled effects of earthquake and rainfall on landslide susceptibility in non-tropical coastal areas: assessing governing mechanisms and innovative slope protection strategy, Discov. Civ. Eng. 2 (1) (2025) 69, https://doi.org/10.1007/s44290-025-00227-7.
[348] Z. He, M. Akiyama, A.K. Alhamid, D.M. Frangopol, Y. Huang, Probabilistic life-cycle assessment of landslides exposed to both rainfall under nonstationary climate change effects and earthquakes, Struct. Saf. 115 (2025) 102599, https://doi.org/10.1016/j.strusafe.2025.102599.
[349] M. Bohnhoff, P. Martínez-Garzón, Y. Ben-Zion, Global warming will increase earthquake hazards through rising sea levels and cascading effects, Seismol Res. Lett. 95 (5) (2024) 2571–2576, https://doi.org/10.1785/0220240100.
[350] S. Martino, G.M. Marmoni, M. Fiorucci, A.F. Ceci, M.E. Discenza, J. Rouhi, D. Tedoradze, Role of antecedent rainfall in the earthquake-triggered shallow landslides involving unsaturated slope covers, Appl. Sci. 12 (6) (2022) 2917, https://doi.org/10.3390/app12062917.
[351] S. Martino, S. Battaglia, F. D'alessandro, M. Della Seta, C. Esposito, G. Martini, F. Troiani, Earthquake-induced landslide scenarios for seismic microzonation: application to the Accumoli area (Rieti, Italy), Bull. Earthq. Eng. 18 (12) (2020) 5655–5673, https://doi.org/10.1007/s10518-019-00589-1.
[352] D.K. Keefer, Landslides caused by earthquakes, Geol. Soc. Am. Bull. 95 (4) (1984) 406–421, https://doi.org/10.1130/0016-7606(1984)95<406:LCBE>2.0.CO;2.
[353] C.E. Rodrıguez, J.J. Bommer, R.J. Chandler, Earthquake-induced landslides: 1980–1997, Soil Dynam. Earthq. Eng. 18 (5) (1999) 325–346, https://doi.org/10.1016/S0267-7261(99)00012-3.
[354] K. Sassa, H. Fukuoka, F. Wang, G. Wang, Landslides induced by a combined effect of earthquake and rainfall, in: K. Sassa, H. Fukuoka, F. Wang, G. Wang (Eds.), Progress in Landslide Science, Springer, Berlin, Heidelberg, 2007, https://doi.org/10.1007/978-3-540-70965-7_14.
[355] F. Faris, F. Wang, Stochastic analysis of rainfall effect on earthquake induced shallow landslide of Tandikat, West Sumatra, Indonesia, Geoenviron. Disaster 1 (1) (2014) 12, https://doi.org/10.1186/s40677-014-0012-3.
[356] V.B.Q. Nguyen, Y.T. Kim, Rainfall-earthquake-induced landslide hazard prediction by Monte Carlo simulation: a case study of MT. Umyeon in Korea, KSCE J. Civ. Eng. 24 (1) (2020) 73–86, https://doi.org/10.1007/s12205-020-0963-8.
[357] V. Ducrocq, I. Braud, S. Davolio, R. Ferretti, C. Flamant, A. Jansa, J. Tamayo, HyMeX-SOP1: the field campaign dedicated to heavy precipitation and flash flooding in the northwestern Mediterranean, Bull. Am. Meteorol. Soc. 95 (7) (2014) 1083–1100, https://doi.org/10.1175/BAMS-D-12-00244.1.
[358] R. Cornes, G. van der Schrier, E.J.M. van den Besselaar, P. Jones, An ensemble version of the E-OBS temperature and precipitation datasets, J. Geophys. Res. Atmos. 123 (2018). https://doi.org/10.1029/2017JD028200.
[359] I. Harris, T.J. Osborn, P. Jones, D. Lister, Version 4 of the CRU TS monthly high-resolution gridded multivariate climate dataset, Sci. Data 7 (1) (2020) 109, https://doi.org/10.1038/s41597-020-0453-3.
[360] A. Fantini, Ph. D. Thesis: Climate Change Impact on Flood Hazard over Italy, 2019. http://hdl.handle.net/11368/2940009.
[361] V. Pavan, G. Antolini, R. Barbiero, N. Berni, F. Brunier, C. Cacciamani, T. Torrigiani Malaspina, High resolution climate precipitation analysis for north-central Italy, 1961–2015, Clim. Dyn. 52 (5) (2019) 3435–3453, https://doi.org/10.1007/s00382-018-4337-6.
[362] F. Desiato, G. Fioravanti, P. Fraschetti, W. Perconti, A. Toreti, Climate indicators for Italy: calculation and dissemination, Adv. Sci. Res. 6 (1) (2011) 147–150, https://doi.org/10.5194/asr-6-147-2011.
[363] F.A. Isotta, C. Frei, V. Weilguni, M. Perčec Tadić, P. Lassegues, B. Rudolf, G. Vertačnik, The climate of daily precipitation in the alps: development and analysis of a high-resolution grid dataset from pan-Alpine rain-gauge data, Int. J. Climatol. 34 (5) (2013) 1657–1675, https://doi.org/10.1002/joc.3794.
[364] D. Waliser, P.J. Gleckler, R. Ferraro, K.E. Taylor, S. Ames, J. Biard, M. Tuma, Observations for model Intercomparison project (Obs4MIPs): Status for CMIP6, Geosci. Model Dev. 13 (7) (2020) 2945–2958, https://doi.org/10.5194/gmd-13-2945-2020.
[365] C. Soci, H. Hersbach, A. Simmons, P. Poli, B. Bell, P. Berrisford, J.N. Thépaut, The ERA5 global reanalysis from 1940 to 2022, Q. J. R. Meteorol. Soc. 150 (764) (2024) 4014–4048, https://doi.org/10.1002/qj.4803.
[366] J. Muñoz-Sabater, E. Dutra, A. Agustí-Panareda, C. Albergel, G. Arduini, G. Balsamo, J.N. Thépaut, ERA5-Land: a state-of-the-art global reanalysis dataset for land applications, Earth Syst. Sci. Data 13 (9) (2021) 4349–4383, https://doi.org/10.5194/essd-13-4349-2021.
[367] A. Giordani, I.M.L. Cerenzia, T. Paccagnella, S. Di Sabatino, SPHERA, a new convection-permitting regional reanalysis over Italy: improving the description of heavy rainfall, Q. J. R. Meteorol. Soc. 149 (752) (2023) 781–808, https://doi.org/10.1002/qj.4428.
[368] R. Bonanno, M. Lacavalla, S. Sperati, A new high-resolution meteorological reanalysis Italian dataset: MERIDA, Q. J. R. Meteorol. Soc. 145 (721) (2019) 1756–1779, https://doi.org/10.1002/qj.3530.
[369] Viterbo, F., Sperati, S., Vitali, B., D'Amico, F., Cavalleri, F., Bonanno, R., Lacavalla, M., Under review. MERIDA HRES: a new High-RESolution reanalysis dataset for Italy. Meteorol. Appl., submitted for publication.
[370] M. Raffa, A. Reder, G.F. Marras, M. Mancini, G. Scipione, M. Santini, P. Mercogliano, VHR-REA_IT dataset: very high resolution dynamical downscaling of ERA5 reanalysis over Italy by COSMO-CLM, Data 6 (8) (2021) 88, https://doi.org/10.3390/data6080088.
[371] S. Wahl, C. Bollmeyer, S. Crewell, C. Figura, P. Friederichs, A. Hense, C. Ohlwein, A novel convective-scale regional reanalysis COSMO-REA2: improving the representation of precipitation, Meteorol. Z. 26 (4) (2017) 345–361, https://doi.org/10.1127/metz/2017/0824.
[372] M. Ridal, E. Bazile, P. Le Moigne, R. Randriamampianina, S. Schimanke, U. Andrae, Z.Q. Wang, Cerra, the copernicus European regional reanalysis system, Q. J. R. Meteorol. Soc. 150 (763) (2024) 3385–3411, https://doi.org/10.1002/qj.4764.
[373] R. Gelaro, W. McCarty, M.J. Suárez, R. Todling, A. Molod, L. Takacs, B. Zhao, The modern-era retrospective analysis for research and applications, version 2 (MERRA-2), J. Clim. 30 (14) (2017) 5419–5454, https://doi.org/10.1175/JCLI-D-16-0758.1.
[374] G. Fosser, M. Tölle, E.J. Kendon, M. Adinolfi, N. Ban, D. Belušić, et al., Convection-permitting climate models offer more certain extreme rainfall projections, npj Clim. Atmos. Sci. (2024), https://doi.org/10.1038/s41612-024-00600-w.
[375] E. Coppola, S. Sobolowski, E. Pichelli, et al., A first-of-its-kind multi-model convection permitting ensemble for investigating convective phenomena over Europe and the Mediterranean, Clim. Dyn. 55 (1) (2020) 3–34, https://doi.org/10.1007/s00382-018-4521-8.
[376] E. Dallan Correa-Sánchez, F. Marra, G. Fosser, M. Borga, Orographic control on bias and uncertainty in extreme sub-daily precipitation simulations from a convection-permitting ensemble, J. Hydrol. 659 (2025) (2025), https://doi.org/10.1016/j.jhydrol.2025.133324. Article 133324.
[377] P. Devò, M.F. Caruso, M. Borga, M. Marani, Estimates of rare rainfall extremes in ungauged areas, Geophys. Res. Lett. 52 (2025), https://doi.org/10.1029/2024GL113576 e2024GL113576.
[378] G. Titti, L. Hu, P. Festi, L. Elia, L. Borgatti, L. Lombardo, An updated version of the SZ-plugin: from space to space-time data-driven modeling in QGIS, Int. J. Appl. Earth Obs. Geoinf. (2025), https://doi.org/10.1016/j.jag.2025.104679.
[379] G. Titti, A. Sarretta, L. Lombardo, S. Crema, A. Pasuto, L. Borgatti, Mapping susceptibility with open-source tools: a new plugin for QGIS, Front. Earth Sci. 10 (2022) 842425, https://doi.org/10.3389/feart.2022.842425.
[380] M. Castelli, G. Torsello, G. Vallero, Preliminary modeling of rockfall runout: definition of the input parameters for the QGIS plugin QPROTO, Geosciences 11 (2) (2021) 88, https://doi.org/10.3390/geosciences11020088.
[381] F. Guzzetti, G. Crosta, R. Detti, F. Agliardi, STONE: a computer program for the three-dimensional simulation of rock-falls, Comput. Geosci. 28 (9) (2002) 1079–1093, https://doi.org/10.1016/S0098-3004(02)00025-0.
[382] C. Sauthier, M. Pirulli, G. Pisani, C. Scavia, V. Labiouse, Numerical modelling of gravel unconstrained flow experiments with the DAN3D and RASH3D codes, Comput. Geosci. 85 (2015) 81–90, https://doi.org/10.1016/j.cageo.2015.09.008.
[383] K.J. Beven, R. Lamb, P. Quinn, R. Romanowicz, J. Freer, Topmodel, in: V.P. Singh (Ed.), Computer Models of Watershed Hydrology, Water Resource Publications, Colorado, 1995, pp. 627–668.

[384] K. Beven, TOPMODEL: a critique, Hydrol. Process. 11 (9) (1997) 1069–1085, https://doi.org/10.1002/(SICI)1099-1085(199707)11:9%3C1069::AID-HYP545%3E3.0.CO;2-O.
[385] S. Peruccacci, S.L. Gariano, M. Melillo, M. Solimano, F. Guzzetti, M.T. Brunetti, The ITAlian rainfall-induced LandslIdes CAtalogue, an extensive and accurate spatio-temporal catalogue of rainfall-induced landslides in Italy, Earth Syst. Sci. Data 15 (7) (2023) 2863–2877, https://doi.org/10.5194/essd-15-2863-2023.
[386] M. Melillo, M.T. Brunetti, S. Peruccacci, S.L. Gariano, A. Roccati, F. Guzzetti, A tool for the automatic calculation of rainfall thresholds for landslide occurrence, Environ. Model. Software 105 (2018) 230–243, https://doi.org/10.1016/j.envsoft.2018.03.024.
[387] F. Rollo, S. Rampello, Influence of the displacement predictive relationships on the probabilistic seismic analysis of slopes, J. Geotech. Geoenviron. Eng. 149 (6) (2023) 04023033, https://doi.org/10.1061/JGGEFK.GTENG-11162.
[388] F. Rollo, G. Buscarnera, Modelling seasonal landslide motion: does it only depend on fluctuations in normal effective stress? Int. J. Numer. Anal. Methods GeoMech. (2023) 1–20, https://doi.org/10.1002/nag.3625.
[389] C. Esposito, S. Martino, F. Pallone, G. Martini, R. Romeo, A methodology for a comprehensive assessment of earthquake-induced landslide hazard, with an application to pilot sites in Central Italy. Landslides and Engineered Slopes: Experience, Theory and Practice 2, Taylor & Francis, 2016, pp. 869–877, https://doi.org/10.1201/9781315375007.
[390] L.M. Giannini, C. Varone, C. Esposito, G.M. Marmoni, G. Scarascia Mugnozza, L. Schilirò, Earthquake-induced reactivation of landslides under variable hydrostatic conditions: evaluation at regional scale and implications for risk assessment, Landslides 19 (8) (2022) 2005–2019, https://doi.org/10.1007/s10346-022-01882-y.
[391] F. Rollo, S. Rampello, Probabilistic assessment of seismic-induced slope displacements: an application in Italy, Bull. Earthq. Eng. 19 (2021) 4261–4288, https://doi.org/10.1007/s10518-021-01138-5.
[392] M. Mergili, I. Marchesini, M. Rossi, F. Guzzetti, W. Fellin, Spatially distributed three-dimensional slope stability modelling in a raster GIS, Geomorphology 206 (2014) 178–195, https://doi.org/10.1016/j.geomorph.2013.10.008.
[393] I.S. Liso, R. Tufano, G. Poneti, E. Scacchia, R. Colacicco, V.L. Presti, S. Martino, Design of a virtual test bed for the Italian territory: proof of concept for multi-hazard scenarios effects in the context of a national resilience assessment, Int. J. Disaster Risk Reduct. (2026) 106110, https://doi.org/10.1016/j.ijdrr.2026.106110.
[394] F. Marra, D. Zoccatelli, M. Armon, E. Morin, A simplified MEV formulation to model extremes emerging from multiple nonstationary underlying processes, Adv. Water Resour. 127 (2019) 280–290, https://doi.org/10.1016/j.advwatres.2019.04.002, 2019.
[395] F. Marra, M. Borga, E. Morin, A unified framework for extreme subdaily precipitation frequency analyses based on ordinary events, Geophys. Res. Lett. 47 (2020), https://doi.org/10.1029/2020GL090209 e2020GL090209.
[396] N. Ban, J. Schmidli, C. Schär, Evaluation of the new convective-resolving regional climate modeling approach in decade-long simulations, J. Geophys. Res. 119 (2014) 7889–7907, https://doi.org/10.1002/2014JD021478.
[397] M. Marani, M. Ignaccolo, A metastatistical approach to rainfall extremes, Adv. Water Resour. 79 (2015) 121–126, https://doi.org/10.1016/j.advwatres.2015.03.001.